2019-09-06

Reactions involving fracturing chemical additives with implication in delayed H2S production

Marrugo Hernandez, Juan Javier

UNIVERSITY OF CALGARY

Reactions involving fracturing chemical additives with implication in delayed H_2S production

by

Juan Javier Marrugo Hernandez

A THESIS

SUBMITTED TO THE FACULTY OF GRADUATE STUDIES

IN PARTIAL FULFILMENT OF THE REQUIREMENTS FOR THE

DEGREE OF DOCTOR OF PHILOSOPHY

GRADUATE PROGRAM IN CHEMISTRY

CALGARY, ALBERTA

SEPTEMBER, 2019

Abstract

Shale gas is fast becoming the primary source of liquefied natural gas, a must needed fuel in a society trying to lower carbon emissions. When producing shale reservoirs, hydraulic fracturing in combination with horizontal drilling are the chosen technologies to extract hydrocarbons economically and efficiently. An issue faced during production from hot shale gas reservoirs ($T > 100$ °C) is the presence of hydrogen sulfide (H_2S) and organo-sulfur compounds (C_xH_y-SH) in the production fluids. These sulfur species can have a significant economic impact on the overall production as the gas now has to be treated to remove the unwanted components.

In this work, the decomposition of selected chemical additives contained within fracturing fluids are investigated as an alternative explanation to the H_2S formation in hot shale sweet gas reservoirs. Initially, high-pressure and high-temperature decomposition/hydrolysis of sulfur-containing biocides and corrosion inhibitors were studied, and the mechanisms of H_2S generation were proposed. Although the results were definitive, sulfur-containing additives are not always applied. Therefore, in researching a more universal explanation of non-biogenic souring, an undeniable fact came to light: the water used in hydraulic fracturing is not degassed, thus it is saturated with oxygen at field conditions. As such, the oxygen present in the fluid can react with *native* H_2S to generate elemental sulfur. Under downhole conditions elemental sulfur can react with hydrocarbons regenerating H_2S. For this reason and to further prove this hypothesis, the kinetics and equilibrium products of sulfur-methanol reaction in aqueous conditions was studied under various downhole conditions *e.g.* temperature, pressure, pH and salinity.

Acknowledgements

I will forever be grateful to my supervisor, Dr. Marriott for the incredible opportunity and support provided during my graduate studies. His understanding, guidance and jokes made the time working on this project gratifying.

Special thanks to Dr. Birss and Dr. Roesler for serving on my committee and providing me with feedback throughout this research.

I would like to recognize Dr. Pirzadeh, who initiated this research. His research and help at the beginning of my graduate studies were invaluable to understanding the future direction of my project.

I want to thank all the people at Alberta Sulfur Research Ltd. (ASRL) for their unlimited help during the course of this research. I would especially like to acknowledge Ms. Nancy Chou for her assistance with all the analytical instruments and Kevin Lesage for sharing with me some of his vast knowledge in electronics and analytical chemistry.

I would like to thank my research group members (past and present) for their help within the research and their friendship. I want to acknowledge Rohen Prinsloo for his tireless assistance in reviewing and proofreading much of my work and Jerry Commodore for his friendship and support.

To Tatiana, Lucia, Samuel and ..., my constants in a life full of variables.

Table of contents

List of tables

List of figures and illustrations

List of symbols, abbreviations and nomenclature

Symbol	Definition
ABT	2-Aminobenzothiazole
ATD	2-amino-1,3,4-thiadiazole
a_i	Activity of specie i
C_2+	Reactive hydrocarbons
CI	Corrosion inhibitors
C_xH_y-SH	Organo-sulfur compounds
Dazomet	3,5-dimethyl-1,3,5-thiadiazinane-2-thione
DMDS	Dimethyl disulfide
DMS	Dimethyl sulfide
DMTD	2,5-dimercapto-1,3,4-thiadiazole
DMTS	Dimethyl trisulfide
E^e	Equilibrium potential
FFCI	Film forming corrosion inhibitors
FID	Flame ionization detector
GC	Gas chromatograph
HF	Hydraulic fracturing
HiP	High pressure equipment
HPV	High-pressure poppet valve
HTHP	High-temperature and high-pressure
I	Ionic strength
k'	Rate constant
$k_{ATD \to H_2S}$	Formation rate of hydrogen sulfide from 2-amino-1,3,4-thiadiazole
k_{ATD}	Hydrolysis rate of 2-amino-1,3,4-thiadiazole
$k_{DMDT \to H_2S}$	Formation rate of hydrogen sulfide from 2,5-dimercapto-1,3,4-thiadiazole
k_{DMTD}	Hydrolysis rate of 2,5-dimercapto-1,3,4-thiadiazole
k_{obs}	Observed kinetic rate
LNG	Liquefied natural gas
NIST	National institute of standards and technology
p	Pressure
PFPD	Pulse flame photometric detector
PRT	Platinum resistance thermometer
REFPROP	Reference fluid thermodynamic and transport properties database software
$S°$	Elemental sulfur
SAGD	Steam assisted gravity
SCD	Sulfur chemiluminescence detector
SDS	Sodium dodecyl sulfate
SLS	Sodium lauryl sulfate/Sodium dodecyl sulfate
SRB	Sulfate-reducing bacteria
SS	Stainless steel

t	Time
T	Temperature
$t_{1/2}$	Half-life
T1	Temperature 1 for pyrolysis tube
T2	Temperature 2 for pyrolysis tube
TCD	Thermochemical conductive detector
TPP	Triphenyl phosphine
TPPS	Triphenyl phosphine sulfide complex
TSR	Thermochemical sulfate reduction
VED	Volt equivalent diagrams
x	Mole fraction
$\Delta_f G^o$	Change in standard Gibbs energy

Chapter One: Introduction

1.1 Motivation

The ability to produce natural gas from unconventional resources has changed the energy landscape worldwide.[1] Hydraulic fracturing in combination with horizontal drilling has been the dominant driving force in the production of hydrocarbons from low-permeability reservoirs that otherwise could not be accessed.[2] A feature found in produced fluids from hot shale gas plays is the presence of variable amounts of hydrogen sulfide (H_2S) and organo-sulfur compounds, which are often absent in the initial assessment of the reservoir.[3] In many of these H_2S-producing wells, the initial fluid testing does not reveal a significant amount of H_2S; however, after production begins the H_2S concentration starts to increase, reaching a maximum concentration of tens to several hundred parts per million in the following months.[4] In addition, unexpected spikes of H_2S in the production fluid can pose significant challenges for downstream treating facilities. This is especially true when the well was initially thought to be sweet (low H_2S, variable CO_2), leaving producers with the additional cost and the unexpected risks associated with H_2S.

In general, the H_2S produced in a reservoir could be formed *via* several mechanisms, some of which are (i) aquathermolysis, (ii) biogenic generation, (iii) thermochemical sulfate reduction (TSR) reaction, (iv) decomposition of hydraulic fracturing additives and (v) sulfur oxidation of chemical additives.[4] The first three sources of H_2S have been studied extensively, and provide an important understanding of how H_2S could be formed. The least explored sources of H_2S in the literature are decomposition of chemical additives at downhole conditions, and the sulfur oxidation of chemical additives. Therefore, the goal of this thesis was to explore the possible kinetics and decomposition mechanisms for chemical additives used in hydraulic fracturing, which could

produce H_2S and organo-sulfur compounds when exposed to reservoir conditions. Consequently, to study these chemical systems the design and construction of a high-pressure high-temperature reactor was initially required. This equipment was used to explore the chemistry of additives such as biocides and corrosion inhibitors at high-pressure ($p = 140$ bar) and high-temperature ($T = 150$ °C) conditions.

1.2 Structure of the thesis

This thesis is a manuscript based thesis and has been organized into six chapters, where chapters 3-5 are published or submitted journal articles. Chapter one includes the motivation and a detailed introduction. It contains the possible souring mechanisms of a reservoir and a review of different chemical entities used as additives in hydraulic fracturing. The delayed H_2S production with the new possible souring mechanisms is also discussed.

The second chapter presents the design of the high-pressure and high-temperature mini autoclave, the instrument later used to collect most of the experimental kinetic data. The mini autoclave is described in detail, along with the modification performed to fully automate the setup. The interface of LabView software for control and monitoring, as well as the Arduino controllers for automatic sampling, also are included. All the analytical techniques along with their respective methodologies and modifications are listed in this chapter. Lastly, the density calculation procedure by using reference quality pure component Helmholtz equations of state are briefly explained in the context necessary for this research. Note that the experimental section for manuscripts in chapters 3 to 5 have been removed to avoid excessive redundancy.

In chapter three, the decomposition mechanisms for sulfur-containing biocides (dazomet and methylisothiazolinone) were discussed. In particular, the decomposition of dazomet under downhole conditions showed interesting behaviour. The decomposition products (H_2S + formaldehyde) reacted to form methyl mercaptan while decomposition of starting material was still taking place. The kinetics and thermodynamic products that were observed are also included in this chapter. The decomposition kinetics for the methylisothiazolinone was established, and a mechanism of H_2S formation was proposed. Manuscript submitted to Industrial and Engineering Chemistry Research, American Chemical Society, on June 28, 2019.

In chapter four, the decomposition of nitrogen and sulfur-containing corrosion inhibitors is presented. Heterocyclic compounds containing both nitrogen and sulfur are often selected for high-pressure and high-temperature applications with low-pH, such as acid stimulation. Three compounds were studied, 2,5-dimercapto-1,3,4-thiadiazole (DMTD) and 2-amino-1,3,4-thiadiazole (ATD) generated H_2S, while 2-Aminobenzothiazole (ABT) did not produce any measurable H_2S under the conditions tested. Manuscript submitted to Applied Energy, Elsevier, on July 17, 2019.

Chapter five discusses an alternative approach in the formation of H_2S without the addition of sulfur-containing additives. In this section, the chemical additive methanol was reacted with elemental sulfur at downhole conditions. The mechanisms of H_2S and organosulfur products are proposed in this chapter, and the explanation is supported by the use of volt-equivalent diagrams (VED). Manuscript published as "Marrugo-Hernandez, J. J.; Prinsloo, R.; Sunba, S.; Marriott, R.

A. Downhole Kinetics of Reactions Involving Alcohol-Based Hydraulic Fracturing Additives with Implications in Delayed H_2S Production. *Energy and Fuels,* **2018**, *32*(4), 4724–4731".

Finally, chapter six summarizes all the significant findings for the decomposition of common additives and a final overview of H_2S occurrence in hot shale gas reserves. Conclusions and potential future research directions are suggested thereby concluding this thesis.

1.3 Unconventional gas and hydraulic fracturing

Many unconventional reservoirs require hydraulic fracturing after drilling, in order to allow for easier fluid flow to the wellbore. Horizontal drilling combined with hydraulic fracturing are the preferred option in producing natural gas from unconventional plays.[5]

When using horizontal drilling, gas producers can reach several kilometres into a production zone in a reservoir, therefore producing larger volumes of hydrocarbons, when compared to traditional vertical drilling.[6] After completing the drilling process, high-pressure water (above the reservoir formation pressure) is injected into the reservoir with proppant (normally sand) and chemical additives, creating fractures in the near-wellbore region from which the gas can flow. Next, water and additives are partially recovered by flowing the aqueous fluids back through the initial well (flowback).[6] Note that acid stimulation can also be part of the completion of a well. Acid stimulation can be performed alone (acid matrix stimulation) or as part of the fracturing fluid (acid fracturing).[7] In both cases the objective is the same, etching the minerals in the rock formation, causing fractures to increase porosity and to clean the open channel from formation damage (acid soluble material). After the completion of a well, the flowback water

may be treated and re-used, although the majority of the recovered water is injected into deep subsurface wells or disposed of into deep brine reservoirs.[8] During flowback, some of the chemical additives are recovered. The remaining fluids are believed to be recovered during production, as the produced gas comes out of the well with excess water.[8] It is worth mentioning that in many cases shale wells can be re-fractured or re-stimulated multiple times to increase production throughout the lifetime of the well.

Downhole conditions are incredibly variable for shale plays. For instance, the Marcellus shale reservoir temperature ranges from 40 to 125 °C and depths between 1,200 to 2,600 m, with pressures from 275 bar to 414 bar. Deeper shales, such as the Haynesville (3,200 to 4,100 m), can have temperatures of 200 °C and pressures up to 690 bar.[4] Downhole environments can also be highly saline, where total dissolved species can range from 50,000 up to 400,000 ppm with Na^+, K^+ and Cl^- being the major ions present.[9] The pH of flowback water has been reported to be in the range from 3.1 to 8.4.[10] However, this may not be the natural pH of the reservoir and will vary depending on the mineralogy (the presence of CO_2 will lead to a buffering capacity) and the pH of the stimulation and fracking fluid used during completion.

It is essential to highlight that downhole conditions are specific to the well location. Two wells drilled within the same formation could potentially have a different temperature and salinity.[11] As such, the chemical additives are exposed to very complex systems that, in many cases, need to be simplified for laboratory studies. Moreover, it is essential to mention that a production well is a dynamic system resulting in variable concentrations of gases, salinity, pH and

sorption-desorption of chemical additives which would impact the decomposition rates of those additives and hence the rate of H_2S being generated.

1.4 Chemical additives used in hydraulic fracturing

Chemical additives used within the fracturing and stimulation fluid are specifically selected for a well. Parameters such as temperature, pressure, mineralogy and pH are important in designing a fracturing fluid. Chemical additives are generally used in low concentrations ($\leq 2\%$ by volume); however, the total volume of fracturing fluid used for each operation can be significant, *e.g.*, 50,000 cubic meters of the total solution.[8] Each chemical additive has an intended use; for example, surfactants are used to reduce fluid friction and biocides are applied to prevent and/or eliminate bacteria. Table 1-1 shows some common additives listed within FracFocus and includes a variety of chemicals used and their specific purposes (FracFocus is a website where companies publicly and voluntarily disclose the chemicals used in hydraulic fracturing operations).[12] The additives can modify the physical and chemical properties of the fluid. As an example, additives such as hydroxyethyl cellulose can be added to increase the viscosity and therefore increase the proppant dragging capacity of the fluid. On the other hand, biocides such as dazomet can be added to sterilize the fluid and avoid unwanted bacterial growth that could negatively impact production. Hundreds of chemicals can be used for a single fracturing operation.[13]

Table 1-1. Chemical additives with their chemical compounds and the purpose for including them in a fracturing fluid.[12]

Additive type	Chemical	Purpose
Surfactant	Sodium dodecyl sulfate (SDS)	Viscosity modifier, emulsion inhibitor, friction reducer
Surfactant	Methanol	Product stabilizer, winterizer
Biocide	Dazomet, Methylisothiazolinone	Eliminates bacteria
Proppant	Silica and quartz sand	Allows the fractures to remain open so gas can migrate to the wellbore
Gel	Guar gum, hydroxyethyl cellulose	Viscosity modifier for carrying proppant
Acid	Hydrochloric acid	Helps dissolve minerals
Biocide	Glutaraldehyde	Eliminates bacteria
Corrosion inhibitor	Methanol	Product stabilizer and winterizing agent
Crosslinker	Boric acid	Maintain fluid viscosity as temperature increases
Friction Reducer	Ethylene glycol	Helps in reducing fluid friction and also used as a winterizing agent
Scale inhibitor	Phosphonic acid	Prevent scale deposit
Iron control	Citric acid	Prevents precipitation of metal oxides
Crosslinker	Sodium tetraborate	Maintain fluid viscosity
Clay stabilizer	Tetramethyl ammonium	Prevents clay shifting

Many of these are well known chemicals and some are commonly used in many household products. As a matter of fact, many hydraulic chemical additives are used in our personal care products, for instance, sodium dodecyl sulfate (SDS) is a commonly used surfactant added to toothpaste and methylisothiazolinone is a common biocide added to mouthwash and makeup.

Not every chemical additive reported on FracFocus or in the open source databases is used in a fracturing fluid. Many of the chemicals reported in these sources are not compatible with all the fracturing techniques used. For example, certain chemicals used for slick water fracturing are not used in gel fracturing. Therefore, fracturing fluids are not only a complex mixture of chemicals, they are specifically tailored for each well and each application.

Many chemical additives are used only once during the fracturing of a well as part of the fracturing package or in the drilling mud. However, additives such as biocides, corrosion inhibitors, hydrate inhibitors and scale inhibitors are often used during fracturing and throughout the lifetime of the production well. These chemicals are important to avoid unwanted production issues such as corrosion by either bacteria or corrosive gases, as well as formation damage caused by scale build-up. Many biocides and corrosion inhibitors contain sulfur as part of the chemical structure. Therefore, decomposition of these compounds at downhole conditions could produce unwanted sulfur species such as H_2S or mercaptans in the fluid being produced. The extent to which these undesirable sulfur species increase over time can vary depending on the mode of chemical injection (batch vs continuous), temperature and kinetics of decomposition.

1.4.1 Corrosion inhibitors

Corrosion inhibitors (CI) used in oil and gas production can be classified as volatile and film forming.[14] Volatile or vapour phase corrosion inhibitors are often used in closed systems and are compounds with enough vapour pressure to diffuse through the fluid and physically adsorb onto metal surfaces. There are many examples, such as diethylamine phosphate, dicyclohexylamine carbonate and trimethylamine, among others.[15]

Film forming corrosion inhibitors (FFCIs) are more commonly used for well application.[16] They can be easily injected continuously or in batches downhole, at the wellhead, or throughout the gathering system. These types of inhibitors rely on the adsorption of the compound onto the metal surface, thereby forming a protective layer that physically prevents contact with corrosive chemicals. Surfactant based film forming corrosion inhibitors are typically amphiphiles, usually consisting of a polar head group and a hydrophobic tail.[17] The hydrophobic tail is designed to interact with the hydrocarbons while the polar head group interacts with the metal.

Besides oxygen and nitrogen, sulfur is another common heteroatom used in the chemical structure of FFCI's, particularly in acidizing corrosion inhibitors.[18] Sulfur-containing inhibitors are typically used in combination with another corrosion inhibitor to reduce pitting corrosion. For example, a film forming corrosion inhibitor containing a thiol can react with an aldehyde (generally cinnamaldehyde) forming a compound that also can be a corrosion inhibitor.[19]

When acid treatments are part of the stimulation or fracturing fluids, acid corrosion inhibitors are applied to protect the integrity of surface and subsurface equipment. Note that acidic conditions tend to accelerate corrosion rates compared to normal operation. Typically, acid

corrosions inhibitors are small heterocyclic rings containing both nitrogen and sulfur atoms, such as, thiadiazoles and aminobenzothiadiazoles, whose decomposition and H_2S generation mechanism are presented in chapter 4.

1.4.2 Biocides

Biocides are bioactive organic chemicals which have been developed for sterilization and preservation purposes. Biocides have been applied in oil and gas reservoirs for many years with significant success in water flooding operation during enhanced oil recovery (secondary recovery).[20] Because hydraulic fracturing is usually a water intensive process, bacterial presence in the fluids is almost inevitable. As such, biocides are extensively applied in the fracturing fluid, drilling mud and during regular operation to control bacterial growth.[21]

There are multiple types of biocides, and they are classified as oxidants and non-oxidants. Oxidant biocides have been used in treating water injection systems but are usually corrosive and difficult to handle.[22] As such, non-oxidizing biocides are often the preferred choice. Non-oxidizing biocides are organic molecules with multiple inhibition mechanisms. Typically, non-oxidizing biocides alter the permeability of the cell walls of bacteria thereby disrupting basic biological processes in order to cause cell death.[20] These types of compounds are easier to handle and are less likely to cause corrosion issues. The list of non-oxidizing biocides is extensive, from small aldehydes to metronidazoles, phenolics or cationic polymers. From the wide-ranging options of biocides, this thesis is concerned with the sulfur-containing species as these could potentially produce H_2S and organosulfur compounds when exposed to downhole conditions.

Sulfur-containing biocides can be classified into four groups: isothiazolones, organic thiocyanates, triazine derivates and dithiocarbamates.[23] Dithiocarbamates are frequently used in the pulp and paper industry.[24] They have been applied with some success in oil fields throughout water injection systems but are not commonly found in hydraulic fracturing fluids. Organic thiocyanates are expensive and suffer from rapid decomposition, and thus having the potential to release toxic hydrogen cyanide.[19] They require a relatively high concentration and are often applied after confirmation of bacterial growth and biofouling. Triazines have been reported to have some microbial properties. However, they are mostly reported to be used as an H_2S scavenger.[25]

Isothiazolones have shown broad-spectrum antimicrobial activity and are also very effective towards sessile bacteria. They inhibit bacterial growth by limiting respiration and food transport through the cell wall.[26] Isothiazolones are known to be very useful in preventing the formation of H_2S by inhibiting sulfate-reducing bacteria (SRB). They are often injected continuously during well production with sporadic aliquots of a second biocide.[26]

1.5 Reservoir souring

Reservoir souring is a phenomenon in which the concentration of H_2S increases over time in production wells. *Native* H_2S or metal sulfides are to be expected, as it is known that oil and gas deposits originate from biomass degradation, which would have contained some sulfur. The increase in H_2S levels in a production fluid could be generated *via* multiple mechanisms, many of which are well known and have been described in various geological systems. As presented before in the motivation, the most known mechanisms by which H_2S can be generated in a reservoir are: (i) Aquathermolysis reaction with kerogen, (ii) biogenic generation *via* sulfate reducing bacteria,

(iii) TSR reaction, (iv) degradation of sulfur-containing chemical additives and (v) sulfide oxidation with dissolved oxygen followed by sulfur oxidation of organic species.

1.5.1 Aquathermolysis

Aquathermolysis of kerogen is a well-known phenomenon occurring during steam-assisted gravity drainage (SAGD) in a bituminous reservoir. In this process, high-temperature and high-pressure water is injected into a reservoir with the final objective of reducing the viscosity of the oil.[27] The oil viscosity can drop by five orders of magnitude from millions of centipoise to tens of centipoise.[28] In heavy oil reserves, the majority of the sulfur is present as organosulfur species, along with small concentrations of metal sulfides. While heavy oil reserves do not contain significant amounts of *native* H_2S, the reduction in viscosity by high-temperature and high-pressure water causes the thermochemical production of H_2S, CO, CO_2, H_2 and CH_4 as the major off-gas species.[29] Therefore, during SAGD or cyclic steam stimulation, the produced fluid can contain levels of up to 5 % H_2S (at the surface), which must be recovered to avoid toxic emissions.[30]

Steam reformation of hydrogen and later hydrogenation of sulfur compounds is not the primary mechanism by which H_2S can be generated in this type of process. It has been reported that steam reformation under these conditions is considerably slower and would not be able to produce such large levels of H_2S in a short period of time.[28-29] On the other hand, water at these conditions undergoes significant dissociation and reacts with molecules present in the kerogen producing the above mentioned thermochemical products.

The aquathermolysis mechanism of H_2S generation has been suggested to occur at elevated pressures and temperatures lower than 300 °C.[4,28-30] At much higher temperatures ($T > 300$ °C) thermal cracking starts to become more prevalent and becomes the major contributor towards hydrocarbon reactions. Clark and Hyne established these two characteristic chemical regimes as, (1) aquathermolysis and (2) pyrolysis, in which they described the aquathermolysis "window" occurring at $T < 300$ °C.[29] At these conditions, aquathermolysis occurred *via* the production of reactive species formed from organosulfur compounds.[29] In particular, Clark and Hyne studied the H_2S and CO_2 formation from organosulfur compounds (thiophenes and sulfide-containing asphaltenes) undergoing aquathermolysis.[27,30,31] It was found that majority of the H_2S was generated by sulfur-containing asphaltenes at temperatures close to 300 °C.

1.5.2 Biogenic generation of H_2S

Sulfate-reducing bacteria are well known microorganisms capable of reducing aqueous sulfate to H_2S. Sulfate reducing bacteria have been observed in various geological settings with variable temperatures from 0 to 80 °C.[32] Machel *et al*. showed that in geological systems with temperatures above 60 °C, metabolism of sulfate reducing bacteria was very slow.[33] As such, the major distinctive isotopic signature of the metabolic product (H_2S) is absent in most high-temperature geological reservoirs. Certain hyperthermophilic sulfate-reducing bacteria have shown to survive to temperatures as high as 110 °C,[34] however these are rarely observed and they appear to be inactive in typical geological environments. Bacterial sulfate reduction can be responsible for both *native* and non-*native* H_2S. When H_2S is biologically generated, the lighter sulfur isotope in H_2S is enriched when compared to the aqueous sulfate. Consequently, in some cases, biogenic H_2S can be confirmed by sulfur isotopic signatures of fractionation of ^{32}S to ^{34}S.[35]

The rates of hydrogen sulfide produced by bacterial sulfate reduction are incredibly high when compared to reactions occurring on a geological time scale.[32,33] This is commonly observed by the hydrogen sulfide concentration in many organic-rich sediments below the depth of atmospheric oxygen penetration. Although the biogenic production rate of hydrogen sulfide could be high under ideal proliferation conditions, sulfate reducing bacteria are often limited by multiple factors, such as temperature, aqueous sulfate availability and reactive organic matter, thereby slowing down the overall hydrogen sulfide production significantly.[32]

Sulfate reducing bacteria can be responsible for souring a reservoir and are commonly observed in low-temperature water flooding systems.[22] Similarly, during a water-intensive process such as a hydraulic fracturing process, the risk of bacterial contamination is high. Water that is obtained from multiple sources and not stored properly could potentially contain enough bacteria to start a souring process in a reservoir if the right conditions are met.[21] Therefore, biocide injection and bacterial control programs during secondary recovery and during hydraulic fracturing are periodically needed. Note that in the case of secondary recovery, nitrate injection (non-biocide) can be used to control hydrogen sulfide production by allowing bacteria to digest nitrate instead of sulfate, which is a more thermodynamically favourable process.[19] Together, high-temperature and biocide application makes the reduction of sulfate by bacteria a controllable and less probable mechanism for H_2S production in hot shale reservoirs. This does not suggest that the native H_2S would not have been initially generated by sulfate reducing bacteria, but that H_2S increase during well production is less likely to be bacterial in nature.

1.5.3 Thermochemical sulfate reduction reaction

TSR reactions are a natural process occurring in multiple carbonate reservoir systems. The majority of geological TSR studies are based on well-documented examples including the Khuff Formation (Middle East), the Smackover formation (United States), and the Nisku Formation (Alberta, Canada), among others.[34,36-37] During TSR, sulfate is reduced to sulfide through the non-bacterial oxidation of hydrocarbons, producing CO_2 and H_2S, along with organo-sulfur intermediates. Note that this reaction happens on a very slow geological timescale.[38]

A simplified TSR mechanism involving aliphatic hydrocarbons was proposed by Marriott *et al.*:[38]

$$\tfrac{3}{4}\cdot x\ H^+ + \tfrac{3}{4}\cdot x\ CaSO_4(s) \rightleftharpoons \tfrac{3}{4}\cdot x\ Ca^{2+} + \tfrac{3}{4}\cdot x\ HSO_4^- \tag{1-1}$$

$$\tfrac{3}{4}\cdot x\ HSO_4^- + \tfrac{9}{4}\cdot x\ H_2S + \tfrac{3}{4}\cdot x\ H^+ \rightleftharpoons 3x\ S° + 3x\ H_2O \tag{1-2}$$

$$3x\ S° + C_{x+1}H_{2x+4} + 2x\ H_2O \rightarrow 3x\ H_2S + x\ CO_2 + CH_4 \tag{1-3}$$

$$\tfrac{3}{4}\cdot x\ CO_2 + \tfrac{3}{4}\cdot x\ H_2O \rightarrow \tfrac{3}{4}\cdot x\ HCO_3^- + \tfrac{3}{4}\cdot x\ H^+ \tag{1-4}$$

$$\tfrac{3}{4}\cdot x\ Ca^{2+} + \tfrac{3}{4}\cdot x\ HCO_3^- \rightarrow \tfrac{3}{4}\cdot x\ CaCO_3(s) + \tfrac{3}{4}\cdot x\ H^+ \tag{1-5}$$
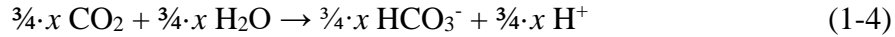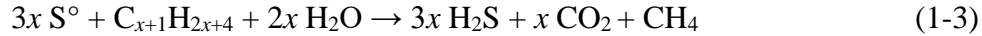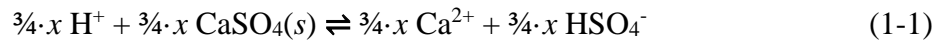
where the net reaction for the oxidation of C_2+ species is

$$\tfrac{3}{4}xCaSO_4(s) + C_{x+1}H_{2x+4} \rightarrow \tfrac{3}{4}xH_2S + \tfrac{1}{4}xCO_2 + \tfrac{1}{4}xH_2O + \tfrac{3}{4}xCaCO_3(s) + CH_4 \tag{1-6}$$

The overall reaction has two distinct limiting steps: the first limitation is the equilibrium dissolution of sulfate mineral (reaction 1-1), and the second is a slow rate for the oxidation of hydrocarbons by sulfur (reaction 1-3).[39] According to reaction 1-2 of the above mechanism, initial H_2S is required to generate the sulfur (S°) intermediate, which then oxidizes the hydrocarbon.

Mougin *et al.* confirmed this by using Gibbs energy minimization calculations, that TSR is a thermodynamically favourable process from $T = 20$ to 240 °C.[34] However, the overall rate of TSR reactions with hydrocarbons at low-temperatures ($T < 250$ °C) is slow. As a result, the majority of laboratory experiments involving TSR reactions are carried out at $250 < T < 600$ °C, in order to obtain sufficient products to perform analytical measurements.[23,26] For this reason, there is little to no agreement in the literature about the overall rate of such reactions, mostly due to this significant temperature difference at which the laboratory reactions are performed versus the reservoir temperatures.

Initially and based on the observations by Orr *et al.*, TSR reactions were suggested to only occur under hot reservoir conditions for $T > 120$ °C.[40] More recently, Zhang *et al.* have shown that the functional groups of the reductant (alcohols, alkenes, alkynes, and acids) can significantly alter TSR reaction rates (primarily due to solubility), resulting in different H_2S yields.[41-43] This information agrees with the mechanism previously presented (reaction 1-1 to 1-5), in which the steady-state S^o is formed from the equilibrium reaction of bisulfate and H_2S, and is consumed in reaction 1-3 during the oxidation of the dissolved hydrocarbon (or other available organic species). Therefore, both the aqueous solubility of the hydrocarbon and the hydrocarbon oxidation rates are important factors during a TSR reaction.

1.6 Delayed onset of hydrogen sulfide in shale gas reservoir

As presented earlier in the motivation section, an unexpected increase in H_2S concentration when producing from hot shale gas is problematic. As such, the understanding of the sources of H_2S in a reservoir is essential. So far, the most common mechanisms available in the open literature

have been reviewed. However, upon closer inspection aquathermolysis and biogenic generation of H_2S does not fully meet the physical and chemical criteria to be the key mechanisms in producing H_2S under hot shale reservoir conditions.

On the other hand, if the chemicals used during hydraulic fracturing are composed of sulfate groups, and reactive hydrocarbons (C_2+) are present, a TSR reaction could be expected. Therefore, H_2S could be observed in the production fluid. This mechanism was first described by the Marriott group and formed the basis of the research presented in this thesis.[4]

1.6.1 Thermochemical sulfate reduction of sulfate surfactant

The Marriott research group has demonstrated that sodium dodecyl sulfate (SDS) in fracturing fluids can also undergo TSR to produce H_2S, CO_2, and some minor organo-sulfur species when exposed to hot shale gas reservoir conditions. The proposed mechanism for the TSR of SDS reported by Pirzadeh *et al.* is included below: [44]

$$H_2O + C_{12}H_{25}SO_4^- + Na^+ \rightarrow C_{12}H_{25}OH + HSO_4^- + Na^+ \qquad (1\text{-}7)$$

$$HSO_4^- + 3H_2S + H^+ \rightleftharpoons 4S° + 4H_2O \qquad (1\text{-}8)$$

$$3S° + C_{12}H_{25}OH + 2H_2O \rightarrow 3H_2S + CO_2 + C_{11}H_{23}OH \qquad (1\text{-}9)$$

$$S° + {}^1\!/_3\,C_{11}H_{23}OH + {}^2\!/_3H_2O \rightarrow H_2S + {}^1\!/_3\,CO_2 + {}^1\!/_3C_{10}H_{21}OH \qquad (1\text{-}10)$$

$$Na^+ + CO_2 + H_2O \rightleftharpoons NaHCO_3 + H^+ \qquad (1\text{-}11)$$

where the net reaction is

$$NaC_{12}H_{25}SO_4(aq) + {}^2\!/_3H_2O \rightarrow NaHCO_3 + H_2S + {}^1\!/_3CO_2 + {}^2\!/_3C_{11}H_{23}OH + {}^1\!/_3C_{10}H_{21}OH \quad (1\text{-}12)$$
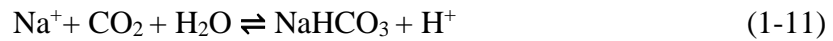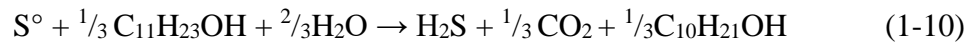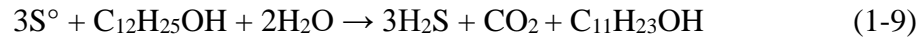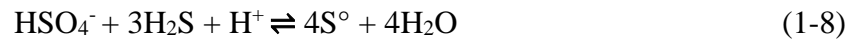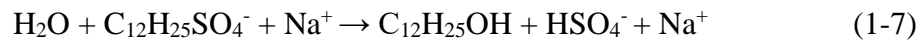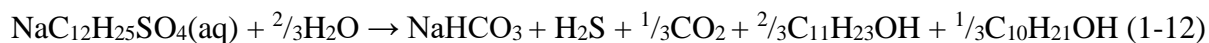
SDS hydrolyzes to 1-dodecanol and sodium bisulfate, which are key components for a TSR reaction. The hydrolysis of SDS is an autocatalytic process affected by temperature, pH, and initial H_2S concentration.[44] SDS is known to hydrolyze rapidly at $T > 80\ °C$; therefore, under hot shale gas conditions ($T > 100\ °C$), the hydrolysis should not be a rate-limiting step. When H_2S is present in a reservoir before fracturing (*native* H_2S), a rapid and favourable reaction 1-8 would temporarily sequester the H_2S as elemental sulfur.

TSR reactions can be initiated with or without initial H_2S under different conditions.[43,45] Therefore, the SDS systems were studied by Pirzadeh *et al.*, with and without initial sulfide concentration and with different sources of sulfur (sulfuric acid, magnesium sulfate, sodium bisulfate).[44] These reactions were initially carried out at a relatively high-temperature ($T = 300\ °C$) to better compare results with previous literature reactions performed at $T \geq 300\ °C$, whereas later studies were performed at lower temperatures ($T = 150\ °C$).[44] With these studies performed at lower temperatures, the rate of H_2S formation was determined at conditions which resemble reservoir temperatures.[44,46] Sulfuric acid was found to produce the fastest kinetic yield, which agrees with previous observations reported in the literature, where acidic conditions favour high reaction rates. CO_2 and H_2S were the major products found after a reaction time of $t = 168$ hours. The experimental system was not buffered, and in all cases the initial pH of the reactants dissolved in water before the reaction was pH = 7 to 8, compared to a final of pH $\approx$ 1 on completion of the reaction. By fitting the data to an Arrhenius equation, the estimated activation energy for the TSR reaction of SDS was found to be *ca.* 83 kJ mol^{-1}. Similar activation energies have been reported

for higher-temperature TSR experiments with a pH range of 2 – 5 and reduced sulfur species.[47]

1.6.2 Decomposition of chemical additives

Recently, several decompositions of hydraulic fracturing additives have been reported in the literature.[11,48-50] While the procedure and chemicals might be different, the end goal of these studies have been similar. In many cases, under downhole conditions, the additives decomposed to a variety of compounds that could potentially be more toxic than the parent molecule, raising concerns about the toxicity of the flowback water. Note, that all of these studies focussed only on liquid phase reactions and did not study the gas phase.

Previous studies showed that sulfate/bisulfate ion generated by the SDS hydrolysis could generate H_2S through a TSR reaction as was discussed in the previous section.[44] However, those studies did not show how H_2S could be generated if sulfur is covalently bound to the organic structure. Biocides and corrosion inhibitors are used during hydraulic fracturing and are replenished over time during normal operation as part of the corrosion protection programs in multiple oil and gas operations. Some of these compounds have sulfur in their chemical structure that could potentially form H_2S as by-products if the right conditions are met. Sulfur-containing biocides and sulfur-containing corrosion inhibitors have been studied here, along with the associated chemistries under downhole conditions.

Dazomet and methylisothiazolinone (biocides) generated H_2S. Similarly, two corrosion inhibitors, 2-amino-1,3,4-thiadiazole (DMTD) and 2-amino-1,3,4-thiadiazole (ATD) also generated H_2S. While many sulfur-containing additives could potentially generate H_2S or organo-

sulfur compounds, the chemical compounds tested in the work presented here should be used as a proof of concept to demonstrate that the decomposition of certain additives could also be involved in the souring of hot shale gas wells. The mechanism and details by which H_2S is being generated are discussed later in the thesis in Chapters 3 and 4.

1.6.3 Oxidation of H_2S followed by S_8 disproportionation/oxidation

Water used for hydraulic fracturing is saturated with oxygen at atmospheric pressure. Therefore under hot shale gas conditions oxygen can oxidize the *native* H_2S to form S^0 when reaching the reservoir (in a reducing environment):[4]

$$O_2 + 2H_2S \rightarrow 2S^0 + 2H_2O \qquad\qquad (1\text{-}13)$$

Similar oxidation reactions were presented previously in the TSR mechanisms, where sulfate was the oxidant (reactions 1-8 and 1-9), *i.e.*, $S^0 + H_2O$ exists in equilibrium with HSO_4^- and H_2S. Thus, H_2S can be reduced from direct oxidation with O_2 or sulfate and be regenerated by reaction with H_2O or organic species. After completion of the organic sulfur oxidation reactions, H_2S levels would then return to *native* reservoir concentrations. It should be noted that isotopic fractions would not be expected to change in this scenario.

Finally, the sulfur oxidation of organic species involves the formation of several intermediate oxidation products (organo-sulfur species), which could be produced before H_2S returns to *native* levels. To study the kinetics and H_2S evolution from the sulfur oxidation reaction, initially, the sulfur-methanol reaction was studied. The results and findings of these reactions are

discussed in Chapter 5.

1.7 Thesis Format

Each manuscript-based chapter (Chapter 3, 4 and 5) presented here begins with a "preface" with the intention of bringing the reader some additional context for a better understanding of the goals and motivations behind the manuscript.

The manuscripts shown here are presented as submitted in the corresponding journal and have been modified and formatted according to the faculty of graduate studies guidelines to improve readability and flow in the thesis document. The changes include:

1. The numbering of figures, tables and equations has been modified to provide continuity throughout the thesis.

2. The experimental chapter encompasses all the details from each manuscript. Therefore, the experimental section in the manuscripts were removed to avoid redundant information for the reader.

3. All references have been renumbered to allow consistency and continuity.

Manuscripts published during completion of this thesis, but not included are:

1) Marriott, R. A.; Pirzadeh, P.; Marrugo-Hernandez, J. J.; Raval, S. Hydrogen Sulfide formation in Oil and Gas. *Can. J. Chem.* **2016**, *94*, 406–413.

2) Lavery, C. B.; Marrugo-Hernandez, J. J.; Sui, R.; Dowling, N. I.; Marriott, R. A. The effect of methanol in the first catalytic converter of the Claus sulfur recovery unit. *Fuel.* **2019,** 238, 385-393.

Chapter Two: Methodology and experimental procedure

2.1 Methods for studying high-pressure and high-temperature kinetics

In order to perform experiments at high-pressure and high-temperature with variable concentrations of H_2S, certain requirements and specifications for the equipment are necessary. Ideally, the equipment should be corrosion resistant, require small volumes for easier handling of toxic gases and be able to operate at elevated pressure and temperatures. Numerous apparatus have been described in the open literature for measuring the kinetics of H_2S formation under high-pressure and high-temperature conditions, each with their respective advantages and disadvantages.[4,30,37,42,43,59]

Gold tubes are commonly used for downhole kinetics and H_2S formation studies. They have been widely used in studying geological processes for high-pressure and high-temperature applications such as thermochemical sulfate reduction.[37,40,42,43] In general, they are 110 to 120 mm long with an internal diameter of 3.5 to 4.5 mm and a wall thickness of 0.2 to 0.4 mm (see Figure 2-1). Gold is the material of choice mainly because of its high chemical inertness. Total volumes are between 40 to 80 µL, and upon loading the reagents, the sample is frozen (usually at $\approx$ -80 °C) as the open end portion is sealed and welded, to avoid loss of sample upon heating. The sealed tubes are then placed into a stainless steel autoclave and inserted into a pyrolysis oven. Temperature controlled is limited by the pyrolysis oven and is usually within ±2 °C. Confinement pressure of the gold tubes is held constant by a water pump.

Although numerous data for interesting geological processes have been obtained using gold tubes, the analytical drawbacks are evident. Despite the high-cost associated with using gold tubes, the fact that the internal volume is very small limits the subsequent analysis of liquid and gas products of each reaction. It is assumed that there is no difference in pressure across the gold tube wall (actual system pressure is less accurate than annulus pressure). A small variation in concentrations obtained by gas chromatography (GC) can significantly impact the total carbon and sulfur recovery. The amount of H_2S formed during the reaction needs to be significant (hundreds of ppm to mol% level) to accurately quantify it, and no continuous concentration monitoring is possible, so each gold tube only generates a single kinetic point.
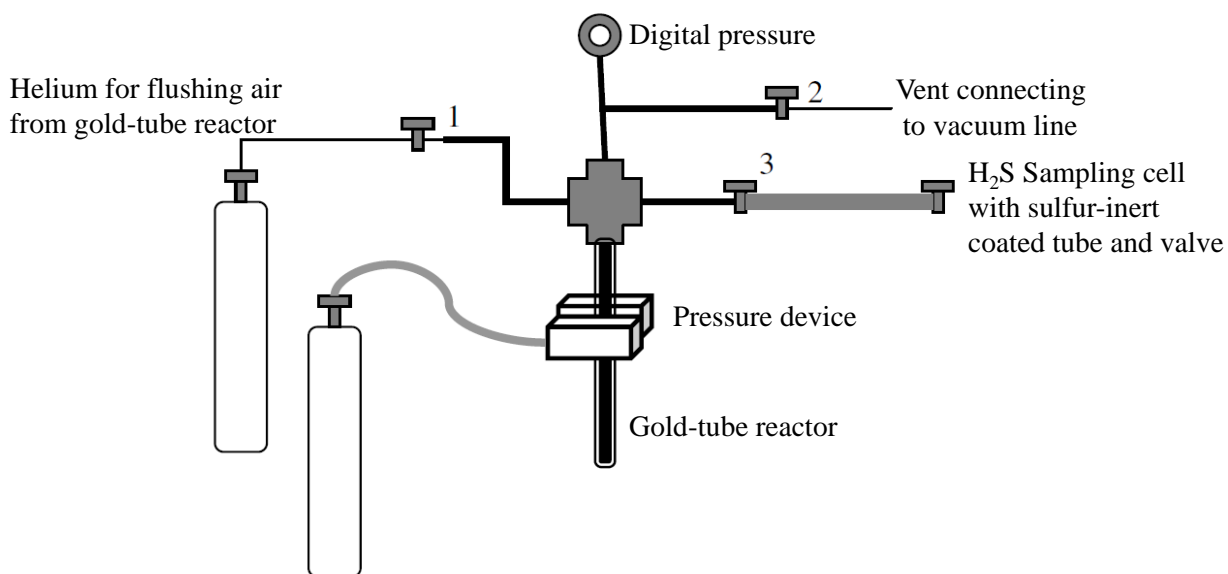
Figure 2-1. Schematic diagram showing the loading into gold-tube reactor. Adapted from Zhang *et al.*[46]

To overcome some of the gold tubes limitations, the Marriott group proposed and tested 5 mL titanium vessels to study high-pressure and high-temperature reactions. The reaction vessels consisted of hollowed out 25.4 mm, grade II titanium HiP plugs (high-pressure gland fitting) mated

to Hastelloy 25.4 – 0.16 mm adapter fittings (see Figure 2-2). A transfer line is connected to a needle valve for sampling and loading of the reactants. The reaction vessel was later connected to a sampling manifold and pressurized to the target pressure (see Figure 2-3). The vessels were then heated up to the target temperature by using a resistive heating jacket. After the required reaction time, the vessel is removed from the heating jacket and air-cooled to room temperature and sampled by GC *via* the manifold.
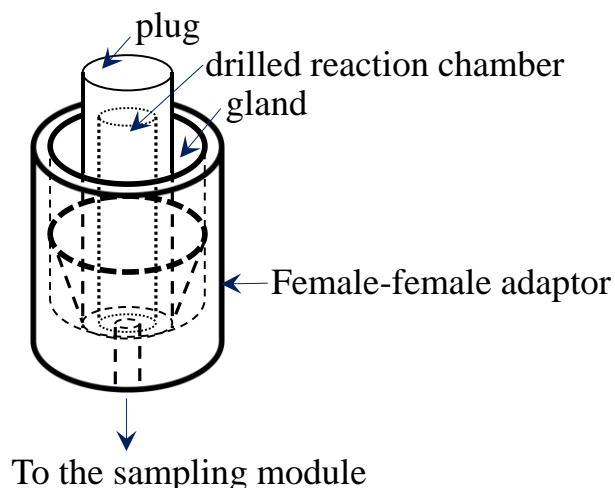
Figure 2-2. Schematic diagram showing the titanium vessel. Adapted from Pirzadeh *et al.*[47]

Pressure control is limited, as the vessel can only be pressurized to lower pressures and reached target pressure by heating up the system. The volume of the reaction mixture is larger than the gold tubes (5 mL of total volume); therefore more reaction mixture is obtained to perform further analysis at the end of each experiment. In a similar fashion as the gold tubes, one experiment can only produce a single kinetic measurement, and no continuous monitoring of species is possible as the reaction must be cooled down to room temperature before quantification.
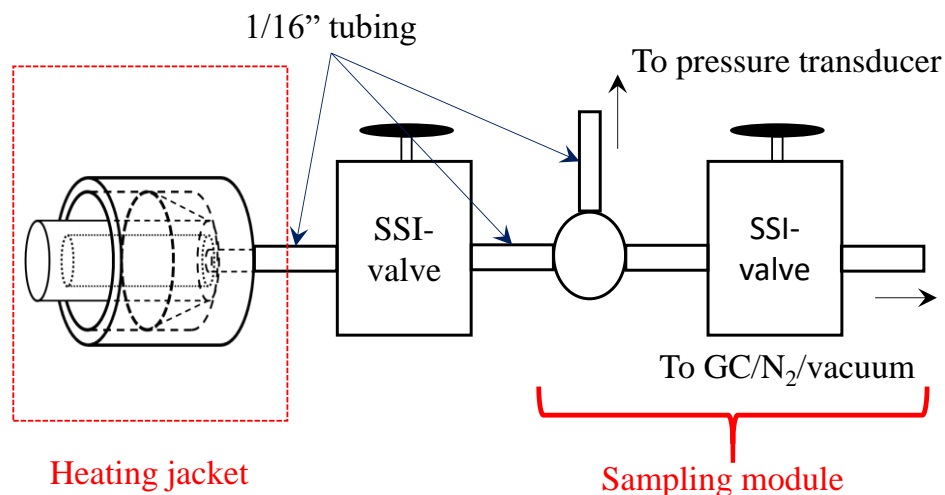
Figure 2-3. Schematic diagram showing the loading into gold-tube reactor. Adapted from Pirzadeh *et al.*[47]

Although high-grade titanium (type 2) was used, acid corrosion was reported to be evident in this type of system. Therefore to overcome this issue, a gold coated high-grade titanium (type 2) vessel was constructed (See Figure 2-4). With the gold coated vessel, several SDS degradation kinetic measurements were repeated and it was found that the corrosion product did not alter (enhance or inhibit) the kinetic rates previously reported. This system was also used to validate previously reported rates by our research group.
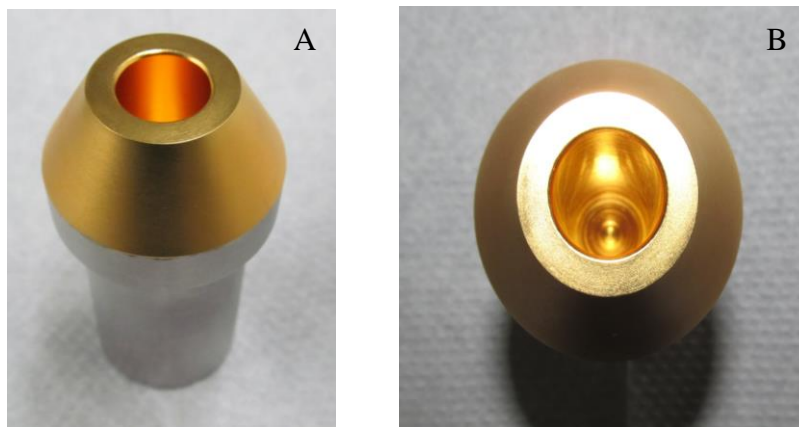
Figure 2-4. Gold coated titanium type 2 vessel: A, side picture; B, aerial picture.

2.2 Experimental apparatus

Taking into consideration the limitation described above for both gold tubes and titanium vessels, a new autoclave was designed and constructed. The goals behind the construction of the new set-up was to make it (i) fully automatic for sampling of gases and liquids, (ii) be acid corrosion resistant, (iii) have an accurate control of temperature and pressure and (iv) be fully interfaced with LabVIEW for data logging.

The final set-up was comprised of an overhead-stirred 50 mL autoclave (Autoclave Engineers) with operating conditions up to $p = 241$ bar and $T = 300$ °C (See Figure 2-5). The autoclave was constructed of SS-316 and fully protected with a corrosion resistant Tantalum film (treatment performed by Tantaline®). The magnetically coupled stirring assembly was controlled by an in-house built Arduino microcontroller, and a dual Hall-effect speed sensor was used to measure the stirring rate. The reactor was held isothermal by a modified Hewlett Packard 5890 GC oven with a stability of ±0.05 °C. The pressure in the system was measured using a

Paroscientific 410KR-HT-101 pressure transducer calibrated to an accuracy of ±0.007%, ranging from $p = 0.1$ to 250 bar using a Pressurement Limited T3800/4 deadweight tester.

The temperature of the modified GC oven and the reactor was measured by two 100-ohm four-wire platinum resistance thermometers connected to a Pico Technology PT- 104 data logger. The sampling of the liquid and headspace was automatically controlled by two high-pressure poppet valves activated by an in-house modified microcontroller. When activated, both high-pressure poppet valves were opened for 90 milliseconds, thus allowing an aliquot of the high-pressure gas from the head space to flow to the online gas chromatograph. Simultaneously, the second high-pressure poppet valve allowed for the collection of *ca.* 1.3 g of the liquid sample.

The reaction mixture was loaded by evacuating the 50 mL high-pressure, high-temperature reactor to a vacuum pressure of $p \leq 3.9$ mbar and allowing 50 mL of the solution to be drawn in through a zero-volume valve. After liquid injection, the setup was pressurized with ultra-high-purity nitrogen (99.998% Praxair) before regulating the temperature of the vessel to the target temperature. Time zero was marked when the temperature came within 0.05 °C of the target (approximate 16 min for 150 °C). Liquid and gas samples were collected at regular time intervals over the duration of each experiment.
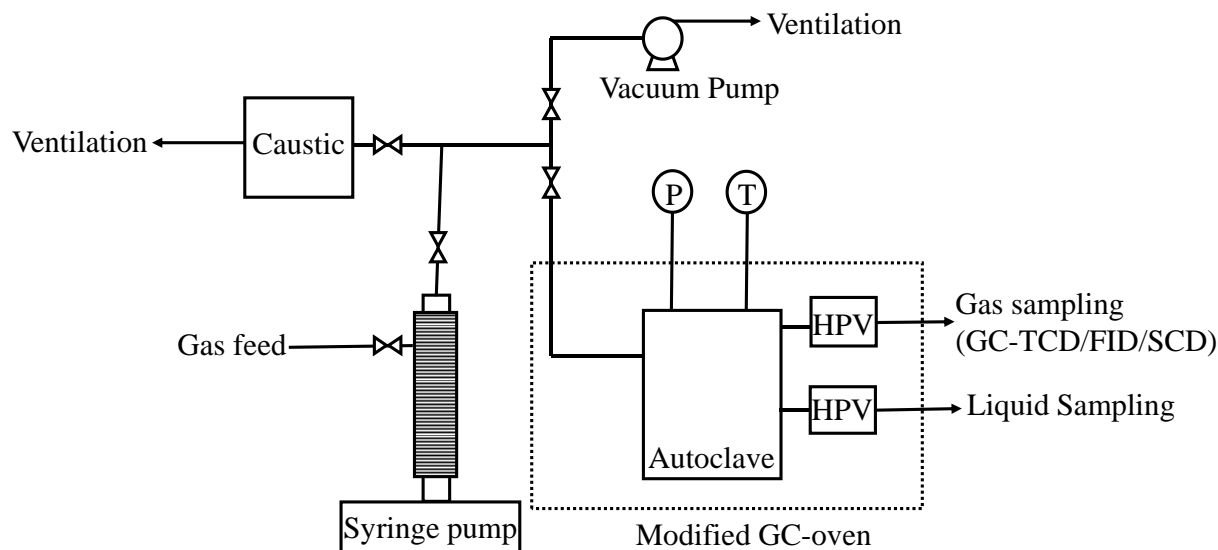
Figure 2-5. Simplified schematics of the modified constant volume, magnetically stirred autoclave. Abbreviation: P, pressure transducer; T, platinum resistance thermometer; HPV, high-pressure poppet valve for headspace and liquid sampling. Adapted from Marrugo-Hernandez *et al.*[59]

2.2.1 Automatic GC-sampling (Arduino microcontroller and LabVIEW)

The microcontroller was programmed in C^{++} to control the stirring *via* a dual hall sensor (to compensate for viscosity), the high-pressure poppet valves for the sampling of both the liquid and gas (headspace), and finally it controlled the injector of the GC (See appendix A.1). During the experiment, the user gives an array to the microcontroller. The array should consist of (i) the stirring rpm, (ii) the equilibrating time, (iii) the sampling time (time that the poppet valve is open for), and (iv) the time before injection. For the experiments reported here, the microcontroller stops the stirring for 5 seconds, allowing the gas-liquid to settle, followed by opening the selected high-pressure valve for 50 to 150 ms, allowing an aliquot of the high-pressure gas to flow from the autoclave to the GC sampling loops (loop volume of 2 x 250 µL). At this stage, all valve switching

was paused for 5 seconds for the high-pressure gas in the injection loop to reach atmospheric pressure because all GC calibrations were performed at atmospheric pressure. Finally the code triggered the GC injector to analyse the gas composition and then to resume stirring in the autoclave. When sampling the liquid, a similar procedure was performed, and the high-pressure liquid aliquot was collected in a sealed glass vial for later analysis.

The microcontroller, the pressure transducer, the PRTs and the Arduino microcontroller were interfaced with LabVIEW (see appendix A.2). As such, pressure, temperature and sampling time are recorded and visualized for the duration of the experiment.

2.3 Materials

Methylisothiazolinone (Catalog No. 725765, ≥95%), phosphoric acid (Catalogue No. 345245), methyl isobutyl ketone (Catalog No. 293261, ≥99.5%), 2-ethyl-1-hexanol (Catalog No. 538051, ≥99.6%), *trans*-cinnamaldehyde (Catalog No. 293261, ≥99.5%), ethylene glycol butyl ether (Catalog No. 537551, ≥99%), propargyl alcohol (Catalog No. P50803, ≥99%), methanol (Catalogue No 494291, ≥99.9%), elemental sulfur (Catalogue No. 213292, trace metal basis grade ≥99.998%) and propylene carbonate (Catalog No. 310328, ≥99.7%) were purchased from Sigma-Aldrich. Monobasic phosphate monohydrate (Catalogue No. 567549), 2-(2-ethoxyethoxy)ethyl acetate (Catalog No. 814635, ≥99.7%) was purchased from Merck. Benzoic acid (Catalog No. 73983, ≥99.7%) was purchased from Fluka. All chemicals were used without further purification. Water was polished to a resistivity of 18.2 MΩ·cm (EMD Millipore model Milli-Q type 1) and then degassed under vacuum for a minimum of 12 hours.

2.3.1 Synthesis and characterization of dazomet

A 40% aqueous solution of methylamine (40 g, 0.52 mols) was added to a round bottom flask and cooled to 15 °C. Carbon disulfide (24.4 g, 0.32 mols) was added dropwise to the solution and the mixture was stirred for 1 hour while maintaining the temperature below 20 °C. 37% formaldehyde (51.95g, 0.64 mols) was added to the reaction flask, and the mixture was stirred for 30 min. The white precipitate was filtered and rinsed with distilled water (3 x 20ml) to yield 88% (45.93g, 0.28 mols) of the desired product. The product was recrystallized in xylene yielding white needle-shaped crystals. ^{1}H NMR (400 MHz, CDCl3) δ 4.36 (s, 2H), 4.30 (s, 2H), 3.44 (s, 3H), 2.61 (s, 3H). ^{13}C NMR (101 MHz, CDCl3) δ 191.4 (C), 73.0 (CH2), 60.1 (CH2), 40.4 (CH3), 39.1 (CH3). The molecular ion was found to be (EI, m/z, %) 162.02 [M+].
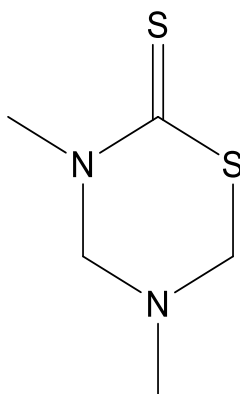
Figure 2-6. Chemical structure of Dazomet, $C_5H_{10}N_2S_2$, 3,5-Dimethyl-1,3,5-thiadiazinane-2-thione.

2.3.2 Preparation of biocides and corrosion inhibitors aqueous solutions

Dazomet and methylisothiazolinone were prepared individually to a target concentration of 500 mg/L. Similarly, 2,5-dimercapto-1,3,4-thiadiazole, 2-amino-1,3,4-thiadiazole and 2-aminobenzothiazole solutions were prepared at variable concentrations and were tested individually. Control of pH was achieved by the addition of 25 mM phosphate buffer. Phosphate

buffer was chosen due to the high chemical stability at high-pressure, and high-temperature environments. Synthetic brine solutions were composed of NaCl and buffer.

2.3.3 Preparation of alcohol (methanol based) solution

Aqueous CH_3OH solutions were mixed in-*situ* by injection of a 1:3 ratio dry-CH_3OH/buffer solution (by volume) into a stirred autoclave (discussed in the next section) with 80 mg of elemental sulfur. Control of pH was achieved by the addition of 25 mM phosphate buffer. Phosphate buffer was chosen for $pH \leq 3.15$ and $pH \geq 6.0$. Citric acid-phosphate buffer solution was used to further inspect the $3.5 \leq pH \leq 5.4$ region. As citric acid can be decomposed (mostly to CO_2) under hydrothermal conditions, blank experiments were performed, and CO_2 values were corrected. Synthetic brine solutions were composed of buffer and NaCl.

2.4 Gas sampling

2.4.1 Online gas chromatograph

When sampling the headspace of the reactor the high-pressure gas aliquot flowed through a Bruker GC-450 coupled with a thermal conductivity detector (TCD), a flame ionization detector (FID) and a sulfur chemiluminescence detector (SCD). The TCD has a linear dynamic range $>10^5$. The FID has a limit of detection <1.5pg C/s and a linear dynamic range $>10^7$. The SCD has a a linear dynamic range $> 10^4$ and a detection limit of 50 ppb. Chromatographic separation was achieved by a Bruker BR-1ms 20 m $\times$ 0.15mm I.D column (Catalog No. BR56198) for the SCD and Restek Rt-U-Bond 30 m $\times$ 0.53 mm I.D column (Catalog No. 19750) for the TCD and FID with helium as a carrier gas at flow rates of 0.6 and 10 mL/min, respectively. Both columns were kept at $T = 40\,°C$ for 1 minute, and the temperature was raised to $T = 190\,°C$ at a rate of 30 °C/min.

The SCD was operated under burner conditions of 40 sccm of hydrogen, 60 sccm of air, 533.3 mbar and $T = 800$ °C.

2.4.2 GC-MS

Upon conclusion of the reactions, an aliquot of the gas phase was collected into a previously evacuated gas sampling cylinder, and 5 µL was injected multiple times into a Bruker Scion-SQ GC-MS equipped with a 15 m × 0.25 mm I.D. BR-5ms column with a mass scanning range of 33 to 500 m/z and a data acquisition rate of 5 Hz. A cryogenic thermal gradient program was applied where the initial temperature of the GC oven was held at 0 °C for 1 minute, and then increased up to $T = 320$ °C at a rate of 10 °C/min.

Table 2-1: Summary table for analyte detection.

Analyte	Detector
N_2	TCD
CO_2	TCD
H_2S	TCD/SCD
COS	SCD
CH_4	FID
CH_3SH	SCD
CH_3SCH_3	SCD
$CH_3S_2CH_3$	SCD
$CH_3S_3CH_3$	SCD/MS

*The TCD and FID detectors were fully calibrated when the instrument was first commissioned, and the calibrations were verified monthly. The SCD was fully calibrated approximately every 3 months and the calibration was verified before each experiment was performed.

2.5 Liquid sampling

2.5.1 Quantification of sulfur-containing biocide in the liquid phase

Liquid samples were collected in sample vials and allowed to cool to room temperature (22 ± 0.5 °C) before direct injection into a GC. Calibration and quantification (analysed in triplicates)

were performed using a Varian CP-3500 equipped with an FID and a Pulsed Flame Photometric Detector (PFPD). Chromatographic separation was achieved using a DB-5 0.32 mm x 15 m 1.0μm column (Catalog No. 13457). The column was kept at $T = 80$ °C for 1 minute, and the temperature was then raised to $T = 295$ °C at a rate of 15 °C/min with a helium flow of 6 mL/min. The FID was operated at 300 °C with a 30 mL/min flow of H_2 and a 300 mL/min air. The PFPD was operated at 300 °C with a photomultiplier voltage of 525 mV, gate delay of 6 ms, gate width 20 s, trigger level of 200 mV and air and H_2 flows of 17 and 13 mL/min, respectively.

2.5.2 Quantification of methanol

Samples were allowed to cool to room temperature (22 ± 0.5 °C) before the addition of the internal standard (200 µL of dimethylformamide). Direct injection, calibration and methanol quantification (analysed in triplicates) were performed using a Varian CP-3500 equipped with an FID. Chromatographic separation was achieved using DB-5 0.32 mm x 15 m 1.0μm column (Catalog No. 13457). The column was kept at $T = 100$ °C for 1 minute, and the temperature was raised to $T = 295$ °C at a rate of 15 °C/min with a helium flow of 6 mL/min. The FID was operated at 300 °C with a 30 mL/min flow of H_2 and a 300 mL/min air.

2.5.3 Sulfur analysis

A quantitative xylene extraction was performed for each liquid sample at the end of each experiment. The xylene layer was removed and dried with $MgSO_4$. An aliquot of the extract was later used for total sulfur analysis, elemental sulfur analysis, and GC-MS.

2.5.3.1 Total Sulfur

An aliquot was diluted at least 10 times and analyzed with a Mitsubishi TS-100, with a T1 of 1000 °C and T2 of 1100 °C for the double pyrolysis tube. An argon gas time of 30 s and an argon plus oxygen time of 600 s. The gas flow rate of main oxygen was 300 mL/min, sub oxygen was 300 mL/min and argon was 400 mL/min. External calibration was performed before each batch of analysis.

2.5.3.2 Elemental sulfur analysis TPP (S_8 + S_x)[51]

An aliquot of the xylene extract was reacted with triphenyl phosphine (TPP) producing a triphenyl phosphine sulfide complex (TPPS) that was quantified in triplicate *via* a GC-PFPD in phosphorous mode. Chromatographic separation was achieved using DB-5 0.32 mm x 15 m 1.0μm column (Catalog No. 13457). The column was kept at $T = 80$ °C for 1 minute, and the temperature was raised to $T = 295$ °C at a rate of 15 °C/min with a helium flow of 6 mL/min. The FID was operated at 300 °C with a 30 mL/min flow of H_2 and 300 mL/min flow of air. The PFPD was operated at 300 °C with a photomultiplier voltage of 525 mV, gate delay of 6 ms, gate width 20 s, trigger level of 200 mV and air and H_2 flows of 17 and 13 mL/min respectively.

The residual sulfur was calculated by taking the difference between total sulfur and S_8 + S_x. The residual sulfur could include H_2S and organic sulfur species such as thiols, sulfides (dimethyl sulfide (DMS), dimethyl disulfide (DMDS)), or any sulfur bound to hydrogen or carbon.

2.5.4 Ion-chromatography (IC) analysis of sulfur species

A 100 µL aliquot of the extracted aqueous mixture was diluted to 10 mL using a preservative solution containing 10 mM mannitol and 50 mM sodium hydroxide to prevent oxidation of sulfide anions. This solution was analyzed on a Dionex DX320 with an IonPac AS17 hydroxide-selective anion exchange column with a CD25 conductivity detector and parallel AD25 absorbance detector for quantitative analysis of anions in the aqueous mixture. A potassium hydroxide concentration gradient from 30 to 70 mM was applied to elute anions from the column.

2.5.5 GC-MS

A 10 times-diluted sample of the xylene extract was prepared and directly injected into a Bruker Scion-SQGC-MS with a 15 m × 0.25 mm I.D. BR-5 ms column. A thermal gradient program was applied where the initial temperature of GC oven was held at 50 °C for 1 min and then increased up to $T = 320$ °C at a rate of 10 °C/min. Data collection started after 3 min of injection and continued for 34 min with a mass scanning range of 33 to 500 m/z and a data acquisition rate of 5 Hz.

Table 2-2: Summary table for analyte detection.

Analyte	Detector/Technique
Dazomet	PFPD/GC
Methylisothiazolinone	PFPD/GC
CH_3OH	FID/GC
Total S	TS-100/Total Sulfur
$S_8 + S_x$	PFPD/ TPP
*$CH_3S_3CH_3$	MS
*$CH_3S_4CH_3$	MS
*$CH_3S_5CH_3$	MS
SO_4^{2-}	CD25/IC
SO_3^{2-}	CD25/IC
$S_2O_3^{2-}$	CD25/IC

Calibratons were performed daily prior to analysis except for the organo polysulfides (*), which were identified by MS.

2.6 Density calculations

2.6.1 Reference quality pure component Helmholtz equation of state

The composition obtained from the GC analysis with the pressure and temperature of the system were used to calculate the density of the gas by using NIST's Reference Fluid Thermodynamic and Transport Properties Database software (REFPROP version 9.1). The calculated density, the gas composition and the calibrated total volume of the system were used to calculate the moles of sulfur species in the gas phase for a complete mass balance analysis.

Chapter Three: An assessment of the decomposition kinetics of sulfur-containing biocides to hydrogen sulfide at simulated downhole conditions.

Preface

Biocides are typically applied during drilling, fracturing and for the long-term maintenance of formations and wells. The goal behind this type of chemical treatment is to inhibit or kill bacteria present in the reservoir or fracturing fluids, with the aim of avoiding reservoir souring and microbial-induced corrosion. In this chapter, the decomposition of two sulfur-containing biocides is discussed. The results presented here showed that under high-temperature and high-pressure certain biocides decompose and can produce H_2S. Thus, while the biocides are injected to control H_2S producing bacteria, abiogenic H_2S and organosulfur compounds can form if the right reservoir conditions are met. Note that the intended biocidic activity of the additive is obviously compromised with degradation.

Manuscript submitted to the Industrial and Engineering Chemistry research journal, ACS, on June 28, 2019.

3.1 Abstract

North American production of liquefied natural gas (LNG) is at an all-time high in large part due to shale gas extraction from unconventional reserves. In producing shale gas, hydraulic fracturing in combination with horizontal drilling, is often used to create a path to free the hydrocarbons embedded in the reservoir. Biocides are incorporated into the fluid during drilling and fracturing for preventing activity from both native and non-native bacteria and potential reservoir souring (biogenic generation of H_2S). Certain sulfur-containing biocides have been reported to be used as part of the fracturing fluid in several reservoirs. Our research has shown that upon reaching downhole conditions (temperature and pressure) some of these compounds can decompose and generate unwanted H_2S and organosulfur compounds as by-products. In the case of dazomet, a sulfur-containing biocide, the decomposition products underwent hydrolysis under downhole conditions to produce undesirable H_2S, CS_2 and CH_3SH. A second biocide tested, methylisothiazolinone, eliminated sulfur and generated H_2S by sulfur dehydrogenation of the reaction intermediates. Our findings highlight the chemical transformation that sulfur-containing biocides could undergo under hydraulic fracturing conditions. In these circumstances H_2S and organo-sulfur compounds can be generated.

3.2 Introduction

The energy requirements for developing and industrialised countries are projected to increase as the world population grows.[52] Currently, most of the energy is expected to be supplied from non-renewable sources such as oil, gas, coal and nuclear.[53] In this regard, liquefied natural gas (LNG) is by far the most promising commodity before transitioning from carbon-based energy towards non-carbon or renewable sources.[53-54] In producing LNG, gas reservoirs are classified as

conventional and unconventional. In recent years, unconventional gas reserves (shale, tight and coal-bed methane) have been widely discovered across the globe, with significant reserves found in North America.[55]

Accessing unconventional natural gas, such as shale, requires the use of hydraulic fracturing commonly referred to as "*fracking*".[53-56] Hydraulic fracturing technologies have been reported since the 1950s;[57] however, in recent years, the combination of low-cost horizontal drilling with hydraulic fracturing have proven to be successful in a wide variety of unconventional plays.[13,54-58] We note that various unwanted concentrations ($< 1\%$) of hydrogen sulfide (H_2S) and organosulfur ($C_XH_Y\text{-}SH$) species exist in production of hot shale reservoirs ($T > 80 \,°C$) such as the Barnet shale ($T \approx 80 \,°C$), Haynesville ($T \approx 150 \,°C$) and Horn River ($T = 80 - 160 \,°C$), among others.[4,44,46,59] Often the initial assessment of these reservoirs does not reveal significant concentrations of H_2S; however, when production is brought on-stream, H_2S starts to appear, reaching a maximum concentration within a few months and later decreasing to lower stable levels.[3] These unexpected levels of H_2S and organosulfur compounds are very challenging to model and also difficult to treat properly, as most removal technologies require a stable H_2S concentration. Therefore, there is a need to explore the chemistry of fracturing fluids under downhole conditions to better understand the composition of the gas being returned to the surface.

When fracturing a well, a combination of water, proppant and chemical additives are rapidly pumped at high-pressure into the reservoir creating fractures in the near-wellbore region, accessing hydrocarbons embedded in the low-permeable gas reserve.[55-57]Although used in low concentration ($< 0.1 \%$ by volume) the chemical additives play an important role in the completion

of the well, as they are used to meet required parameters such as density, viscosity, stability and dragging capacity for the fracturing fluid.[60,61] While the majority of the chemicals used in hydraulic fracturing have been used in multiple industrial applications and are common in many household products, the understanding of the degradation pathways and products under downhole conditions such as variable pH, high salinity, high-pressure and high-temperature (HTHP) is limited. [11,48-50,62,63]

Among the chemical additives, biocides are very important. During the fracturing of a well, large volumes of water are used from multiple sources (river, lakes, municipal water supplied or fresh water wells) which can contain some bacteria.[64] To avoid microbial contamination and reservoir souring from both *native* and non-*native* bacteria, biocides are added during drilling (as part of the drilling mud), during fracturing (as a chemical additive in the fracturing fluid) and for long-term bacterial control in the formation and gathering system.[65,66] Ideally, a biocide or a combination of biocides should sterilize the reservoir during a hydraulic fracturing procedure, as reservoir souring in the fractures is known to be very difficult to treat. In reality, complete sterilization is not achievable, and long-term treatment is often required as part of a microbial control strategy. In general, the biocides used in hydraulic fracturing are nonoxidizing organic chemicals, due to the inherent risk of oxidizing biocides corroding equipment.[23,67] The nonoxidizing organic biocides can be divided into two categories: the membrane-active (lytic) and electrophilic biocides. The lytic biocides are surfactant-based molecules capable of binding to anionic functional groups at the membrane, thereby disrupting the lipid bilayer which results in lysis of the cell. On the other hand, electrophilic biocides make use of an electron-accepting functional group that reacts with chemical groups present in membrane proteins.[68] Two common additives of interest, dazomet (3,5-dimethyl-1,3,5-thiadiazinane-2-thione) and

methylisothiazolinone, are sulfur-containing electrophilic biocides. Dazomet is classified as a pesticide, which has been reported to hydrolyse to form methyl isothiocyanate, formaldehyde and other by-products. Methylisothiazolinone is a well-known biocide commonly used in many personal care products. Dazomet has been frequently used in the Marcellus Shale to limit microbial activity while methylisothiazolinone has been reported to be part of the fracking fluid for shale plays in California and Texas.[22,69]

Our research group is particularly interested in studying chemical additives capable of producing H_2S under HTHP conditions. Previously, we have shown how a well-known chemical such as sodium dodecyl sulfate can hydrolyse to 1-dodecanol and sulfate/bisulfate (pH dependent) and produce H_2S under HTHP conditions *via* a thermochemical sulfate reduction (TSR) reaction.[4,44,46,59] Although some HTHP decomposition research has been done on different liquid systems (glutaraldehyde, polyacrylamide and various halogenated additives), most studies focused on the wide variety of products generated in the aqueous phase, as these new chemicals can be brought up to surface as part of the flowback water after fracturing or later as part of the produced water.[11,48-50,62,63] While these results have given insights into the multiple reaction paths than additives can undergo under HTHP conditions, very few studies have aimed at measuring or understanding the gas phase portion of these reactions. Many products of chemical decomposition end up in the gas phase, depending on the vapour pressure and solubility of the compounds at HTHP conditions. In this work, we performed multiple experiments at HTHP conditions over a wide variety of scenarios in which sulfur-containing biocides could be present. To evaluate the impact of downhole conditions, the kinetics and final/equilibrium products of the decomposition reaction in saturated aqueous conditions were systematically evaluated. Parameters such as temperature, pH, initial H_2S concentration and salinity were changed to evaluate their impact on

the decomposition kinetics. Finally, chemical mechanisms for the H_2S production and decomposition of dazomet and methylisothiazolinone have been proposed.

3.3 Results and discussion

When a biocide is applied in a hydraulic fracturing process, it requires some time to travel from the chemical mixer to the wellhead, down the tubing and finally the production zone within the reservoir. As many of the hydraulic fracturing procedures are at large depths of 1,200 m (Marcellus Shale) to 4,100 m (Haynesville), depending on the injection rate, the fluid injected from the surface can take hours to fully reach the production zone. Therefore, it is important to know the rate at which these biocides are hydrolysed.

3.3.1 Mechanism of dazomet hydrolysis.

In our experiments, the gas phase was monitored, and the concentrations of sulfur species were quantified over time (see Figure 3-1). Dazomet rapidly hydrolyses to give carbon disulfide (CS_2) as the only sulfur species, along with formaldehyde (CH_2O) and methylamine (CH_3NH_2) as described by Reaction 3-1 (CH_3NH_2 and CH_2O are shown for simplicity; however, the cyclic tertiary triamine, monomethyl amine triazine, would likely be the major species in solution).

Hydrolysis of dazomet occurs near quantitatively to give only CS_2 within the first 30 min. This is followed by CS_2 hydrolysis (Reaction 3-2), a well-described process where CS_2 reacts stoichiometrically with water to produce H_2S and CO_2 in a ratio of 2:1. The H_2S produced in Reaction 3-2 could be readily scavenged by the triazine. Triazines are commonly used to capture H_2S when producing natural gas containing low levels of H_2S ($< 1\%$ H_2S) and at lower gathering-

line temperatures ($T < 80$ °C). Our observations show that at 150 °C, H₂S is converted to CH₃SH as the major sulfur containing product. Note that under these HTHP conditions, no methyl isothiocyanate was detected by GC-SCD or GC-MS.
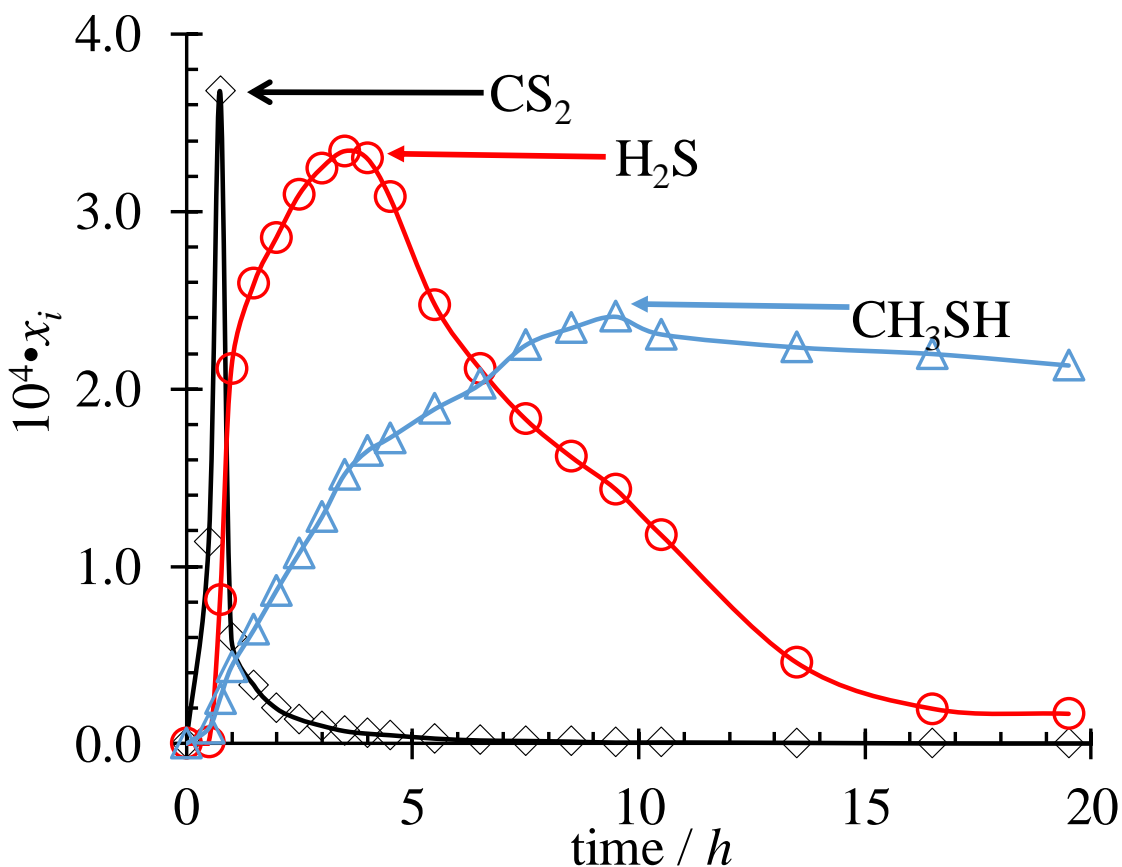
Figure 3-1. Mole fraction (xi) of each sulfur compound in the gas phase for dazomet at pH $=7$, $T = 150$ °C and $p = 143$ bar.

The mechanism for generating H₂S and CH₃SH *via* CS₂ is summarised by

$$C_5H_{10}N_2S_2 + 2\ H_2O \rightarrow CS_2 + 2\ CH_2O + 2\ CH_3NH_2 \tag{3-1}$$
[dazomet]

$$CS_2 + H_2O \rightarrow 2\ H_2S + CO_2 \tag{3-2}$$

$$CH_2O + 2\ H_2S \rightarrow CH_3SH + H_2O + 1/8\ S_8 \tag{3-3}$$

With a net reaction of

$$C_5H_{10}N_2S_2 + H_2O \rightarrow CO_2 + CH_2O + 2CH_3NH_2 + CH_3SH + S \qquad (3\text{-}4)$$
[dazomet]
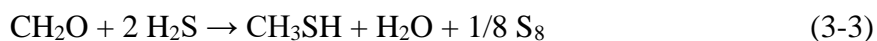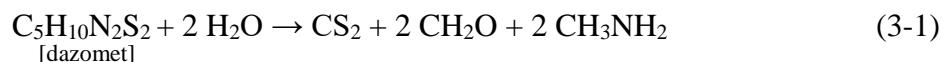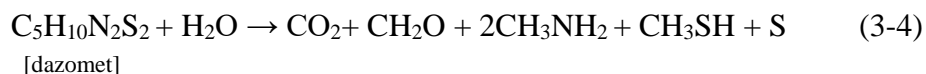
CH_3SH was produced from CH_2O and H_2S (Reaction 3-3). Elemental sulfur was isolated and quantified after the reactions were quenched. The mechanism for producing mercaptans from thioketones was previously described by Lucien $et\ al.$[70] In our case, a thioformaldehyde intermediate could be reduced by CH_3NH_2 to form CH_3SH and $H_2C=NH$.

H_2S was previously reported as a by-product of dazomet by Ruzo[71,72] and Roberts $et\ al.$;[73] however, in their studies the biocide was used as a soil fumigant at room temperature and atmospheric pressure. They found that under certain soil conditions the release of a highly odorous gas was detected. They also proposed a degradation pathway with multiple intermediates and highlighted that H_2S could be a decomposition product. Additionally, when using formaldehyde to scavenge H_2S, formation of the trithiane ($C_3H_6S_3$, 1,3,5-Trithiane) is possible, which under pressure and temperature can form a thioaldehyde known to be very unstable.[74] Nevertheless, trithiane was not detected in the GC-MS extracts after thermal quenching the reaction and, although it could be an intermediate, it is unlikely that it would be kinetically stable enough to be observed using our techniques. Overall, hydrolysis of dazomet yields transient H_2S, which reacts in the presence of formaldehyde to give CH_3SH as the major sulfur species.

To determine the source of carbon in the product (CH_3SH), reactions were performed to sequester the formed H_2S from the CS_2 hydrolysis reaction. In these experiments, equimolar amounts of $AgNO_3$ or $Cu(NO_3)_2$ were added and reacted at $T = 150\ °C$ and $p = 143$ bar. In both cases, no H_2S was detected due to the formation of Ag(I)sulfide or Cu(II)sulfide precipitate, and

we did not observe CH_3SH (see Figure 3-2). To rule out CH_3SH forming from H_2S reacting with

CH_3NH_2, a control experiment was performed by reacting only H_2S (3000 ppmv) and methylamine

(3000 ppmv) under aqueous conditions. No CH_3SH was detected in the gas phase, but rather the

$CH_3NH_3^+SH^-$ salt had formed through the acid base ionization reactions.
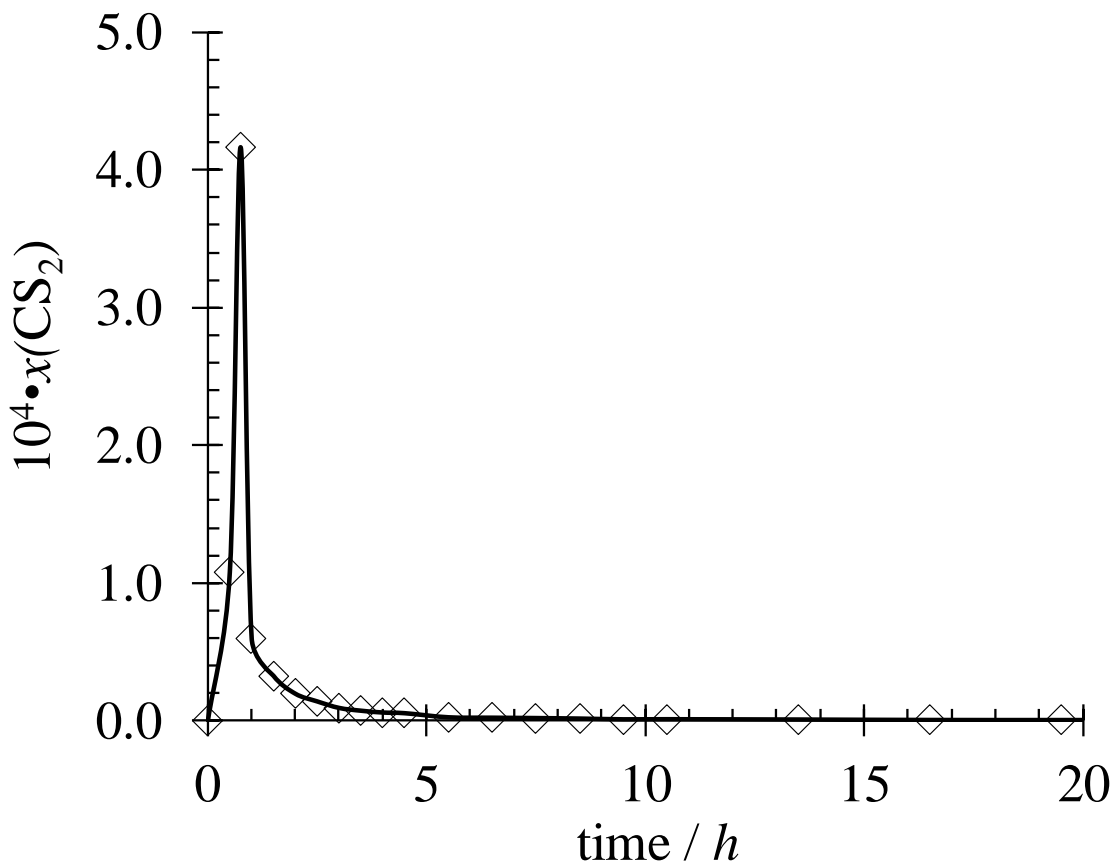
Figure 3-2. Mole fraction of CS_2 in the gas phase for of dazomet at pH =7, T = 150 °C and p = 143 bar, quantitatively amounts of $Cu(NO_3)_2$ were added to block the formation of H_2S and later CH_3SH.

3.3.2 Kinetics of dazomet hydrolysis.

As illustrated in Figure 3-3a, approximately 1 hour was required to fully hydrolyse a 500

mg/L solution at 125 °C and 30 minutes at 200 °C. The reaction was monitored for 20 h in the

aqueous portion using the loss of dazomet concentration. An Arrhenius plot was constructed (Figure 3-3(b)), and an activation energy of 33.4 ± 1.4 kJ mol^{-1} ($R^2 = 0.97$) was found for this reaction through least-squares regression (reproducibility shown at the 95% confidence interval). For each temperature tested, the (a) maximum concentration of CS_2, (b) maximum concentration of H_2S, and (c) maximum concentration of CH_3SH was calculated (see Table 3-1). The overall rate equation was found to be first order with respect the dazomet concentration

$$Rate = -\frac{d[C_5H_{10}N_2S_2]}{dt} = k[C_5H_{10}N_2S_2] \qquad (3-5)$$

Table 3-1: The initial reaction parameters and maximum product concentration during dazomet decomposition from 125 to 200 °C.

T / °C	pH	$10^3 \cdot x(CS_2)$	$10^3 \cdot x(H_2S)$	$10^3 \cdot x(CH_3SH)$	k_{obs} / h^{-1}	R^2	$t_{1/2}$ / h
125	7.2	3.65	3.41	2.24	4.85 ± 0.03	0.99	0.14
150	7.1	3.67	3.31	2.40	10.0 ± 0.5	0.98	0.07
175	7.1	3.88	3.51	2.55	17.1 ± 1.2	0.98	0.04
200	7.2	3.90	3.48	2.60	23.7 ± 4.5	0.93	0.03

The initial concentration of CS_2, H_2S and CH_3SH was zero.

The rate of CS_2, H_2S and CH_3SH formation was measured and found to be pseudo-first-order with respect to each species concentration (Table 3-2), *i.e.*, $d[CS_2]/dt = k'[CS_2]$, $d[H_2S]/dt = k'[H_2S]$ and $d[CH_3SH]/dt = k'[CH_3SH]$. In order to understand how various chemical environments commonly encountered in a shale well could impact the sulfur containing product distribution, we measured the H_2S and CH_3SH rate of formation by adding different initial H_2S concentrations, changing total pressure, adding ionic strength through NaCl(aq) and lowering the pH.

When the reaction is initiated with 205 ppmv H_2S, no significant effect on the rates was observed; however, a larger H_2S pre-loading (2850ppmv) did increase the formation rate of CH_3SH. This agrees with our observation within Figure 3-1 and the mechanism shown previously, where CH_3SH is not limited by the rate of CS_2 hydrolysis to produce CH_3SH.

There was no significant ionic strength effect found for the formation of any sulfur containing species. While some intermediates may be cationic during proton transfer reaction, addition of NaCl did not show any stabilising effect; therefore, there appears to be no rate limiting ion-ion reactions. As expected, the pressure did not significantly affect any of the kinetics parameters, as there is no appreciable change in volume associated with the formation of the activated complex and the reaction was expected to be occurring in the aqueous phase (at high-pressure). At low pH, the rate of CS_2 hydrolysis decreased; however, the CH_3SH formation rate increased. We have previously shown that under similar conditions, decreasing the pH favours the steady state concentration of S_8, but this does not explain the increased CH_3SH formation rate.[4,44,46,59] A more detailed mechanism in the future may reveal why reaction 3-3 is enhanced at low pH.

Figure 3-3. (a)The degradation of dazomet versus time at 125 to 200 °C and (b) the corresponding Arrhenius plot. △, 125 °C; ⊙, 150 °C; □, 175 °C; ✕, 200 °C.

More recently, Consolazio[75] studied the interaction of some biocides with minerals such as pyrite. They too report a pseudo first order reaction for the hydrolysis of dazomet when performed at low temperature and atmospheric pressure (80 °C), indicating that the decomposition mechanism could be similar for $T \geq 80$ °C. Although there were no data analysed for the gas phase, and limited experiments under relevant shale gas conditions, some of their results in the liquid phase are comparable to the data presented here, which were performed at a much higher temperature and pressure.

Table 3-2: The initial reaction parameters and rates of CS_2 hydrolysis, H_2S and CH_3SH formation at $T = 150$ °C and $p = 140$ bar.

Initial condition modified	k'_{CS_2} / h^{-1}	k'_{H_2S} / h^{-1}	k'_{CH_3SH} / h^{-1}
Normal condition*	0.491	0.222	0.313
205 ppm H_2S	0.490	0.228	0.310
2850 ppm H_2S	0.492	0.213	0.510
1 M NaCl	0.490	0.212	0.312
2 M NaCl	0.489	0.230	0.311
3 M NaCl	0.490	0.214	0.314
pH = 1.15	0.305	0.237	0.467
pH = 2.18	0.321	0.241	0.435
p = 80 bar	0.487	0.252	0.316
p = 200 bar	0.489	0.235	0.315

*Normal conditions are considered to be $T = 150$ °C, $p = 140$ bar, pH ≈ 7, 0 M NaCl. The initial concentration of CS_2, H_2S and CH_3SH was zero.

3.3.3 Kinetics and mechanism of methylisothiazolinone

Methylisothiazolinone hydrolysis under HTHP conditions was found to produce H_2S and CO_2, while no other organosulfur compounds were detected. Under these conditions, methylisothiazolinone was more kinetically stable than dazomet and required longer times to

decompose completely. When following the methylisothiazolinone concentration over time, we found that it took more than 20 h to completely hydrolyse to below detection limit concentrations (see Figure 3-4). The rate of reaction was calculated using the concentration of methylisothiazolinone (aq) which was followed for 45 h.

By measuring the rate of reaction at various temperatures (see Figure 3-4), an Arrhenius plot was constructed (Figure 3-4(b)), and activation energy of 53.4 ± 1.0 kJ mol^{-1} ($R^2 = 0.97$) was found through least-squares regression (reproducibility shown at the 95% confidence interval, see Table 3-3). The overall rate equation was found to be second-order with respect to the methylisothiazolinone concentration:

$$Rate = -\frac{d[C_4H_5NOS]}{dt} = k[C_4H_5NOS]^2 \qquad\qquad (3\text{-}6)$$

Curiously, the highly functionalised organic structure of methylisothiazolinone did not show any reactivity to H$_2$S, as no other organosulfur species were observed. To better understand the decomposition pathway and determine the mechanism of H$_2$S production, the liquid phase was analysed for organic products by GC-MS and thin layer chromatography. Thin layer chromatography revealed a single major by-product (N,1-dimethyl-6-oxo-1,6-dihydropyridine-3-carboxamide). An experiment was performed at a higher loading of biocide and the reaction was quenched after two hours to isolate the intermediates. Characterization data can be found in the supplemental data. The proposed mechanism is illustrated in Figure 3-5.
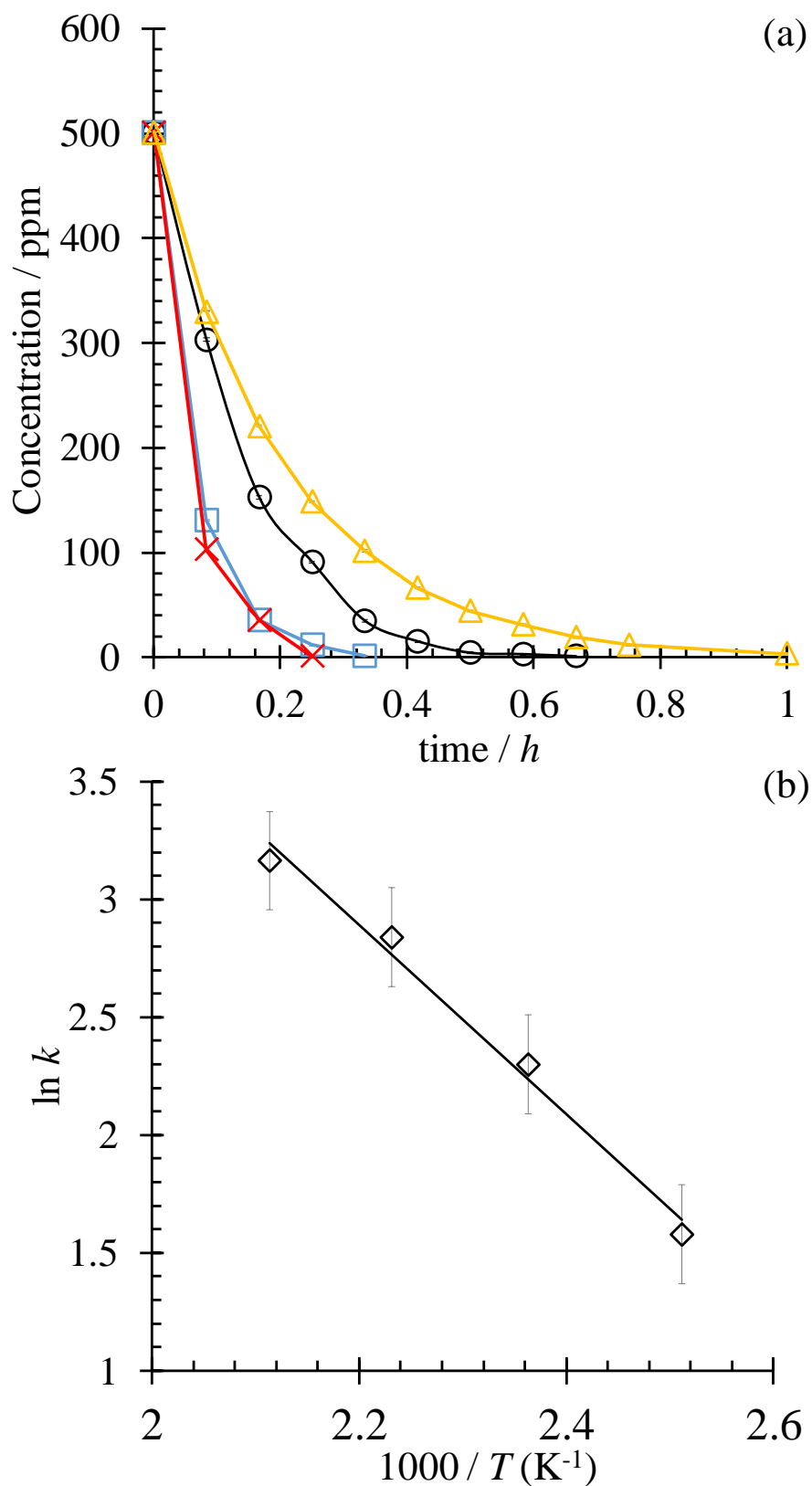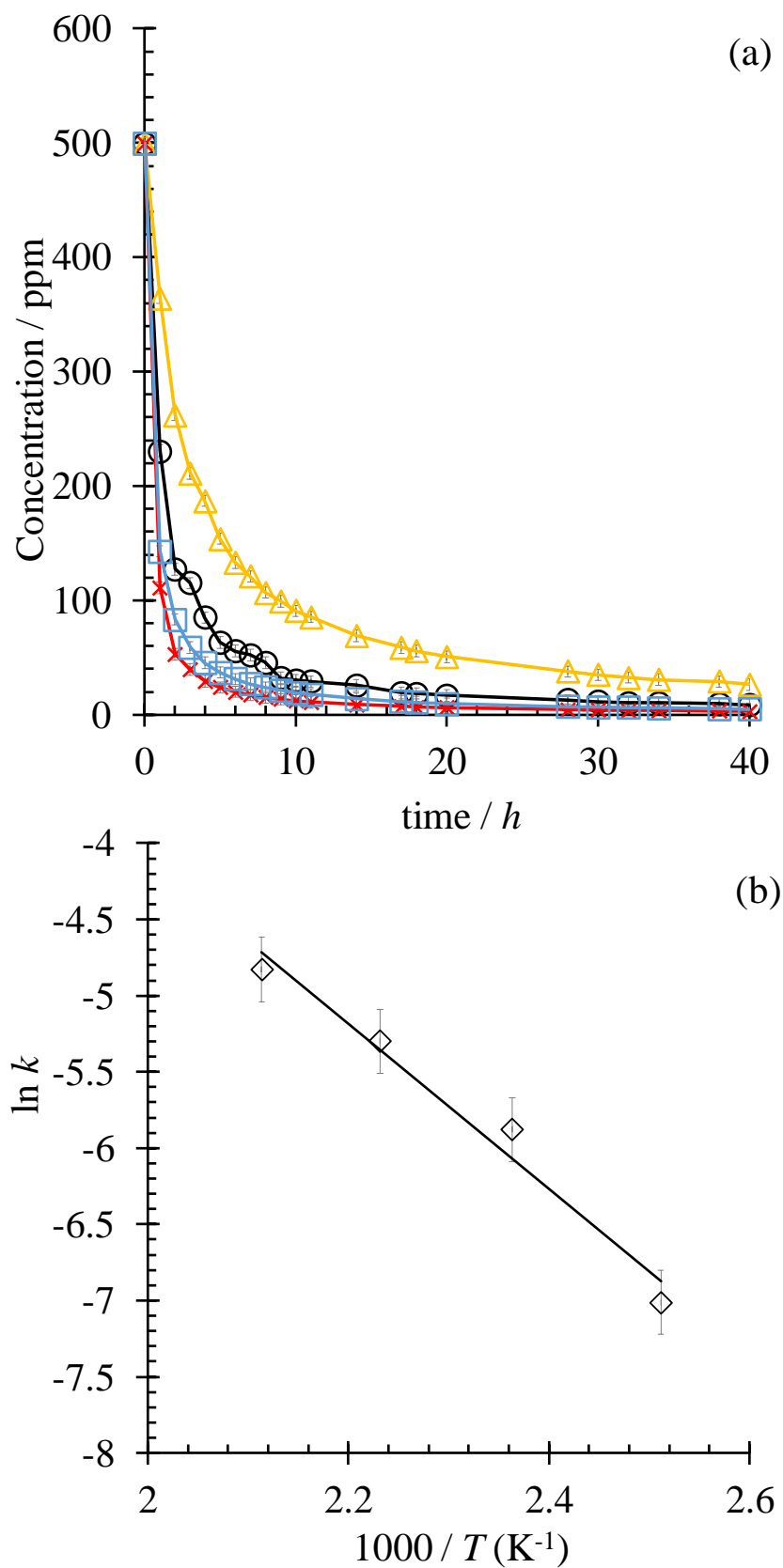
Figure 3-4. (a)The degradation of methylisothiazolinone versus time at 125 to 200 °C and (b) the corresponding Arrhenius plot. △, 125 °C; ☉, 150 °C; ☐, 175 °C; ✕, 200 °C.

51

Table 3-3: The initial reaction parameters and maximum concentration of H_2S during the decomposition of methylisothiazolinone from 125 to 200 °C.

T / °C	pH	$10^3 \cdot x(H_2S)$	$10^3 \cdot k_{obs}$ / h^{-1}	R^2	$t_{1/2}$ / h
125	7.0	1.01	0.94 ± 0.02	0.98	2.22
150	7.2	1.21	2.85 ± 0.04	0.99	0.71
175	7.1	1.11	5.21 ± 0.02	0.98	0.4
200	7.0	1.43	8.6 ± 0.3	0.96	0.25

The initial concentration of H_2S was zero.

Initially, two molecules of **1** (methylisothiazolinone) can dimerize to form **2**, a 10 member ring containing a disulfide. The resonance form, **3**, can undergo an intermolecular conjugate addition and cyclization to give **4**. Rearrangement will eliminate sulfur to give **5**. In the larger scale
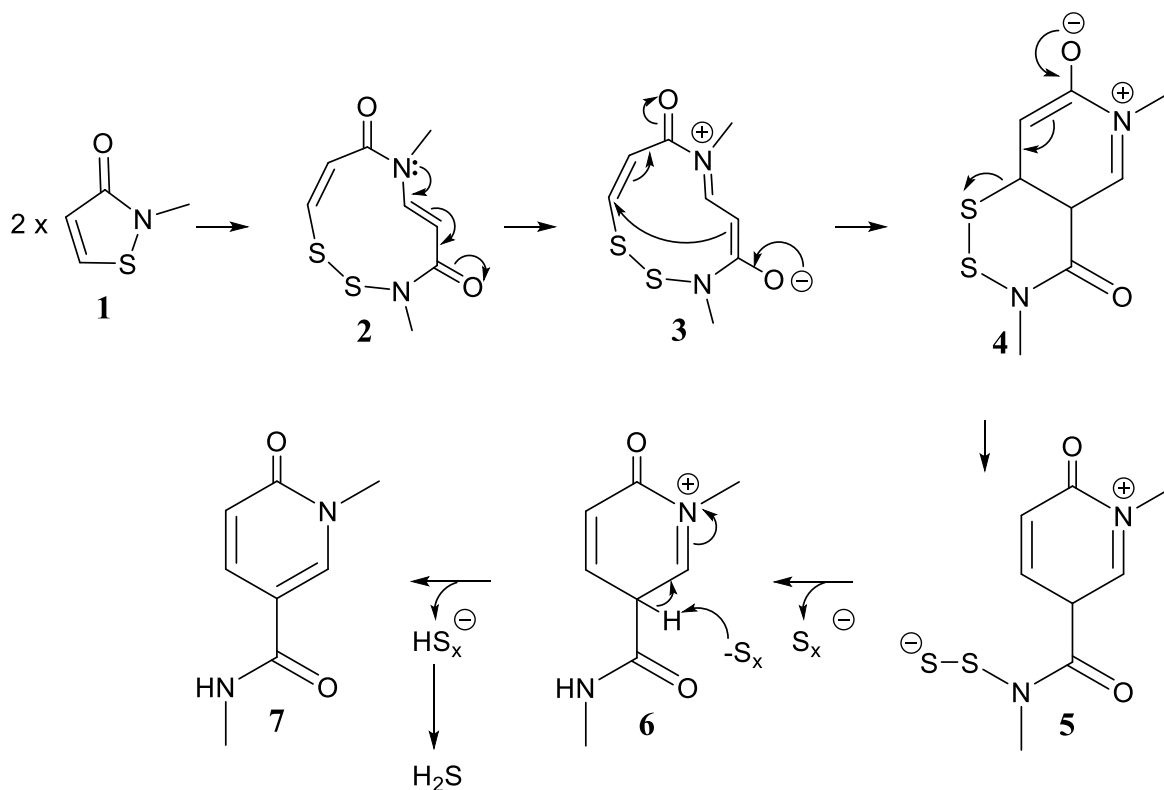
Figure 3-5. Proposed mechanism for decomposition of methylisothiazolinone in aqueous phase at $T = 150$ °C and $p = 140$ bar to form N,1-dimethyl-6-oxo-1,6-dihydropyridine-3-carboxamide.

reaction from which **7** was isolated, elemental sulfur and H_2S were also found, which agrees with the above mechanism. The highly conjugated system favours deprotonation of **6** to yield **7** as the major decomposition product (N,1-dimethyl-6-oxo-1,6-dihydropyridine-3-carboxamide).

Methylisothiazolinone decomposition was also studied under various initial reaction conditions similar to the previous experiments reported above for dazomet (see Table 3-4). When decomposing methylisothiazolinone in the presence of H_2S (205 and 2850 ppmv) an increased rate of H_2S formation was observed. This could possibly be explained by H_2S reacting with intermediate **4,** shown in Figure 3-5, thus enhancing the formation of the hydropolysulfide, and therefore increased H_2S formation. If the decomposition mechanism involves a sulfide in the rate determining step, we should have observed additional intermediates. Isolating intermediates in a high-pressure H_2S system is challenging without increasing H_2S concentrations beyond our practical reaction conditions.

Table 3-4: The initial reaction conditions and H_2S formation constants.

Initial condition modified	k'_{H_2S} / h^{-1}	R^2
Normal condition*	0.059 ± 0.002	0.94
205 ppm H_2S	0.079 ± 0.002	0.97
2850 ppm H_2S	0.13 ± 0.01	0.74
1 M NaCl	0.046 ± 0.002	0.92
2 M NaCl	0.0327 ± 0.002	0.95
3 M NaCl	0.0173 ± 0.001	0.92
pH = 1.15	0.083 ± 0.003	0.96
pH = 2.18	0.072 ± 0.002	0.97
p = 80 bar	0.052 ± 0.003	0.84
p = 200 bar	0.059 ± 0.003	0.87

*Normal conditions are considered T = 150 °C, p = 140 bar, pH $\approx$ 7, 0 M NaCl. If not stated the initial concentration of H_2S was zero.

Again, pressure had no effect on the H_2S being generated, suggesting the reaction occurs in the aqueous phase. Similar behaviour was previously observed for dazomet and our previously studied systems.[4,44,46,59] Unlike our studies of other additives for fracture fluids, this decomposition was not found to be acid catalysed. On the other hand, the rate of H_2S production decreased significantly by adding 1 to 3 M of NaCl. A primary salt effect was ruled out as the rate decreased rather than increasing with increasing ionic strength. To distinguish between an ion-pair and a secondary effect a log k versus $I^{1/2}$ graph was constructed (Figure 3-6). The data exhibits a reasonable fit with a correlation factor of $R^2 = 0.942$. This ionic strength effect suggests that the limiting rate involves the reaction of two anions or two cations. It is important to note that at reservoir conditions, brine concentrations are much higher and the rate of methylisothiazolinone decomposition would likely be slower than reported here.
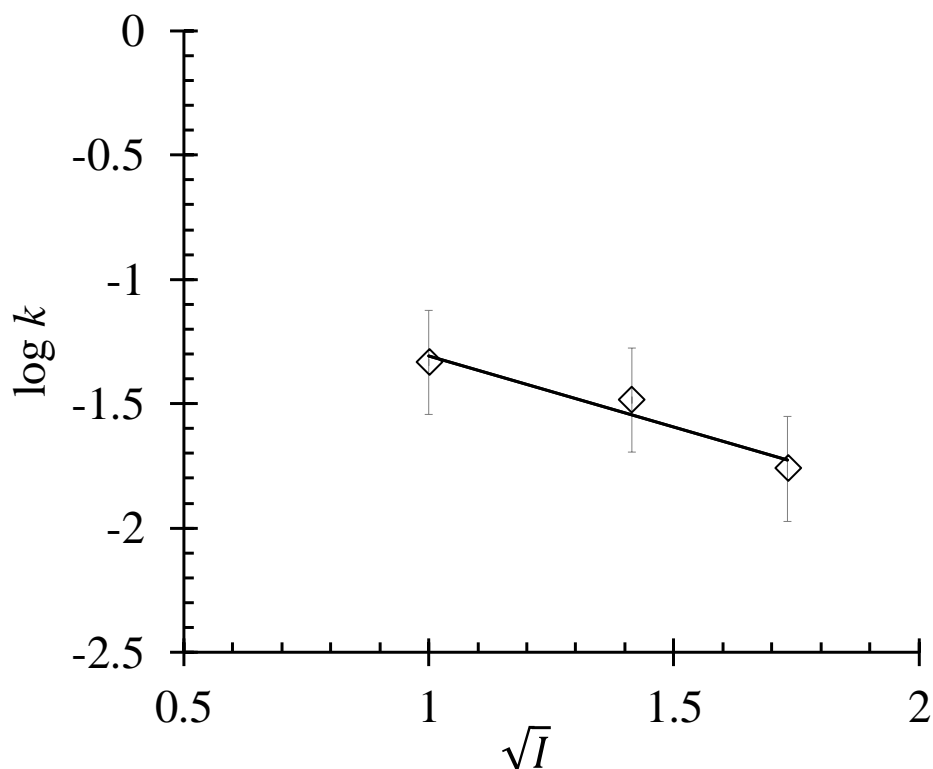
Figure 3-6. Effect of Ionic strength on the reaction rate at pH = 3.1 and p = 140 bar, T = 150 °C.

3.4 Conclusion

In conclusion, we have measured the decomposition of two common sulfur-containing compounds under HTHP conditions and identified the major products. Hydrolysis of dazomet (Tetrahydro-3,5-dimethyl-1,3,5-thiadiazine-2-thione) follows a first order reaction at downhole conditions, by decomposing into CS_2, CH_3NH_2 and CH_2O. CS_2 is then hydrolysed to H_2S, which reacts with CH_2O to produce CH_3SH as the major sulfur species. We noted that formation of CH_3SH was not reported in previous studies of dazomet decomposition. We also found that acidity, pressure and salinity did not affect the rate of H_2S production under the condition studied.

The decomposition of methylisoziolizone was found to follow a second order reaction at downhole conditions, where the only sulfur product was found to be H_2S. A proposed mechanism for H_2S generation was proposed by analysing both gas phase and liquid phase products. The rate of H_2S production from methylisothiazolinone was affected by salinity. In the case, a secondary salt effect was found as the rate decreased with increasing ionic strength.

Hydraulic fracturing fluids can be composed of hundreds of chemical additives, each one selected and tailored for a specific well. Therefore, the results here presented are part of an ongoing effort toward the identification and understanding of the multiple pathways of H_2S formation under high-pressure and high-temperature conditions. The use of sulfur-containing compounds in fracturing fluids is common practice; however, it is important to highlight that the library of these compounds is quite extensive and not all of them are capable of producing H_2S. Souring of a shale reservoir is a complex process that could, in fact, be a combination of multiple chemical reactions involving many chemicals, some of which may not even contain sulfur. Thus, these reactions cannot be solely responsible for the souring of a reservoir, but rather can contribute to the total H_2S observed in delayed souring of sweet wells.

Chapter Four: Downhole chemical degradation of corrosion inhibitors and their role in delayed H$_2$S generation in shale gas

Preface

Based on the results obtained in the study of the decomposition of biocides, the next logical step was to expand this research into other sulfur-containing molecules that could be used as part of the hydraulic fracturing fluid and acid treatments. In this regard, corrosion inhibitors are another group of additives that are often added to fracturing fluid and can be used during the production life of a well. In this study, the previously developed methodology to study high-temperature and high-pressure conditions was applied to investigate the decomposition of 2,5-dimercapto-1,3,4-thiadiazole and 2-amino-1,3,4-thiadiazole. Both compounds were capable of generating H$_2$S under hydraulic fracturing conditions. Additionally, 2-aminobenzothiazole was also tested under the same conditions and did not generate any measurable amount of H$_2$S nor was degradation (hydrolysis) observed at the condition tested. This result can be used for future design of high-temperature and high-pressure corrosion inhibitors.

Manuscript submitted to Journal of Natural Gas Science and Engineering, Elsevier, on August 14, 2019.

4.1 Abstract

Hydraulic fracturing combined with horizontal drilling and acid stimulation has allowed for the development of vast shale gas reserves, an important low-carbon energy source. Chemical additives used in hydraulic fracturing have been studied for various properties; however, little research has been published on the stability of these compounds under downhole conditions. Recent studies have focused on understanding the decomposition rate and products of chemical additives when exposed to laboratory hydraulic fracturing or acid stimulation conditions (high-pressure, high-temperature and variable-pH). Among common additives, corrosion inhibitors are necessary to protect the integrity of the wellbore materials (tubing) and eventually the production facilities. In this study, we report the hydrolysis rates for sulfur-containing corrosion inhibitors (2,5-dimercapto-1,3,4-thiadiazole and 2-amino-1,3,4-thiadiazole), which both decomposed to H_2S and CO_2. Increased ionic strength accelerated the H_2S formation rate for these systems while preloading with H_2S showed no impact when compared to normal conditions. An additional corrosion inhibitor, 2-aminobenzothiazole, did not decompose under the conditions tested. Data presented here provide insight into the degradation mechanisms and perhaps future designs of corrosion inhibitors.

4.2 Introduction

The production of natural gas from unconventional reservoirs has steadily increased together with the world's growing demand for low-carbon energy.[55] Technologies such as horizontal drilling and hydraulic fracturing have made the exploration and production of gas from low permeability reservoirs, such as shale gas reservoirs, economically feasible.[58,76] Together with

58

hydraulic fracturing, acid stimulation is common practice for increasing permeability before, during or after fracturing a well. Acid stimulation is accomplished by fracture acidizing or an acidizing matrix technique. It is important to note that fracturing is achieved hydraulically with or without the use of acids; however, in both cases, the primary objective is to create long open channels from the near-wellbore region deep into the formation. The majority of the fracturing fluid is water, while proppant and chemical additives make up approximately 10% and 0.5-3% respectively.[77] The purposes of these additives are intentional and diverse. This includes surfactants to reduce surface tension, biocides to prevent problematic bacteria, and sometimes gelling agents to increase viscosity and suspend proppant material.[22,78-79]

Corrosion inhibitors are important for protecting surface and subsurface equipment against highly corrosive fluids (general acid attack, embrittlement and stress cracking). If decomposition of the corrosion inhibitor were to happen too fast, the equipment could be unprotected, and the integrity of the metallurgy might be compromised. Corrosion inhibitors are particularly important during an acid stimulation, where the highly acidic fluid can lead to severe general corrosion. Corrosion rates during an acid stimulation are much higher than under normal production conditions. Corrosion inhibitors designed for acid treatments are usually chemically different from the ones used during treatment during normal well operation. Also, acid corrosion inhibitors used during acid stimulation are injected at much higher doses.

In general corrosion inhibitors are classified into four categories: passivating, cathodic, volatile and film forming.[80] Many film forming corrosion inhibitors are amphiphiles by design, with a portion of the molecule being polar to interact with the metal and a lipophilic tail to attract

hydrocarbons, forming a film to further protect the corrosive aqueous media from interacting with the metallurgy. Therefore, the performance of acid film forming corrosion inhibitors is partly determined by its adsorption to the metal surface. Among all the families of corrosion inhibitors, the film forming corrosion inhibitors have shown the best performance under low-pH and high-pressure and high-temperature conditions. Imidazolines and amidoamines are among the most common families of acid corrosion inhibitors (note that these two families of corrosion inhibitors lack lipophilic tails), which seem to inhibit corrosion by adsorption onto the metal surface, thereby inhibiting the interaction between the metal and the producing fluids.

Research has shown that compounds containing nitrogen and sulfur, particularly in heterocyclic structures are good corrosion inhibitors.[81-83] Amidoamines and imidazolines are known corrosion inhibitors that perform relatively well under high-temperature and high-pressure conditions.[84] However, a full study of the decomposition products and rates for both liquid and gas phase are not available in the open literature for these families of compounds. Thiadiazoles such as 2,5-dimercapto-1,3,4-thiadiazole (DMTD) and 2-amino-1,3,4-thiadiazole (ATD) are effective corrosion inhibitors. [80,85,89] 2-Aminobenzothiazole (ABT) is also an effective corrosion inhibitor, especially under low pH environments where the protonated amine may enhance inhibition.[90,91] The ability to inhibit corrosion is related to the cyclic structure and the functional groups containing heteroatoms which act as centers for adsorption.[84-87] These corrosion inhibitors can be exposed to a wide variety of downhole conditions. Variations in shale formation depth will impact the temperature and pressures to which these corrosion inhibitors are exposed (typically $T < 250°C$ and $p < 300$ bar).

In recent years, the decomposition of certain chemical additives under high-temperature and high-pressure conditions has been reported; however, the fate of corrosion inhibitors under actual well conditions remains uncertain.[11,49,50,77] In most cases, the gas phase analysis of these experiments are overlooked or have not been reported. Moreover, the focus of these studies was to observe the variation of by-products in the liquid phase, because, if left untreated, aqueous products can contaminate ground water when returned to the surface as part of the flowback or produced water.

Detection of highly toxic sour gas, hydrogen sulfide (H_2S), in production fluids believed to be sweet, has brought into question the nature of chemical additives being used and whether H_2S observed in these circumstances is a by-product of additive decomposition at downhole conditions. Chemical additives can react under downhole conditions *via* a thermochemical sulfate reduction reaction (TSR) producing H_2S.[44,46] Multiple chemicals have been evaluated under downhole conditions; for example, SDS was found to undergo rapid hydrolysis to form 1-dodecanol and bisulfate.[44,46] Under high-temperature and high-pressure, bisulfate will undergo TSR to produce H_2S. Our research group has also shown how sulfur-containing biocides can hydrolyze or decompose to produce not only H_2S but also CS_2, CH_3SH and elemental sulfur. In this study, we investigate the decomposition products and kinetics of H_2S production of two sulfur-containing corrosion inhibitors (2,5-dimercapto-1,3,4-thiadiazole and 2-amino-1,3,4-thiadiazole) under high-temperature and high-pressure conditions. We also investigated the effect of initial H_2S concentration and ionic strength towards the H_2S formation rate. The mechanisms by which these compounds decompose to generate H_2S is also proposed.

4.3 Result and Discussion

4.3.1 H₂S evolution and hydrolysis kinetics of 2-amino-1,3,4-thiadiazole (ATD)

When monitoring the ATD hydrolysis in the gas phase under acidic conditions (pH = 3.1-3.2), the only sulfur species observed was H_2S (see Figure 4-1). The rate of H_2S production is rapid and remains relativity linear over the first 5 hours, generating approximately 50 % of the total H_2S observed throughout the experiment. The remaining H_2S evolution occurred over 15 hours at a significantly slower rate until all the starting material has decomposed after 20 hours. Thus, multiple rates for H_2S formation could be calculated. If initial formation rate is the objective, the importance of the sampling rate for studies during high-pressure and high-temperature reactions is clearly highlighted here. However, for the purpose of this study, the data was fitted over the total experimental time and the overall rates are reported.
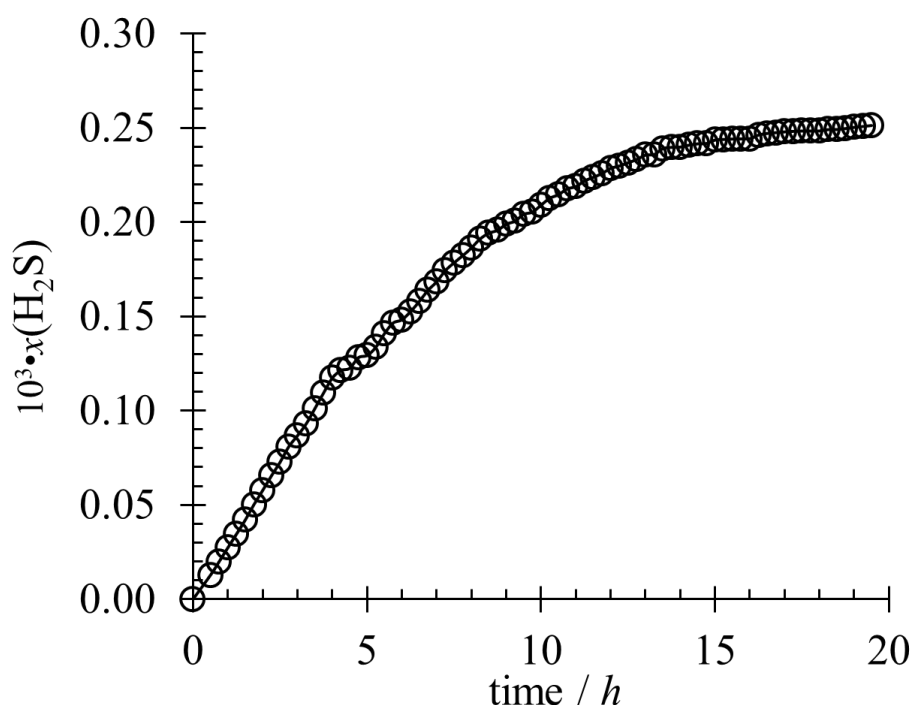
Figure 4-1. Mole fraction of H_2S in the gas phase from hydrolysis of 2,5-dimercapto-1,3,4-thiadiazole (ATD) at pH =3.0, T = 150 °C and p = 143 bar, sampling every 15 min.

Analysis of the gas phase showed H_2S and CO_2 (Equation 4-1) as the major products for hydrolysis of ATD, whereby

$$2\ C_2H_2N_3S + 8\ H_2O \rightarrow 2\ H_2S + 4\ CO_2 + N_2H_4 + 4\ NH_3 \qquad (4\text{-}1)$$

$$2\ N_2H_4 \rightarrow 2\ H_2 + N_2 \qquad (4\text{-}2)$$
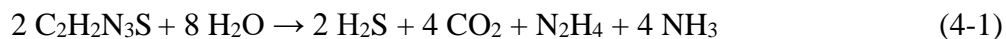
and hydrazine being the most likely nitrogen by-product. Hydrazine will then rapidly decompose to ammonia, nitrogen and hydrogen. No organic nitrogen compounds were detected by GC/MS, and ammonia was detected by cation ion-chromatography but not quantified. Due to N_2 being the bulk of the gas mixture, quantification of the N_2 produced was not possible. It should be noted that these experiments were all performed under aqueous conditions and thermal decomposition cannot be differentiated from hydrolysis reactions. For the purpose of this discussion, decomposition and hydrolysis are used interchangeably.

In the liquid phase, we followed the hydrolysis of ATD (see Figure 4-2a) and we found the overall reaction rate to be first order with respect to ATD concentration (see Equation 4-3)

$$\text{Rate} = -\frac{d[C_2H_2N_3S]}{dt} = \frac{d[H_2S]}{dt} = k[C_2H_2N_3S]^1 \qquad (4\text{-}3)$$

All rates were determined using linear least squared regression of the first order integrated rate law equation, where zero and second order plots were not as linear. Using the rate constants at the four temperatures, an Arrhenius plot was constructed (Figure 4-2b), and the activation energy was found to be $E_a = 52.8 \pm 2.2$ kJ mol^{-1} ($R^2 = 0.95$) through least-squares regression. For

each temperature, the cumulative measurements of total H_2S and total CO_2 generated are reported in Table 4-1. The reaction products for all temperatures showed a 1:2 ratio of H_2S to CO_2, supported by the reaction shown in Equation 4-1.

Table 4-1: The initial reaction parameters of ATD hydrolysis at various temperatures and the total moles of products and the kinetic rates.

T / °C	pH	$10^4 \cdot H_2S$ / mol	$10^4 \cdot CO_2$ / mol	k_{ATD}* / h^{-1}	$t_{1/2}$ / h
125	3.1	1.5	3.2	0.6 ± 0.2	1.16
150	3.2	2.6	5.3	1.2 ± 0.1	0.58
175	3.1	2.7	5.5	2.5 ± 0.1	0.28
200	3.2	2.7	5.6	8.3 ± 0.1	0.09

*Rate of hydrolysis of ATD, all the fitted values had an $R^2 \geq 0.92$. The initial concentration of H_2S and CO_2 was zero.
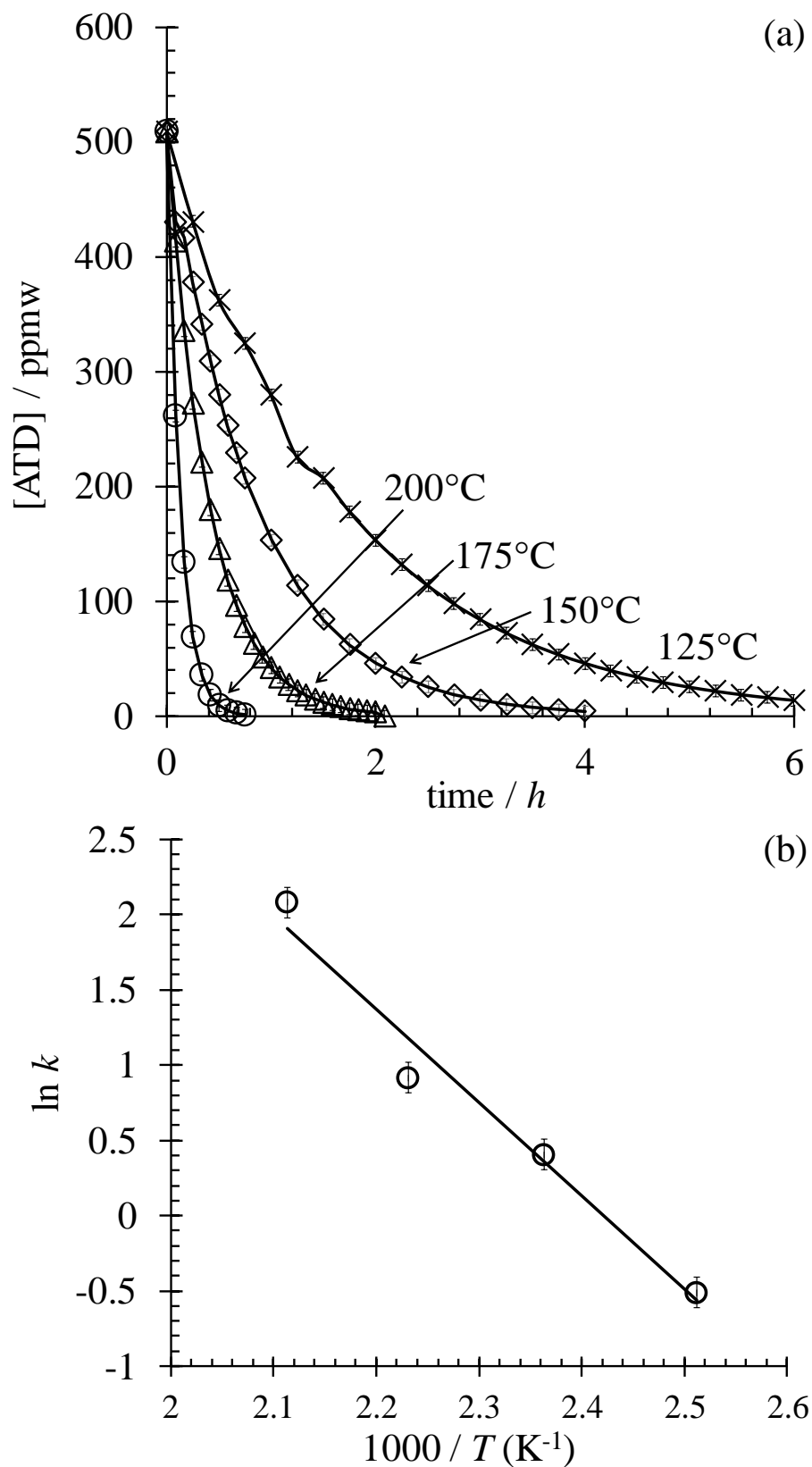
Figure 4-2. (a)The degradation of ATD versus time at 125 to 200 °C and (b) the corresponding Arrhenius plot.

Due to the variability in downhole conditions at which corrosion inhibitors can be used, hydrolysis of ATD was explored at variable pH, salinity and initial amounts of H_2S. The parameters tested and the corresponding rates of H_2S are listed in Table 4-2. The rate of H_2S production remained unchanged under two different loadings of initial presence of H_2S, which implies that the hydrolysis does not involve H_2S, like a typical TSR mechanism would. ATD had a slower rate of H_2S production at pH = 7.2 compared to pH = 3.1. One explanation is that hydrolysis occurs at a faster rate under acidic conditions due to the molecule being protonated at the pendant amino group. When exposed to high saline environments, the rate of H_2S production was accelerated indicating a primary salt effect. When constructing a graph of log k_{H_2S} vs $I^{1/2}$, a small but positive slope was observed ($R^2 = 0.91$); therefore, the limiting rate of reaction involves ions holding opposite charges and an increase in the reaction rate is observed when the Debye length or electrostatic shielding of the reactants is decreased (See Figure 4-3).

Table 4-2: The initial reaction parameters and rates of H_2S formation ($k_{ATD \to H_2S}$ at $T = 150$ °C and $p = 143$ bar).

Parameter modified	$k_{ATD \to H_2S}$ / h^{-1}
Normal condition*	0.09 ± 0.02
205 ppm H_2S	0.09 ± 0.01
2850 ppm H_2S	0.10 ± 0.02
1 M NaCl	0.19 ± 0.01
2 M NaCl	0.19 ± 0.01
3 M NaCl	0.22 ± 0.03
4 M NaCl	0.23 ± 0.05
pH = 7.18	0.04 ± 0.02

*Normal conditions are considered $T = 150$ °C, $p = 140$ bar, pH ≈ 3.0, 0 M NaCl
** $k_{ATD \to H_2S}$ corresponds to the formation rate of H_2S from ATD, all the fitted values had an R^2 ≥ 0.90. If not stated the initial concentration of H_2S was zero.
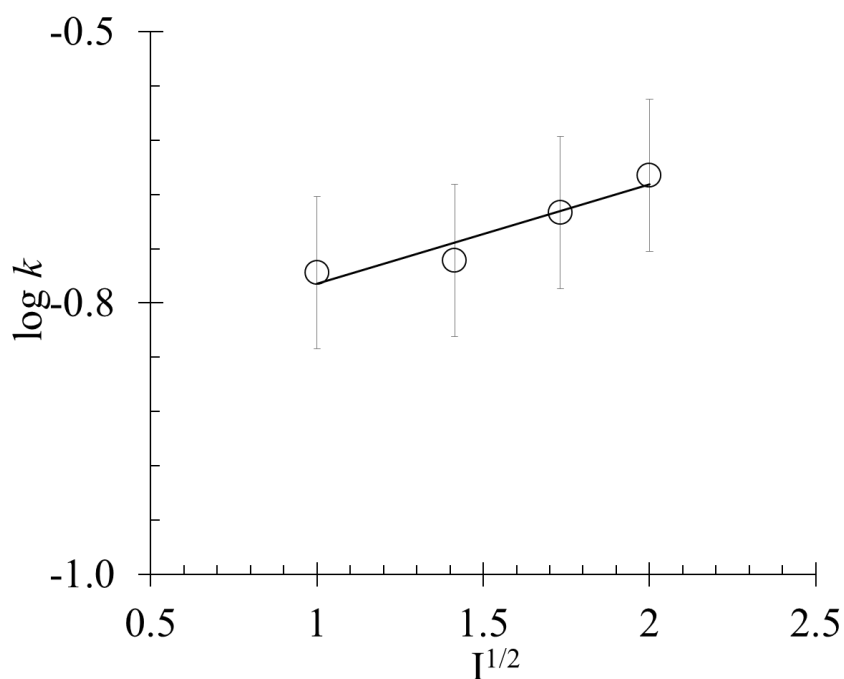
Figure 4-3. Effect of the ionic strength on the reaction rate at pH = 3.1, T = 150 °C, and p = 143 bar.

Reservoir environments are known to be highly saline, which could affect the H_2S evolution from hydrolysis of ATD when the fracking fluid mixes with the reservoir fluids. Gradient concentration effects, as well as adsorption/desorption processes by ATD and H_2S, could also affect the overall H_2S observed at the surface over time. The rate of H_2S formation was not pressure dependent, agreeing with previous degradation mechanisms studied by our group and various other researchers; *i.e.*, the reactions are not occurring in the gas phase. [26,28,33]

4.3.2 Kinetics and H₂S evolution of 2,5-dimercapto-1,3,4-thiadiazole (DMTD)

DMTD at downhole conditions in acidic media also was found to decompose to H_2S and CO_2 (Equation 4-4). Once again, the nitrogen atoms initially form hydrazine, but most likely react rapidly to form N_2 and NH_4^+. Each mole of DMTD can theoretically produce 3 moles of H_2S and 2 moles of CO_2. Our results show that the final mole ratio of the products, H_2S and CO_2, are 1:1 within the experimental error (see Table 4-3). Note that some H_2S can disproportionate to elemental sulfur and other sulfur-oxy species at these conditions.

$$C_2H_2N_2S_3 + 4\ H_2O \rightarrow 3\ H_2S + 2\ CO_2 + N_2H_2 \qquad\qquad (4\text{-}4)$$
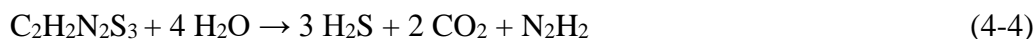
To study the kinetics of this reaction, we followed the concentration of DMTD over time in the liquid phase. The hydrolysis of DMTD was found to follow a first order reaction rate with respect to DMTD concentration thorough comparison of integrated rate law plots. Following a similar procedure as described with ATD, we constructed an Arrhenius plot and found an activation energy of 65.2 ± 1.2 kJ mol⁻¹ (see Figure 4-4).

Table 4-3: The initial reaction parameters and product concentration for hydrolysis of 2,5-Dimercapto-1,3,4-thiadiazole (DMTD) at various temperatures.

T / °C	pH	$10^4 \cdot H_2S$ / mol	$10^4 \cdot CO_2$ / mol	k_{DMTD}* / h⁻¹	$t_{1/2}$ / h
125	3.1	2.10	3.01	0.012 ± 0.002	55.9
150	3.0	2.93	3.28	0.056 ± 0.001	12.4
175	3.0	3.10	3.14	0.125 ± 0.001	5.56
200	3.2	3.21	2.94	0.301 ± 0.001	2.31

*Rate of hydrolysis of DMTD, all the fitted values had an $R^2 \geq 0.95$. The initial concentration of H_2S and CO_2 was zero.
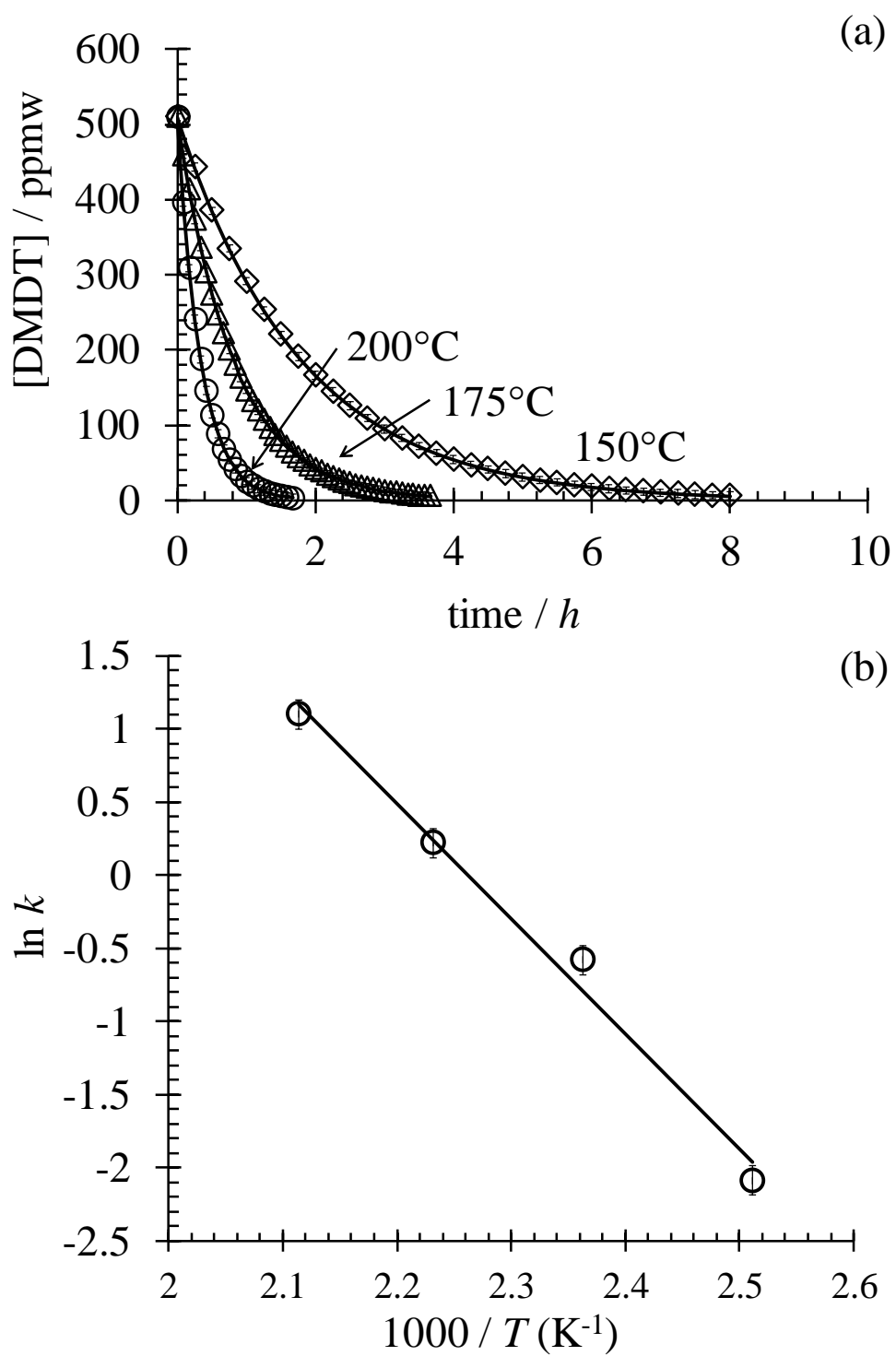
Figure 4-4. (a) The degradation of DMTD versus time at 150 to 200 °C and (b) the corresponding Arrhenius plot. Note that the 125°C data was not shown in Figure 4(a) for clarity.

We evaluated the impact of the different chemical environments at downhole conditions to which DMTD could be exposed. Again, we evaluated variable salinity, pH, pressure and initial H_2S loading on the rate of H_2S production (Table 4-4). The initial presence of H_2S and variable pressure did not play any significant role in the rate of formation of H_2S. The rate of formation of H_2S increased with increasing ionic strength in acidic media (see Figure 4-5). Therefore, higher rates could be expected during an acid stimulation when exposed to saline conditions. Although the results presented here show that this hydrolysis mechanism could contribute to souring, the total H_2S generated was very small compared to previous chemical additives.[4,44,46] As such, hydrolysis of DMTD will likely not significantly influence the total H_2S observed at the surface.
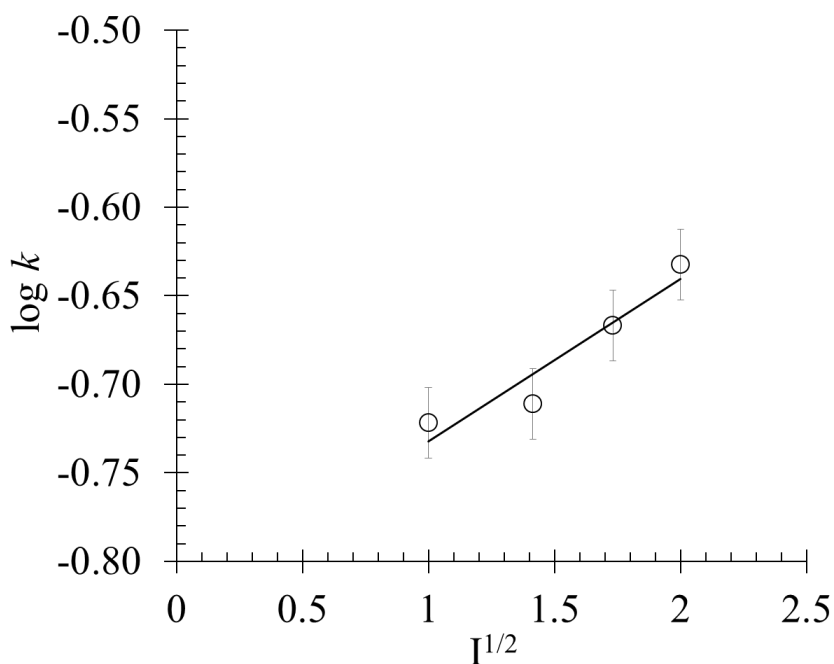
Figure 4-5. Effect of the ionic strength on the reaction rate at pH = 3.0, T =150 °C, and p = 143 bar for the formation rate of H_2S.

Table 4-4: The initial reaction parameters and rates of H_2S formation at ($k_{DMDT \to H_2S}$ at $T = 150$ °C and $p = 143$ bar for DMDT).

Parameter modified	$k_{DMDT \to H_2S}$ / h^{-1}
Normal condition*	0.17 ± 0.01
205 ppm H_2S	0.19 ± 0.02
2850 ppm H_2S	0.17 ± 0.01
1 M NaCl	0.17 ± 0.01
2 M NaCl	0.20 ± 0.01
3 M NaCl	0.37 ± 0.01
4 M NaCl	0.52 ± 0.01
pH = 7.18	0.13 ± 0.01

*Normal conditions are considered $T = 150$ °C, $p = 140$ bar, pH ≈ 3.0, 0 M NaCl
** $k_{DMDT \to H_2S}$ corresponds to the formation rate of H_2S from DMDT, all the fitted values had an $R^2 \geq 0.90$. If not stated the initial concentration of H_2S was zero.

4.3.2.1 Aminobenzothiazole

When testing 2-aminobenzothiazole no H_2S was generated. In fact, almost no degradation was observed when tested under the similar conditions of ATD and DMDT. This is an important finding as this compound can sustain our lab generated hydraulic fracturing conditions with almost no chemical modification (hydrolysis) and minimum thermal decomposition. In fact, crystallographic quality crystals were obtain from our autoclave experiments after 7 days at high-temperature conditions.

4.4 Conclusion

The results presented here showed that both ATD and DMTD slowly decompose and generate H_2S under various downhole conditions, whereas 2-aminobenzothiazole was not found to decompose. Hydrolysis for both ATD and DMTD compounds was found to be first order and the activation energies have been reported. In all cases, no significant amounts of other sulfur compounds were observed in the gas or liquid phase during the reactions. Although H_2S was the

only sulfur species detected, disproportionation to a variety of other sulfur species is possible over time depending on temperature and pH (specifically oxosulfur ions). As such, the reported H_2S formation rates in the gas phase over the course of the hydrolysis reactions (20 to 25 hours) are considered kinetic products. Given sufficient time, disproportionation products may impact production fluids differently.

We found that ionic strength increases the rate of H_2S formation at the conditions studied here for both corrosion inhibitors. This indicates that in both cases the rate limiting step involves the reaction of oppositely charged intermediates which is indicative of a hydrolysis reaction. Also, the fact that 2-aminobenzothiazole did not show any degradation under the condition tested shows that this compound can withstand downhole conditions, and can possibly be useful in the future design of high-temperature acid corrosion inhibitors. These results add to our ongoing effort to identify possible pathways of H_2S formation in hot shale reservoirs, where the accumulation of additive degradation rates can be used to anticipate and treat production fluids.

Chapter Five: Downhole kinetics of reactions involving alcohol-based hydraulic fracturing additives with implications in delayed H$_2$S production

Preface

In the effort to better understand the chemistry involved in the delayed souring of shale gas, the sulfur-oxidation of organic additives has been proposed as a possible mechanism. When the oxygen-saturated fracturing fluid enters the production zone in a reservoir, the oxygen present in the fluid will rapidly oxidize the *native* H$_2$S or metal sulfide to elemental sulfur. The produced sulfur can later react with hydrocarbons present in the fluid media, regenerating the H$_2$S over a longer period of time. Methanol is widely used as a chemical additive in hydraulic fracturing applications, and could also be used as a solvent for various applications. In this chapter, sulfur-methanol reactions are discussed under a wide range of downhole conditions. Similar to the previous chapter, the kinetics of the system are also described. In addition, the implications of the ionic strength and acidity on the reaction rates are explored. The results herein further the understanding of the dehydrogenation of fracturing additives by elemental sulfur.

Published as "Marrugo-Hernandez, J. J.; Prinsloo, R.; Sunba, S.; Marriott, R. A. Downhole Kinetics of Reactions Involving Alcohol-Based Hydraulic Fracturing Additives with Implications in Delayed H$_2$S Production. *Energy and Fuels,* **2018**, *32*(4), 4724–4731".

5.1 Abstract

Horizontal drilling in combination with hydraulic fracturing has dramatically changed the energy landscape as it allows for the more efficient extraction of natural gas from less accessible reservoirs. An issue being explored in greater detail is the increase of hydrogen sulfide (H_2S) and mercaptan (C_xH_y-SH) content during the early production from hot shale gas reservoirs (T >100 °C). Hydraulic fracturing technologies rely on the use of chemical additives for modifying the physical and chemical properties of fracturing fluids to drag proppant into the reservoir. Under downhole conditions, *native* H_2S or metal sulfides can be partially oxidized by dissolved oxygen or other aqueous species, thus producing elemental sulfur. Over time, this elemental sulfur can slowly oxidize the chemical additives, thus regenerating H_2S and other organosulfur species. In this work, we focus on the reaction kinetics of sulfur and alcohol reaction under downhole conditions. Rates and reactions are presented and discussed as an alternative mechanism for the delayed production of mercaptans and H_2S.

5.2 Introduction

The world's desire for energy has motivated industry to look for and extract natural gas resources from unconventional locations, such as shale formations. While the expansion rate of shale exploration has decreased in recent years, it is inevitable that the industry will need to explore more challenging formations to meet the world's energy demands. Hydraulic fracturing (HF) offers many advantages for meeting this demand; however, some questions have arisen regarding hydraulic fracturing technologies. Apart from low overall recovery and environmental concerns, the increase in hydrogen sulfide (H_2S) content in the production fluids from hot (deep) shale gas reservoirs ($T > 100$ °C) has been a recent focus of our research.

A variety of chemical additives are used in modern fracturing applications where each chemical component of the additives has an intended purpose. For instance, acids can be used to partially dissolve minerals, while biocides eliminate bacteria, and surfactants reduce surface tension and improve fluid recovery.[12,58,78] Alcohols are frequently used chemicals for HF applications as reported in FracFocus.[12] In particular, methanol has been reported in 76.5% of the wells contained in the database.[92] Alcohols have physicochemical properties that allow them to act as winterizing agents, solvents for corrosion-scale inhibitors and friction reducers.[92,93] Alcohol-based mixtures (more commonly known as water-free solutions or gelled methanol) can be used as an alternative fluid when reservoirs either have a high-clay content with low-permeability and minimal load fluid recovery or low-bottomhole pressures.[94-96]

Compounds functionalised with alcohol groups are highly reactive chemicals in thermochemical sulfate reduction (TSR) reactions, in regard to total H_2S production and thermal decomposition rates.[42] TSR reactions are known to affect petroleum composition through oxidation and thermal cracking processes and are well documented in several natural petroleum systems across the globe.[34,97]

Previously, it was shown that a commonly used surfactant for HF application (Sodium Dodecyl Sulphate, SLS) could rapidly undergo hydrolysis, thus producing 1-dodecanol and sulfate ions. These products under shale reservoir conditions (high-pressure and -temperature) can produce H_2S *via* the TSR reaction route through a slow oxidation of hydrocarbon species.[4,58,98] These findings provided experimental evidence of a possible mechanism, where TSR reactions with chemicals not *native* to the reservoir could be responsible for the H_2S and sulfur related

compounds in the production streams. As it was shown in our previous research,[44,46,98] these reactions occur through an elemental sulfur intermediate, which upon generation, has the capability of dehydrogenating hydrocarbons contained in the HF fluid.

It has also been suggested that the water used for HF is saturated with oxygen at atmospheric pressure; therefore, the dissolved oxygen can react with the native H_2S or metal sulfides to form S_8:

$$O_2 + 2\ H_2S \rightarrow 1/4\ S_8 + 2\ H_2O \qquad (5\text{-}1)$$
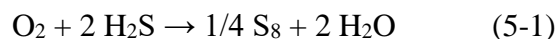
The S_8 produced *via* reaction 5-1 could temporarily sequester the *native* or TSR produced H_2S and re-release it later upon reacting with the chemical additives or hydrocarbons from the reservoir. This can result in a delay before an increased H_2S concentration by up to 6 months, *i.e.*, an H_2S roll up effect. S_8 has limited solubility in water; therefore, the sulfur produced likely precipitates out of the water phase and is left deposited downhole with the proppant.

It is important to highlight that a delayed production of H_2S can cause numerous and problematic operational issues for the gas processing plants where amine units may not have been optimized for H_2S removal during the design stage. Furthermore, continuous variation of H_2S concentration in the production streams (10 to 500 ppm) is not only difficult to treat appropriately but also complex to predict.

Downhole conditions such as temperature and pressure tend to vary greatly between shale reservoirs.[11,77] For instance, deeper shales such as Haynesville with depths from 3.2 to 4.2 km, downhole temperature could reach 200 °C with pressures up to 690 bar.[11,77] Comparatively, in shallow shales such as the Marcellus (1.2 to 2.6 Km well depths) temperature can range from 40 to 125 °C with pressures up to 414 bar.

To evaluate the impact of downhole conditions and chemical stressors in the production of H_2S and organosulfur species, the kinetics and final/equilibrium products of methanol-sulfur reaction in saturated aqueous conditions were systematically evaluated. The most relevant physicochemical parameters under downhole conditions, *i.e.* temperature, pressure, pH and salinity, were monitored. The reference conditions chosen for comparison purposes were 150 °C, 110.3 bar, pH 7 and 0 M NaCl. Methanol and sulfur species concentrations were measured in the liquid and gas phase over time as the chemical and physical parameters were varied. The following parameters were tested: 100, 125, 150 and 175 °C; 5.52, 110.3 and 172.0 bar; pH 7.14, 6.5, 6.0, 5.3, 4.6, 3.9, 3.5, 3.15, 2.4, 2.13, 1.16; 0, 1, 2 and 3 M $[NaCl]_{aq}$. The results from the aqueous reaction of sulfur-methanol reactions show that significant quantities of H_2S and organo-sulfur compounds (mainly CH_3SH, CH_3SCH_3, and CH_3SSCH_3) have been found after various reaction times and conditions. Our results show that the formation rate of metastable organosulfur intermediate increases at pH < 4.5.

5.3 Results and discussion

Methanol undergoes a dehydrogenation reaction (partial oxidation) with sulfur producing various amounts of H_2S, CO_2, and organosulfur compounds. This has been identified as the

limiting rate in previous thermal sulfate reduction mechanisms; however, with previous studies the gas phase products have been followed and pH was not buffered.[4] For the buffered experiments studied here, cumulative measurements of (a) total H_2S, (b) total CO_2 and (c) total organosulfur species generated from 10 mL of CH_3OH at $T = 100$ to 150 °C and pH = 1 to 7 are reported in Table 5-1.

Unlike our previous studies, which show a 3:1 H_2S/CO_2 product ratio (Reaction 5-2),

$$CH_3OH + 3\ S + H_2O \rightarrow 3\ H_2S + CO_2 \qquad\qquad (5\text{-}2)$$
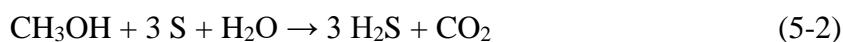
the results for sulfur reaction with methanol show a H_2S/CO_2 ratio closer to unity. This is due to H_2S reaction with methanol to form the organosulfur compounds (thiol and dimethyl sulfides):

$$CH_3OH + H_2S \rightarrow CH_3SH + H_2O \qquad\qquad (5\text{-}3)$$

$$CH_3SH + CH_3OH \rightarrow (CH_3)_2S + H_2O \qquad\qquad (5\text{-}4)$$

$$H_2S + 2\ CH_3OH \rightarrow (CH_3)_2S + 2H_2O \qquad\qquad (5\text{-}5)$$
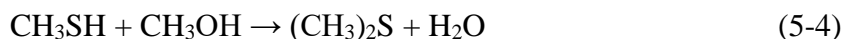
Given enough time, all organosulfides would form H_2S in an aqueous reducing environment.

5.3.1 Methanol decomposition rate and the influence of pH

The instantaneous rate of reaction has been calculated using $CH_3OH(aq)$ the concentration which was followed for 150 hours at various intervals from 1 to 24 hours. An Arrhenius plot was constructed (Figure 5-2), and an activation energy of 48 ± 2 kJ mol^{-1} was found for this reaction through least square regression (reproducibility shown at the 95% confidence interval).

Table 5-1. The initial reaction parameters and final products of methanol (aq) and elemental sulfur at various temperatures at pH = 7 as well as various pH at T = 150 °C.

T / °C	pH	$10^5 \cdot H_2S$ / mol^b	$10^3 \cdot CO_2$ / mol	$10^5 \cdot$ organosulfur species / mol	k_{obs} / h^{-1}	$t_{1/2}$ / h
100	7.0	5.02	6.21	11.21	0.002 ± 0.001	330.07
125	7.0	7.34	6.58	12.24	0.009 ± 0.002	81.55
150	7.0	9.35	10.97	13.76	0.017 ± 0.002	42.01
175	7.0	11.76	13.85	13.24	0.024 ± 0.001	28.76
150	7.0	9.28	9.34	11.45	0.017 ± 0.002	42.01
150	6.5	10.47	10.98	11.29	0.011 ± 0.001	64.78
150	6.0	10.24	9.87	12.35	0.016 ± 0.003	44.43
150	5.3	10.48	10.45*	13.47	0.015 ± 0.001	47.48
150	4.6	11.05	11.74*	14.37	0.014 ± 0.002	48.47
150	3.9	11.57	11.78*	15.1	0.025 ± 0.001	28.06
150	3.5	11.68	12.08*	16.29	0.032 ± 0.002	21.87
150	3.2	11.33	11.21	16.28	0.031 ± 0.001	22.07
150	2.4	11.75	11.41	16.95	0.063 ± 0.003	11.00
150	2.1	11.47	11.25	17.34	0.138 ± 0.003	5.03
150	1.2	11.74	11.98	18.24	0.145 ± 0.002	4.77

*Values were corrected by citric acid phosphate buffer blank. The initial concentration of H_2S and CO_2 was zero.

Experimental kinetic data at various pH resulted in correlation values of $0.87 \leq R^2 \leq 0.99$ matching a linearized pseudo first-order rate with respect to methanol. The overall rate equation was found to be

$$Rate = -\frac{d[CH_3OH]}{dt} = k[CH_3OH]^1[H_3O^+]^{0.33} \qquad (5\text{-}6)$$

The first order reaction with respect to methanol is in agreement with literature on the dehydrogenation of methanol over a wide range of conditions.[99] The rate order for $[H_3O^+]$ was determined to be between zero- and first order at 0.33. The fractional reaction order of 0.33 arises because, under acidic conditions, the reaction rate is pH dependent, whereas, at near neutral pH, the reaction order follows a zero order rate with respect to H_3O^+ (see Figure 5-1).

Several authors have presented results which indicated that pH significantly influences the TSR of hydrocarbons at relatively similar conditions (similar pressures but higher temperatures).[43,97,100] In previous work, we concluded that lowering the pH favours the equilibrium reaction of aqueous oxo-sulfur species and H_2S forming S.[4,44,46] As a result, the steady-state concentration of S will increase at low pH and the instantaneous rate constant is expected to increase with time. In this particular case, we are assuming that the S has already formed inside the reservoir either by shifting chemical equilibrium or by oxidation of H_2S with dissolved oxygen (this oxidation is rapid). In both cases, S under these conditions has the capacity to oxidize the hydrocarbons present in the HF fluid, thus changing the distribution and identities of sulfur species in both liquid and gas phase.

Initially, H_2S could be produced *via* direct oxidation of methanol by S to yield H_2S and CO_2 (reaction 5-2). However, in a shale reservoir, *native* H_2S or metal sulfides are expected to already be present prior to HF, thus, initiating the reactions in a comparable manner. In this case, under acidic conditions, methanol also can be protonated, making it more susceptible to nucleophilic attack by H_2S (reactions 5-4 and 5-5). These ionic reaction schemes are shown in Figure 5-3. Under acidic conditions, Figure 5-1 shows that the rate of methanol hydrolysis

increases as pH decreases. However, it is important to point out that the reaction 5-2 will proceed under both near-neutral and acidic conditions.

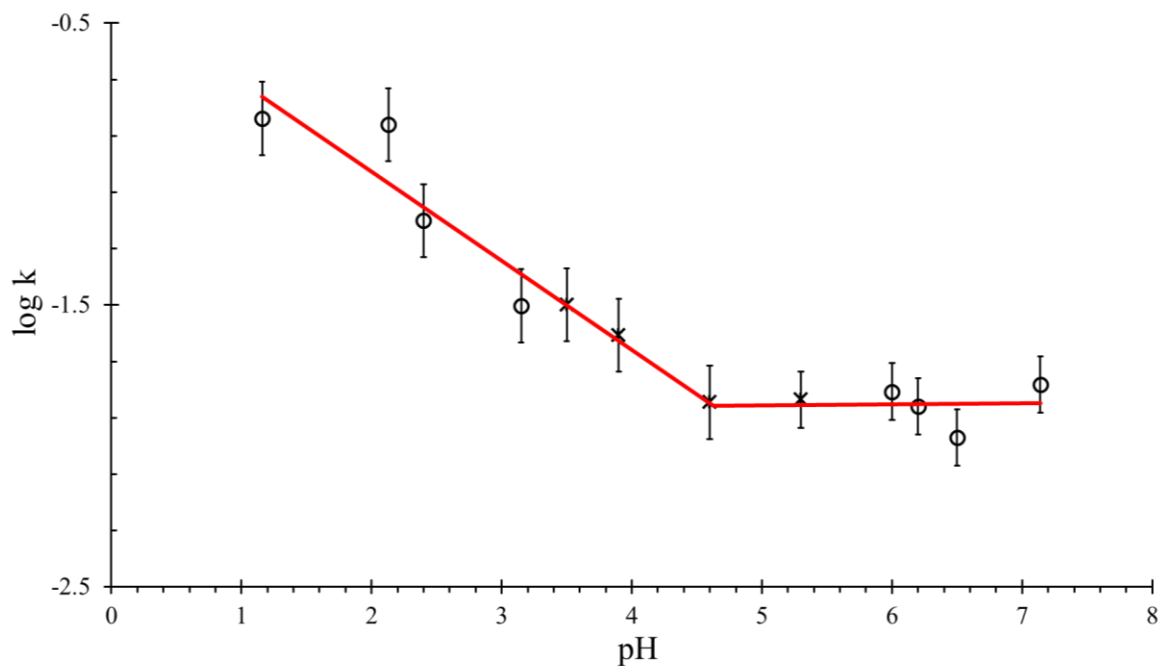**Figure 5-1.** Effect of pH on rate constant of the methanol-sulfur reaction at 150 °C, emphasizing the acid catalysis for pH < 4.6.
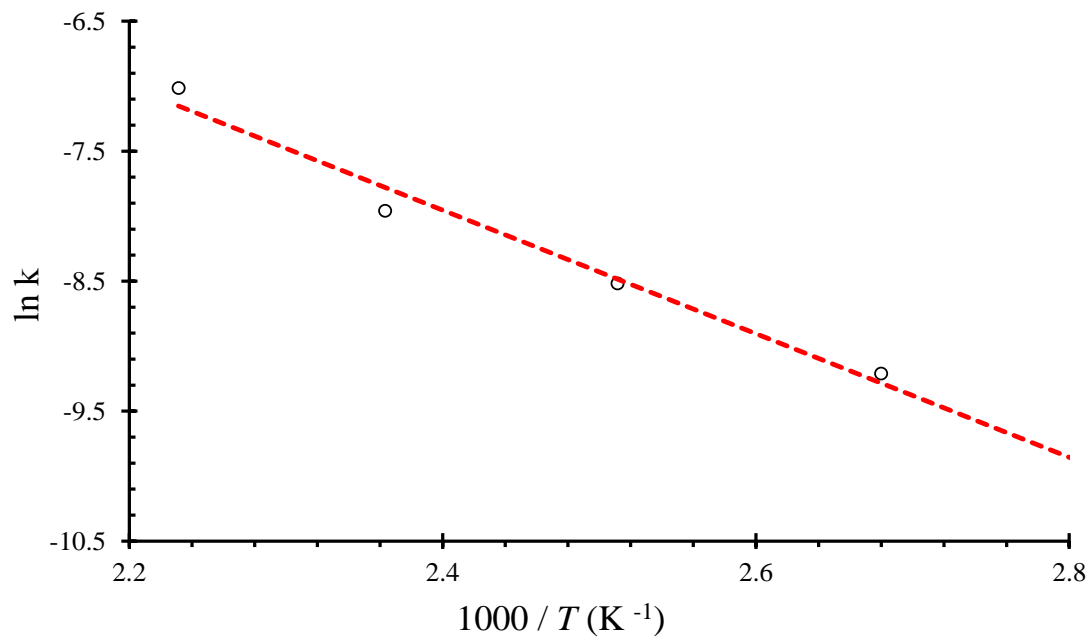

Figure 5-2. Arrhenius plot of reaction constant versus reciprocal temperature for the methanol-sulfur reaction.

Because the protonation of methanol can also form dimethyl ether through the acid catalysed condensation reaction, dimethyl ether could also be an intermediate in producing DMS.[101] However, during our experiments, no dimethyl ether was detected. Small amounts of CS_2, DMDS and DMTS, were also identified by both the SCD during the online sampling and
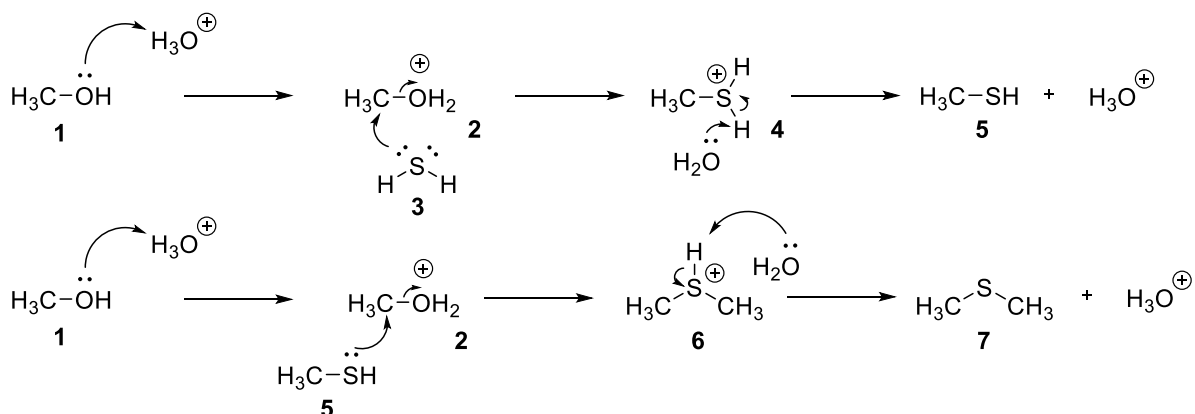

Figure 5-3. Proposed mechanisms for reaction occurring in aqueous phase under acidic conditions (reactions 4 and 5). Initially, methanol **1** can be protonated to form cation intermediate **2**. Nucleophilic attack by H_2S **3** would yield sulfonium **4**. Finally, deprotonation would yield methylmercaptan **5**, and regenerate the hydronium ion. In reaction 2, after protonation of methanol, nucleophilic attack by methylmercaptan **5** would yield intermediate **6**. Deprotonation by water would regenerate the hydronium ion and yield dimethlysulfide **7** as the major product.

through GC-MS from aliquots of the gas phase. Although the presence of these organosulfur compounds was limited in near neutral pH experiments, the concentration increased significantly at lower pH. Additionally, the reaction rates were found to be independent of pressure (see Table 5-2). These results imply that there is no measurable change in volume associated with the formation of the activated complex and that the reaction is within the aqueous phase.[4,46] Similar results were presented by Kahrilas *et al*[22] and concluded by Sumner and Plata[77], where pressure did not have a significant impact in the reaction rate for a variety of reaction chemistry.

Table 5-2. The initial reaction parameters and final products of methanol(aq) and elemental sulfur at various pressures.

| T / °C	pH	$10^5 \cdot$ H$_2$S / mol^b	$10^5 \cdot$CO$_2$ / mol	$10^5 \cdot$Organo sulfur species / mol	p/ bar	k_{obs} / h^{-1}	$t_{\frac{1}{2}}$ / h
150	7.0	9.28	9.34	11.45	110.3	0.017 ± 0.001	42.01
150	7.0	9.38	9.74	11.37	55.2	0.016 ± 0.001	42.79
150	7.0	9.61	11.2	11.89	17.2	0.017 ± 0.002	40.77

k_{obs} calculated by following the methanol decomposition. The initial concentration of H$_2$S and CO$_2$ was zero.

5.3.2 *Influence of pH on H$_2$S formation and Volt-Equivalent-Diagrams (VED)*

Many authors have previously reported a pH influence on reactions similar to TSR. In all cases, much faster reaction rates were measured at pH < 6, allowing the study of these reactions within a reasonable timeframe for laboratory experiments (days to months).[4,43,44,46,102] However, controlling and measuring pH under high-pressure and high-temperature conditions is challenging and often more time-consuming, where little detail is discussed in the literature. Frequently, pH is not measured due to experimental constraints; consequently, the pH is estimated either by a Raman shift or by the use of High-Pressure High-Temperature (HPHT) software.[103,104] The importance of pH on overall reaction rates is highlighted by the wide range of activation energies reported in the literature, where much lower energies are observed in low-pH systems, even without the addition of any catalyst.[4,36] With our experimental setup, pH was controlled by the addition of a phosphate or citrate buffer and pH values were verified throughout the reaction by the use of online liquid phase sampling versus just the evolution of H$_2$S or CO$_2$ gases. In all the experiments, only minor pH changes were observed (±0.2 pH units of the initial pH).

A convenient way to represent sulfur, oxy-sulfur and organosulfur species distribution at equilibrium is by using a Volt-Equivalent Diagram (VED).[4] Sharif-Asl *et al.*[105] previously

discussed the complexity of S-H$_2$O systems as it pertains to pH and temperature effects, in which sulfur species undergo disproportionation to more stable species under high-temperature conditions, and in some cases produces H$_2$S. By using the VEDs, the thermodynamic stability of sulfur species can be compared at high-temperature and various pH by using the volt-equivalent difference between any species. For an example of how a VED is constructed for bisulfate: we first consider the reaction of bisulfate in acidic media to elemental sulfur and water (Equation 5-7)

$$\text{HSO}_4^- + 7\,\text{H}^+ + 6\,\text{e}^- \rightarrow \text{S} + 4\,\text{H}_2\text{O} \tag{5-7}$$
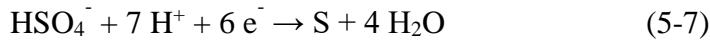
The equilibrium potential, E^e, for reaction 5-7 is

$$E^e = \frac{-\Delta_f G^o}{6F} - \left(\frac{2.303RT}{6F}\right)\log\left(\frac{1}{a_H^7 a_{HSO4^-}}\right) \tag{5-8}$$

Where $\Delta_f G^o$ is the change in standard Gibbs energy, T is the temperature, and a_i is the activity for species i.[4,105] Later the E^e is multiplied by the average oxidation state of sulfur, obtaining the Volt-Equivalent for the HSO$_4^-$. The carbon containing species were calculated using a similar approach with sulfur reacting with methanol to produce the sulfur carbon species. By using the same approach a Volt-equivalent is then calculated for each sulfur species at a specific pH and temperature. Subsequently, a Volt-Equivalent Diagram is constructed by plotting the VED versus average oxidation state of sulfur. Notice that the equilibrium potential is dependent on temperature and pH (a_H^7).

To interpret the VED diagram, we first draw a line connecting two species of interest, and we examine which species lay below, above and on the line connecting these two species. If a third

species is above the line, that species will tend to disproportionate into the other two tied compounds. On the other hand, if the third species lies below the line, the initial two chemicals will tend to react to produce the third. Lastly, if the third species lies on the tie line or very close to it, the third species will be in thermodynamic equilibrium with the other two.

Figure 5-4 shows the sulfur and organosulfur speciation at $T = 150$ °C at pH = 7 (Figure 5-4a) and (Figure 5-4b) at pH = 1. We note that DMS, DMDS, H_2S and HS- are all of the same oxidation rate, with H_2S being the lowest volt-equivalent. This is in agreement with the eventual decomposition of DMS and DMDS to form H_2S.[106] Lines numbered 1 and 2 connect sulfur species observed during the experiments (H_2S, DMS and S_8), and line 3 connecting H_2S with HSO_4^- is shown for reference purposes, as increased reaction rates are often attributed to bisulfate ion catalysis.[41,107] Each line represents a particular equilibrium reaction between the two-species of different oxidation states. Line 1 (S_8-DMS) shows a significant change when moving from pH 7 to 1. As illustrated in Figure 4a the only species with isolated thermodynamic equilibrium observed at neutral pH is CH_3SSCH_3, shown in the middle of the tie line. However, when decreasing the pH (Figure 5-5b), the hydropolysulfide species which were previously located below line 1 at approximately -0.5 volt-equivalents (blue circle), are now in thermodynamic equilibrium. This is in agreement with the light-yellow colour observed when sampling the low-pH solution. It is important to point out that the yellow colour diminishes within seconds of taking the sample, due to rapid decomposition to H_2S and S_8, as it is known that hydropolysulfides are not very stable. In addition, elemental sulfur approaches the H_2S-HSO_4^- line (line 3) when pH = 1. Therefore, at lower pH, elemental sulfur is more thermodynamically favoured by the reaction of H_2S-HSO_4^-. These

results are in agreement with our earlier studies performed at much higher temperatures ($T = 200$ – 250 °C).[44,46,98]

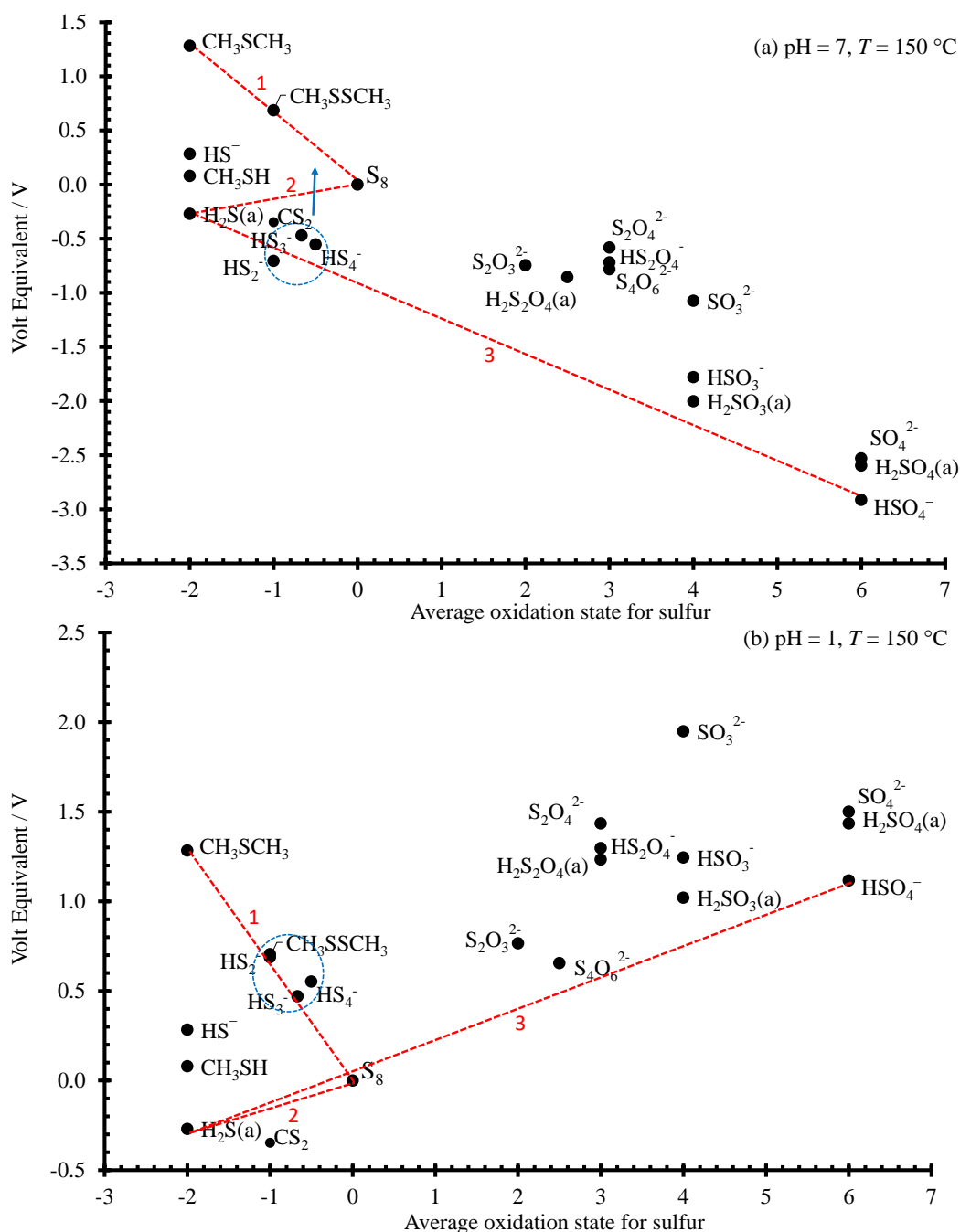**Figure 5-4.** Volt-Equivalent diagrams for the different sulfur species at $T= 150$ °C (a) pH = 7 and (b) pH = 1.

5.3.3 Catalytic effect of H₂S and influence of salt effect

The initiation of a TSR reaction may proceed without initial H_2S, but the reaction mechanism is unclear. Previously, it has been reported that the initial partial pressure of H_2S correlates positively with the rate of a TSR reaction at temperatures much higher than those found in reservoirs ($T > 300$ °C) and the overall rate has been found to be autocatalytic. It is worth pointing out the two major arguments in the literature regarding this effect:

(i) most researchers are interested in the sulfate or bisulfate reduction rates at high-pressure and high-temperature. The system usually has high concentrations of sulfate or bisulfate (depending on the pH of the system); consequently, they would react rapidly with H_2S to produce sulfur as an intermediate. The sulfur generated will later react with a hydrocarbon, *via* a dehydrogenation reaction, producing H_2S and the corresponding olefin. This is applicable to low-pH systems as we have demonstrated using VED's here and in previous publications.[4,46]

(ii) it has also been shown that no measurable TSR rates were obtained at high initial H_2S loading at pH ~ 5. In this scenario, produced H_2S, CO_2 and bisulfate result in lowering the pH of the solution below 3.2 at $T > 300$ °C in an unbuffered system. Therefore, to address the effect of initial H_2S concentration, the pH and H_2S loading should be considered for any particular system.

Initially, we studied H_2S loading in two different buffered systems to study the methanol-sulfur oxidation rates and the effect on reaction rate of H_2S. These experiments are important for establishing baseline reactivity as our hypothesis involves the reaction of dissolved oxygen in the HF-fluid with *native* H_2S. We note that all reservoirs are a reducing environment.

The first two experiments served as our standard conditions ($T = 150$ °C, $p = 140$ bar, pH = 7.1, 0 M NaCl) with loadings of 200 and 1000 ppm of H_2S respectively (Table 5-2). Both concentrations of H_2S had little impact on the rate or products observed in liquid and gas phase samples. At high H_2S loading (1000 ppm) lower methanethiol was observed, thus lowering the organic sulfur value, while the remaining products were within experimental error. When lowering the pH to 2.10 at a high H_2S loading (1000 ppm), the rate and product distribution changed significantly. A much higher amount of methanethiol was generated, approximately double compared to an analogous experiment at low-pH, without the addition of initial H_2S. The decomposition rate for methanol also doubled with respect to the standard conditions. Additionally, low amounts of DMDS and DMTS were detected in this experiment. This suggests that a continued monitoring of wellbore fluids may indicate the change in the average pH within the near wellbore region.

Table 5-2. The initial reaction parameters and final products of methanol (aq) and elemental sulfur while varying the initial H_2S at pH = 2 and 7 ($T = 150$ °C).

T / °C	pH	$10^5 \cdot H_2S$ / mol^b	$10^5 \cdot CO_2$ / mol	$10^5 \cdot$ Organo sulfur species / mol	initial H_2S / ppm	k_{obs} / h^{-1}	$t_{1/2}$ / h
150	7.0	9.4	9.0	11.3	1000	0.020 ± 0.001	43.1
150	7.0	9.3	9.4	11.0	200	0.020 ± 0.001	42.8
150	2.1	11.6	11.2	25.1	1000	0.21 ± 0.02	4.6
150	2.1	11.4	11.9	19.2	200	0.14 ± 0.02	5.0

k_{obs} calculated by following the methanol decomposition, the initial concentration of CO_2 was zero.

Two ionic strength solutions were used at neutral and acidic conditions. As expected the rate at neutral conditions did not change significantly as the intermediates do not involve charged species (oxidation by neutral sulfur only). On the other hand, the rate was decreased by approximately 20% in the case of 2 M NaCl. The salt effect can be categorized into three groups, primary, secondary and ion-pairing. In the case of the sulfur-methanol kinetics, the salt effect is either an ion-pairing or a secondary effect. As the kinetic rate does not follow a primary effect, where rates would increase by changing ionic activities, this effect may be ruled out. A secondary salt effect could be inducing the lower rates; however, secondary salt effects are known to accelerate acid catalysed reactions such as hydrolysis. To further test if the salt effect is indeed a secondary effect, a plot of log k vs $I^{1/2}$ was constructed (Figure 5-5). The data display an excellent fit with a correlation factor of $R^2 = 0.9956$, thus suggesting a secondary salt effect in fact slows down the kinetics in this reaction. The ion-pair formation between the hydropolysulfide and the Na^+ could be an explanation of the decrease in kinetics, where the Na^+ ion would shield the hydropolysulfides, thereby stabilising them and thus rendering them less reactive. However, an ion-pair effect is not considered significant in polar solvents such as water. Nevertheless, this effect could play an important role, despite the polar solvent, because of the physical condition at which the reaction is taking place. The HF applications are performed under a high saline environment where water can have a significant drop in the electric permittivity, thus behaving more as a non-polar solvent which can increase the ion pairing effect. The data also show a good fit to support the ion-pairing effect. When plotting log k and 1/[NaCl] the correlation coefficient was found to be $R^2 = 0.9279$. Although the R^2 is not as strong as in the secondary effect it is significant; therefore the ion-pair effect should not be ruled out. With either explanation, the results show that the

methanol decomposition at low-pH is dependent on ionic strength, as opposed to the production

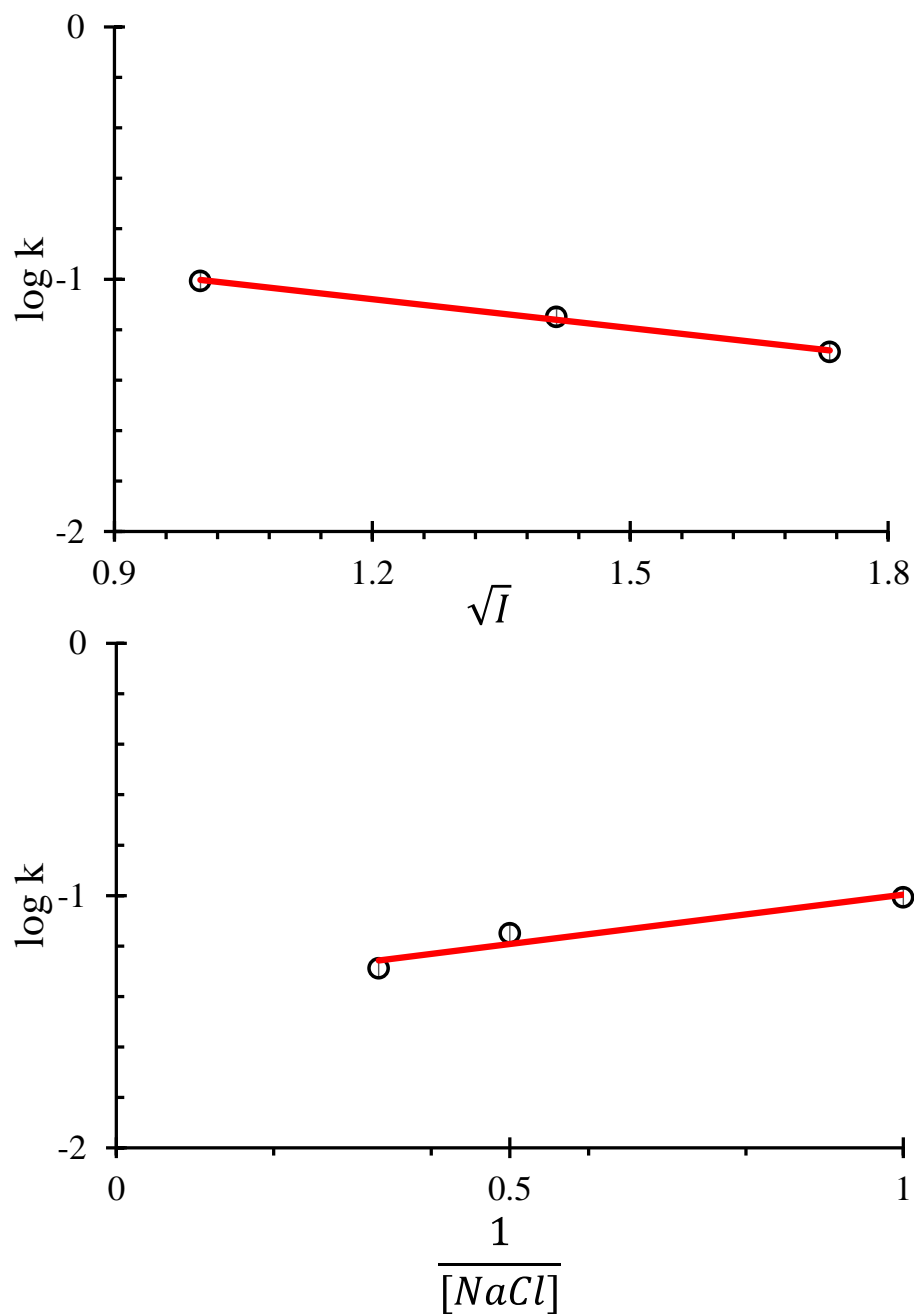of H_2S, *i.e.*, long-lived organosulfur intermediates exist at low-pH.

Figure 5-5. Effect of ionic strength on the reaction rates at pH = 2, Secondary effect (upper graph) and Ion pair effect (lower graph).

5.4 Conclusion

In conclusion, the results presented here support that the methanol, present in a HF fluid, is capable of reacting to generate H_2S, DMS and DMDS under hydrothermal conditions when in contact with elemental sulfur. To further understand the increases in H_2S level during shale production, the formation of hydropolysulfides could be important in understanding the delayed H_2S appearance and the organosulfur species found in production streams during the following months after well completion/stimulation. At low-pH, these organosulfur species are generated at increased rates.

We also note that with un-degassed HF fluid prior to the application, oxygen is introduced in a reducing environment which can oxidize H_2S or metal sulfides, producing elemental sulfur. This elemental sulfur under hydrothermal conditions (T, p, pH, salinity) is capable of reacting with chemical additives. Equally important, scavengers are often used in HF applications to remove oxygen; however, the most common oxygen scavengers are based on generating thiosulfate ions, which upon reaction with oxygen produce sulfate and protons. As discussed in our previous work and shown in the VED diagrams of this study, sulfate and H_2S will react to produce elemental sulfur at low-pH.

A salt effect on methanol reaction with sulfur was evident at low-pH and could be a result of a combination of ion-pairing and a secondary salt effect. We highlighted that hydropolysulfides likely play an important role in the low-pH systems where increases in the reaction rates were observed. Although difficult to measure, but also influential, pH plays an important role in the kinetics of the sulfur-methanol reactions at high-pressure and high-temperature. Furthermore, as

many other components in the HF can contribute through similar chemistry toward H_2S and organosulfur generation, future research in this area is required.

Chapter Six: General conclusion and future work

6.1 Conclusion

6.1.1 Direct production of H₂S by sulfur-containing additive degradation

In this thesis, the construction of a fully automated high-pressure and high-temperature stirred autoclave was accomplished. The main goal behind this instrument was to study the degradation of chemical additives that may produce H_2S and organosulfur compounds as by-products when exposed to downhole conditions. The intention of building this new experimental setup was to improve high-temperature and pressure control from the previous single batch reactors, as well to incorporate on-line sampling capabilities of both liquid and gas phases *via* automation, at relatively low volumes, especially when dealing with toxic gases such as hydrogen sulfide.

When evaluating sulfur-containing biocides, it was found that when exposing dazomet to downhole conditions, H_2S was generated *via* carbon disulfide hydrolysis. H_2S was found to be a sulfur intermediate that was later converted to methyl mercaptan. It was found that neither pressure nor salinity affected the formation of hydrogen sulfide under the conditions tested. A second sulfur-containing biocide, methylisothiazolinone, was found to generate H_2S upon hydrolysis when exposed to hydraulic fracturing conditions. In that case, an organic intermediate was isolated and characterized in order to propose a simplified chemical degradation mechanism. Variable H_2S formation rates were observed when exposed to highly saline or acidic environments. Specifically, a secondary salt effect was found during the formation of hydrogen sulfide. In addition to H_2S generation, biocide degradation reduces the effectiveness of the additive.

When evaluating the degradation of sulfur-containing corrosion inhibitors, 2,5-dimercapto-1,3,4-thiadiazole and 2-amino-1,3,4-thiadiazole were found to generate H_2S under laboratory generated hydraulic fracturing conditions. Both of these rates for hydrogen sulfide formation were found to increase with increasing ionic strength. A third sulfur-containing biocide, 2-aminobenzothiazole, was found to be stable at downhole conditions. No hydrolysis or H_2S was observed during all the conditions tested. The stability of this compound suggests that the benzothiazole motif should be explored further for corrosion inhibitors.

When considering the sulfur-containing biocides and corrosion inhibitor results, one can conclude that upon reaching downhole conditions (pressure, temperature, pH and variable salinity) hydrolysis is a common first degradation pathway. In many cases, results illustrated that the half-life of these compounds were relatively short; therefore, hydrolysis rates could help to correct for effective concentrations in applications where longer residence times are required. It should be noted that souring or hydrogen sulfide generation was observed in the majority of cases. Consequently, if the right conditions are met, these additives could degrade faster than expected and also impact production once hydrogen sulfide starts to appear.

The degradation results observed in this work highlight the fact that more stability testing should be done for chemicals used in hydraulic fracturing either for safety or operational purposes. When hydrogen sulfide is unexpectedly generated, it impacts both the production facilities as well as the environment. The produced gas must be treated to remove hydrogen sulfide before transportation to the end-user and by-products of this process could be left in the produced or flowback water.

6.1.2 Production of H₂S by sulfur oxidation

In trying to understand additional souring mechanisms, the hypothesis for oxidation of *native* hydrogen sulfide to elemental sulfur with oxygen present in the hydraulic fluid coupled with the sulfur-dehydrogenation of organics was shown to be a possible reaction pathway. In fact, this likely is the more significant contributor to shale gas souring due to the amount of possible native sulfide and the fact that the fluids tend to achieve a steady state of H₂S versus a finite release. Native sulfides (metal sulfide or H₂S) are rapidly oxidized to elemental sulfur; therefore, the formation of elemental sulfur could simply be a process which causes the initial fluid testing to be incorrect, *i.e.*, there was H₂S there the whole time, but was temporarily sequestered/fixed through fracturing. Note that sulfur dehydrogenation of sp^3 carbons above 150 °C is well known.

When testing this hypothesis and trying to understand organosulfur formation under hydraulic fracturing conditions, the sulfur-methanol dehydrogenation reaction was studied successfully under various hydraulic fracturing conditions. When exposing a reaction mixture of methanol and sulfur to these conditions, hydrogen sulfide, dimethyl sulfide and dimethyl disulfide was generated. It was also found that the formation of hydropolysulfides played a role in the formation of organosulfur compounds. The effect of pH on the rate constant for the sulfur-methanol system was measured, and the acid enhancement of the rate was experimentally determined at low-pH.

Both sulfur-containing additives, as well as sulfur-dehydrogenation reactions, were shown to be possible mechanisms by which hydrogen sulfide and organosulfur compounds are generated in a laboratory reactor when mimicking downhole conditions. A shale gas well is a dynamic

system; therefore, the souring mechanism is a complex process. The mechanisms described here are particular to the additives tested; as such, more data is needed to understand the mechanisms of decomposition of other chemical additives.

Finally, this thesis is the result of a continuous effort to broaden our understanding of the various mechanisms for souring of shale gas. It is fair to conclude that the results presented here opens the door to further studies about downhole kinetics and the degradation products of fracture fluid chemical additives.

6.2 Future Work

This thesis described the design, construction and procedures for studying the degradation of chemical additives used in hydraulic fracturing fluids. From the literature, it was found that the gas phase is mostly unstudied in the degradation of chemical additives, as most of the research is focused on the products found in the liquid phase. Our results suggested that analysis of the gas phase in degradation of chemical additives could further the understanding of all decomposition products.

The next logical step is to expand the sulfur dehydrogenation studies to various common additives. In this regard, early attempts to study the hydrogen sulfide generation of common additives were completed. In particular, a subgroup of the chemical additives listed by Sumner *et. al.*[77] were reacted with elemental sulfur in high-temperature and pressure aqueous fluids (*trans*-cinnamaldehyde, propylene carbonate, propargyl alcohol, ethyl acetate, 2-butoxyethanol and 2-ethylhexanol). In all cases, hydrogen sulfide was generated in various amounts. However, carsul

formation (carbon sulfur polymerization) affected the reproducibility, as different sulfur loading led to different product recoveries. Based on the early results, it appears that once hydrogen abstraction is initiated, new carbon-carbon bonds can form due to the reactivity of the intermediates, thus affecting the total carbon balance, *i.e.*, the olephinic mixtures undergo polymerization. In these cases, stable organic products may form, and further analysis should be performed to characterize these products. Nevertheless, the formation of hydrogen sulfide was observed. Future research could focus on identifying these compounds to enhance the understanding of the sulfur dehydrogenation mechanism of chemicals with various functional groups. Additionally, the incorporation of complementary analytical techniques such as GC-TOF-MS for this system could provide sufficient information in the possible reaction pathways.

The latter data and complications with carsul formation, meant that the results were poor and less reproducible. Nevertheless, a preliminary plot of H_2S versus time for a laboratory fracturing solution composed of trans-cinnamaldehyde, propylene carbonate, propargyl alcohol, ethyl acetate, 2-butoxyethanol, benzoic acid and 2-ethylhexanol with a concentration of 500 ppmw of each compound is shown in Figure 6-1
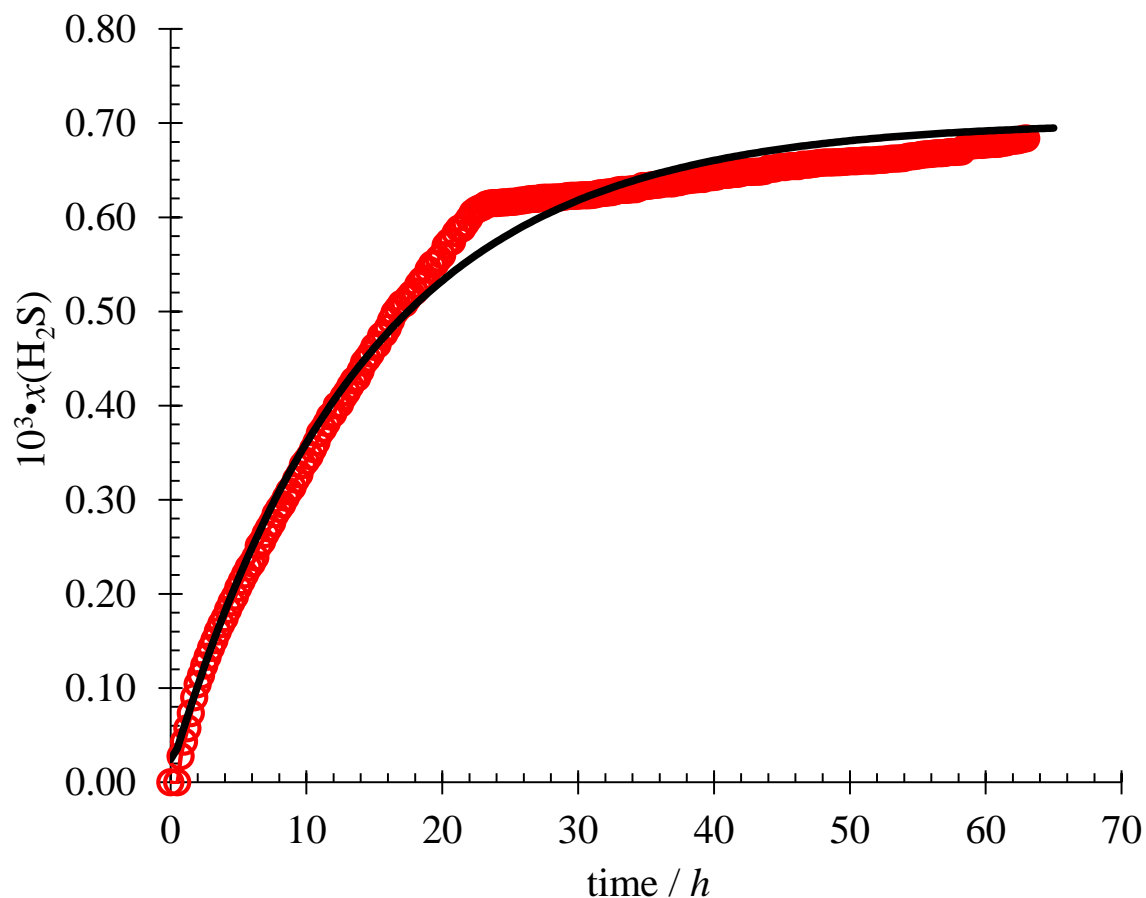
Figure 6-1. H$_2$S evolution for the sulfur oxidation of trans-cinnamaldehyde, propylene carbonate, propargyl alcohol, ethyl acetate, 2-butoxyethanol and 2-ethylhexanol.

Based on the kinetic data present here and incorporating new hydrogen sulfide formation data for commonly used additives, a semi-empirical kinetic model could be developed. Initial efforts of modelling souring of shale gas has been done by Ellis *et al.*[108], and found possible ppb levels of hydrogen sulfide in the production fluids with early rates obtained from our research group. An updated version of a similar reservoir modelling program would benefit both producers and chemical companies.

Finally, this research would benefit from post-fracture hydrogen sulfide production data being made available in combination with the fracturing fluid composition in order to validate some of these results in the field.

Appendices

A.1 Arduino (microcontroller code)

This program controls the speed of an autoclave motor and samples *via* a poppet valve. Data is set in the COM port in the format:-RPM Set, Quiescent Time (seconds), Poppet Valve Time (millisec) and Wait Time before starting the GC (seconds).

```
#include <Wire.h>

int rpmSETPOINT = 60  // Initial RPM Setpoint; Will round down to a multiple of 30

int quiet = 0;  // Quiecient time (seconds) between stopping motor and sampling

int poppet = 0;  // Time (milliseconds) the sampling valve remains open

int SamDelay = 0; // Time (seconds) between sampling and starting the GC

const int motorpin = 9;      // the pin that switches the MOSFET (PWM) for motor

const int poppetpin = 8; // the pin that opens the sampling valve

const int GCpin = 13;  // the pin that starts the GC (reed relay)

const int LEDpin = 12;  // the indicator LED on the Unit

const int SpeedSensorPin = A5;

volatile byte half_revolutions; // pulses from Hall sensor

unsigned int Hallpps;

unsigned int motor_control;

int rpm_previous;

unsigned int rpm;

unsigned long timeold;
```

```
void setup()

{

 // initialize the serial communication:

  Serial.begin(9600);

 // initialize the motor pin as an output:

  pinMode(motorpin, OUTPUT);

  pinMode(3, INPUT);          // set Hall sensor pin to input

  pinMode(poppetpin, OUTPUT);

  pinMode(GCpin, OUTPUT);

  pinMode(LEDpin, OUTPUT);

  digitalWrite(3, LOW);       // turn off pullup resistors

  digitalWrite(poppetpin, LOW);

  digitalWrite(GCpin, LOW);

  digitalWrite(LEDpin, LOW);

  attachInterrupt(1, rpm_fun, RISING);

   Hallpps = rpmSETPOINT / 30;

   Hallpps = constrain(Hallpps, 0, 40);

   rpmSETPOINT = Hallpps * 30;

   motor_control = Hallpps * 12;

   analogWrite(motorpin,motor_control);

   half_revolutions = 0;

   rpm = 0;

   timeold = 0;
```

```
}

void loop() { // if there's any serial information available, read it:

 while (Serial.available() > 0) { // look for the next valid integer in the incoming serial stream:

   rpmSETPOINT = Serial.parseInt();

   quiet = Serial.parseInt();  // read quiet(seconds) if available

   poppet = Serial.parseInt();  // read poppet(milliseconds) if available

   SamDelay = Serial.parseInt();  // read Sample Delay(seconds) if available


   // look for the next value, then timeout

   Serial.setTimeout(250);

  if (poppet > 0)

 {

 digitalWrite(LEDpin, HIGH);  // indicates that the Unit is doing a sampling cycle

 analogWrite(motorpin,0);  // stops the autoclave motor

 Serial.println("Autoclave Motor Stopped - Settling Period");

 delay((quiet * 1000));  // wait for quiet seconds

 digitalWrite(poppetpin, HIGH);  // start sampling

 Serial.println("Valve Open - Sampling");

 delay(poppet);  // sample

 digitalWrite(poppetpin, LOW); // end sampling

 Serial.println("Valve Closed - Sampling Completed");

 delay((SamDelay * 1000));  // delay before GC starts

 digitalWrite(GCpin, HIGH); // start GC
```

```
Serial.println("GC Started - Stirring Resumed");

delay(500);

digitalWrite(GCpin, LOW);

analogWrite(motorpin,motor_control);  // turn the autoclave stirrer back on

poppet = 0;  // set the poppet time back to zero

digitalWrite(LEDpin, LOW); // turns off the sampling LED

}

 if (rpmSETPOINT != rpm_previous)

  {

    Hallpps = rpmSETPOINT / 30;


    // constrain the values from 0 to 40; in case you entered something stupid

    // this gives a maximum RPM of 1200

    Hallpps = constrain(Hallpps, 0, 40);

    rpmSETPOINT = Hallpps * 30;

    motor_control = Hallpps * 12;

    analogWrite(motorpin,motor_control);  // sets the Autoclave motor to an initial value

  }

 }
if (half_revolutions >= 60  || (millis() - timeold) > 1000)

{

  //Update RPM every 60 counts or every second,

  //increase half_revolutions for better RPM resolution
```

```
rpm = (30*1000/(millis() - timeold))*half_revolutions;

timeold = millis();

half_revolutions = 0;

Serial.print(rpmSETPOINT);

Serial.print(" , ");

Serial.print(rpm);

Serial.print(" , ");

float volts0 = (motor_control / 255.0) * 24.0;

Serial.println(volts0);


if (rpm < rpmSETPOINT)

{

 motor_control = motor_control + 1;

 motor_control = constrain(motor_control,0,255);

 analogWrite(motorpin,motor_control);

}

if (rpm > rpmSETPOINT && motor_control != 0)

{

 motor_control = motor_control - 1;

 motor_control = constrain(motor_control,0,255);

 analogWrite(motorpin,motor_control);

}

rpm_previous = rpmSETPOINT;
```

```
 }

 }

void rpm_fun()

 {

  half_revolutions++;

  //Each rotation, this interrupt function is run twice

 }
```

A.2 LabVIEW interface

LabVIEW is a programming language designed for the control and measurements of experimental systems. LabVIEW provides an integrated platform where all component can be controlled under the same panel, therefore allowing the user to operate and read from multiple controllers. The LabVIEW platform provides two different views, first the block diagram which contains all the graphical programming language used to control sensors and equipment, and second, the front panel where all the controls are displayed and are accessible by the user. As illustrated in Figure A.2-1, the front panel has all of the instrument controls consolidated as well as all of the data displayed for the PRTs, pressure transducer and the microcontroller interface. The coding presented here was developed to fully automate the experimental systems used in this thesis
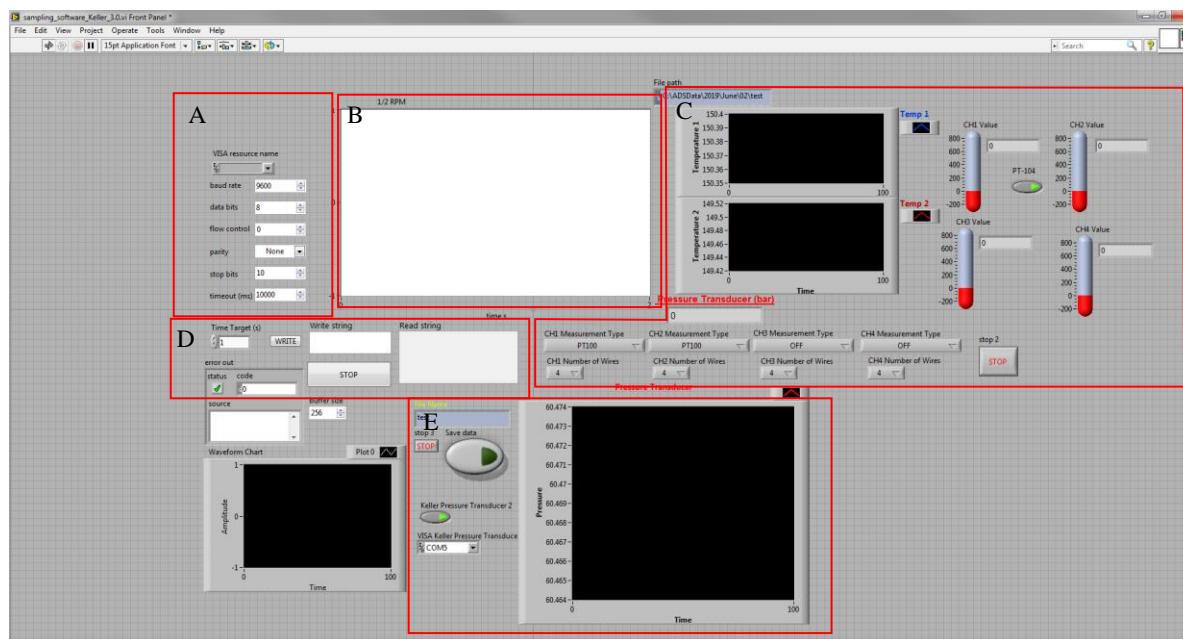

Figure A.2-1. LabVIEW front control panel for the control of the 50 mL high-pressure high-temperature reactor: A, controls for device communication and data collection; B, live-update rpm of reactor; C, live-update PRTs; D, Arduino microcontroller interface for sampling configuration; E, live-update pressure transducer measurements.

A.3 Characterization of N,1-dimethyl-6-oxo-1,6-dihydropyridine-3-carboxamide

The reaction described for decomposition of methylisothiazolinone was performed on a larger scale (1g, 6.02 mols) than described in chapter 3, in order to isolate the intermediate. The aqueous mixture was extracted with chloroform (3x25mL), dried with magnesium sulfate and concentrated under vacuum. The crude product was purified by column chromatography on silica gel (4% MeOH/DCM) which gave 3-pyridinecarboxamide as a pale brown precipitate. ^{1}H NMR (400 MHz, CDCl$_3$) δ 4.36 (s, 2H), 4.30 (s, 2H), 3.44 (s, 3H), 2.61 (s, 3H). ^{1}H NMR (400 MHz, CDCl$_3$) δ 8.11 (d, $J = 2.6$ Hz, 1H), 7.58 (dd, $J = 9.5$, 2.7 Hz, 1H), 6.17 (br, 1H), 6.51 (d, $J = 9.5$ Hz, 1H), 3.58 (s, 3H), 2.96 (d, 3H).^{13}C NMR (101 MHz, CDCl$_3$) δ 164.8 (C), 162.9 (C), 141.6 (CH), 136.3 (CH), 119.5 (CH), 113.3 (C), 38.3 (CH$_3$), 26.9 (CH$_3$). Mass spectrum (CI, *m/z*) 166.1 [M$^+$], 136.1. HRMS (EI) calc'd for C8H10N2O2 166.0742 [M$^+$], found 166.0740.
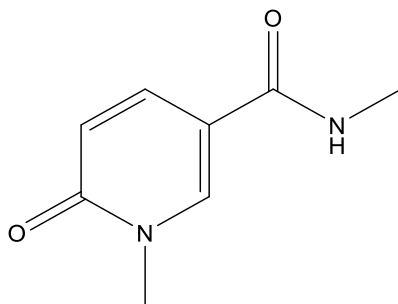
Figure A.3-1. Chemical structure of C$_8$H$_{10}$N$_2$O$_2$, N,1-dimethyl-6-oxo-1,6-dihydropyridine-3-carboxamide.

13C - NMR
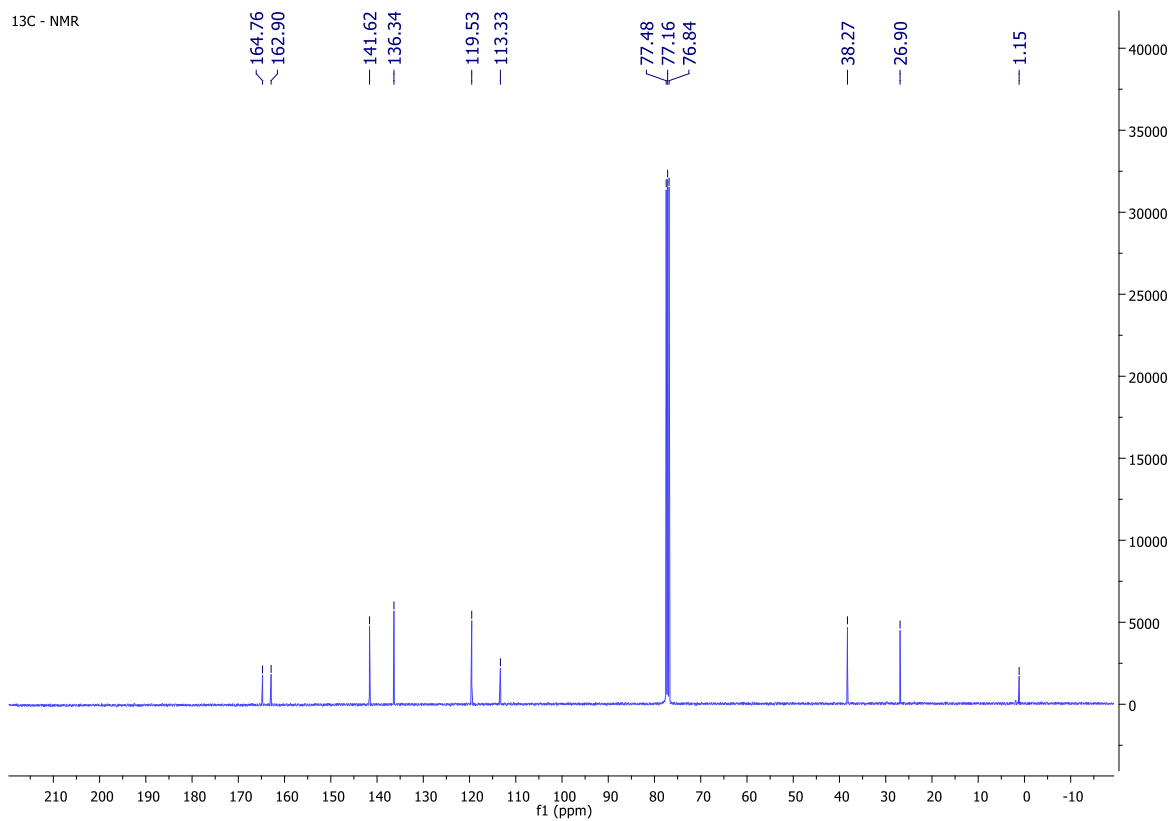

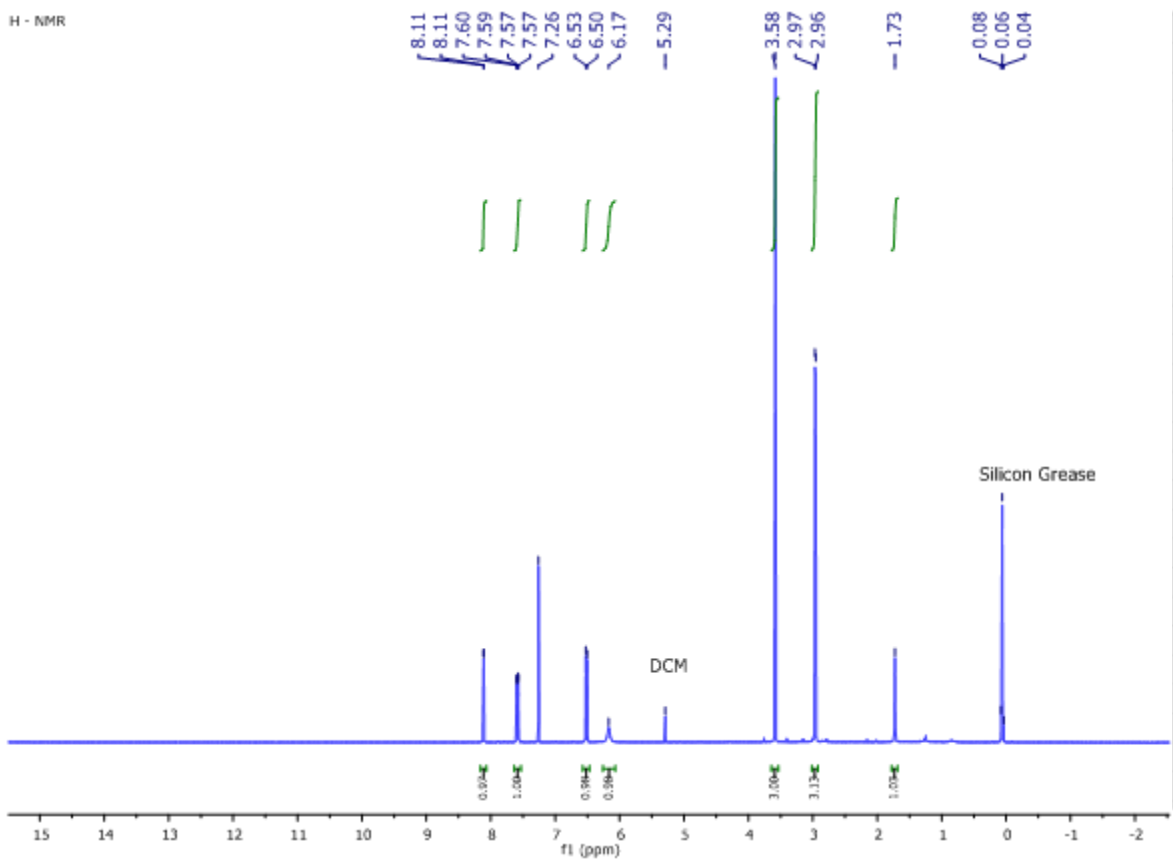**Figure A.3-2.** ^{13}C NMR of intermediate 3-pyridinecarboxamide

H - NMR

Figure A.3-4. H[1] for 3-pyridinecarboxamide

Figure A.3-5. Elemental sulfur extracted from the decomposition of methylisothiazolinone.

A.4 Permission of second authors

1. Dr. Marriott

Juan, the manuscripts you've listed below are primarily your work and are well suited for your PhD thesis. I agree.

Rob

--
Robert Marriott
ASRL Director of Research, Associate Professor, and
NSERC ASRL Industrial Research Chair in Applied Sulfur Chemistry
Department of Chemistry
University of Calgary
2500 University drive N.W.
Calgary, AB, T2N 1N4

Tel: (403)-220-2417, (403)-220-3144
Email: rob.marriott@ucalgary.ca

From: Juan Marrugo-Hernandez <juan.marrugohernande@ucalgary.ca>
Sent: July 22, 2019 2:38 PM
To: Robert Marriott <rmarriot@ucalgary.ca>
Subject: Co-author permission for thesis

Dear Dr. Robert Marriott,

As you know, I wish to include the following manuscripts, in which you are a co-author, to my thesis:

1) Marrugo-Hernandez, J. J.; Prinsloo, R.; Sunba, S.; Marriott, R. A. Downhole Kinetics of Reactions Involving Alcohol-Based Hydraulic Fracturing Additives with Implications in Delayed H_2S Production. *Energy and Fuels,* **2018**, *32*(4), 4724-4731.

2) Marrugo-Hernandez, J. J.; Prinsloo, R.; Marriott, R. A. An assessment of the decomposition kinetics of sulfur-containing biocides to hydrogen sulfide at simulated downhole conditions. *Submitted* to the Industrial and Engineering Chemistry research journal, ACS, on June 28, 2019.

3) Marrugo-Hernandez, J. J.; Prinsloo, R.; Fischer, J.; Marriott, R. A. Downhole chemical degradation of corrosion inhibitors and their role in delayed H_2S generation in shale gas. *Submitted* to the Applied Energy journal, Elsevier, on July 17, 2019.

In addition to being part of my thesis, it will also be added to the University of Calgary Theses Repository – The Vault (http://theses.ucalgary.ca/) and Library and Archives Canada (http://www.bac-lac.gc.ca/eng/services/theses/Pages/theses-canada.aspx)

Please confirm by responding to this email that you agree.

Sincerely,

Juan Marrugo-Hernandez

2. Mr. Rohen Prinsloo

Mon 2019.07.22 15:39

Rohen Prinsloo

RE: Co-author permission for thesis

To   Juan Marrugo-Hernandez

Dear Juan,

I give you permission to include the manuscripts in your thesis.

Congratulations on a great achievement!

Rohen Prinsloo

From: Juan Marrugo-Hernandez <juan.marrugohernande@ucalgary.ca>
Sent: July 22, 2019 14:30
To: Rohen Prinsloo <rprinslo@ucalgary.ca>
Subject: Co-author permission for thesis

Dear Mr. Rohen Prinsloo,

As you know, I wish to include the following manuscripts, in which you are a co-author, to my thesis:

1) Marrugo-Hernandez, J. J.; Prinsloo, R.; Sunba, S.; Marriott, R. A. Downhole Kinetics of Reactions Involving Alcohol-Based Hydraulic Fracturing Additives with Implications in Delayed H_2S Production. *Energy and Fuels,* **2018**, *32*(4), 4724-4731.

2) Marrugo-Hernandez, J. J.; Prinsloo, R.; Marriott, R. A. An assessment of the decomposition kinetics of sulfur-containing biocides to hydrogen sulfide at simulated downhole conditions. *Submitted* to the Industrial and Engineering Chemistrtry research journal, ACS, on June 28, 2019.

3) Marrugo-Hernandez, J. J.; Prinsloo, R.; Fischer, J.; Marriott, R. A. Downhole chemical degradation of corrosion inhibitors and their role in delayed H2S generation in shale gas. *Submitted* to the Applied Energy journal, Elsevier, on July 17, 2019.

In addition to being part of my thesis, it will also be added to the University of Calgary Theses Repository – The Vault (http://theses.ucalgary.ca/) and Library and Archives Canada (http://www.bac-lac.gc.ca/eng/services/theses/Pages/theses-canada.aspx)

Please confirm by responding to this email that you agree.

Sincerely,

See more about Rohen Prinsloo.

3.Ms Jade Fischer

Mon 2019.07.22 15:01

Jade Fischer Fischer

Re: Co-author permission for thesis

To   Juan Marrugo-Hernandez

Dear Juan,

Please accept this email as my confirmation and I wish you the best of luck on your Thesis.

Best,
Jade Fischer

From: Juan Marrugo-Hernandez <juan.marrugohernande@ucalgary.ca>
Sent: Monday, July 22, 2019 2:34:12 PM
To: Jade Fischer Fischer <jade.fischer1@ucalgary.ca>
Subject: Co-author permission for thesis

Dear Ms. Jade Fishcher,

As you know, I wish to include the following manuscript, in which you are a co-author, to my thesis:

1) Marrugo-Hernandez, J. J.; Prinsloo, R.; Fischer, J.; Marriott, R. A. Downhole chemical degradation of corrosion inhibitors and their role in delayed H2S generation in shale gas. *Submitted* to the Applied Energy journal, Elsevier, on July 17, 2019.

In addition to being part of my thesis, it will also be added to the University of Calgary Theses Repository – The Vault (http://theses.ucalgary.ca/) and Library and Archives Canada (http://www.bac-lac.gc.ca/eng/services/theses/Pages/theses-canada.aspx)

Please confirm by responding to this email that you agree.

Sincerely,

Juan Marrugo-Hernandez
PhD candidate
Vanier Scholar
University of Calgary
#6 – 3535 Research Road N.W.

4. Saud Sunba

Mon 2019.07.22 16:51

Saud Sunba

Re: Co-author permission for thesis

To   Juan Marrugo-Hernandez

Hi Juan,

I agree!
Best of luck,

Sincerely,
Saud

From: Juan Marrugo-Hernandez <juan.marrugohernande@ucalgary.ca>
Sent: Monday, July 22, 2019 2:32:04 PM
To: Saud Sunba <saud.sunba@ucalgary.ca>
Subject: Co-author permission for thesis

Dear Mr. Saud Sumba,

As you know, I wish to include the following manuscript, in which you are a co-author, to my thesis:

1) Marrugo-Hernandez, J. J.; Prinsloo, R.; Sunba, S.; Marriott, R. A. Downhole Kinetics of Reactions Involving Alcohol-Based Hydraulic Fracturing Additives with Implications in Delayed H_2S Production. *Energy and Fuels,* **2018**, *32*(4), 4724-4731.

In addition to being part of my thesis, it will also be added to the University of Calgary Theses Repository – The Vault (http://theses.ucalgary.ca/) and Library and Archives Canada (http://www.bac-lac.gc.ca/eng/services/theses/Pages/theses-canada.aspx)

Please confirm by responding to this email that you agree.

Sincerely,

Juan Marrugo-Hernandez
PhD candidate

See more about Saud Sunba.

A.5 Statement of contribution

Co-author contribution (Dr. Marriott)

I will like to use this section to acknowledge the contribution of Dr. Marriott, who has been involved in the development, supervision and publication of all the work presented in this thesis. His support has been essential in all aspects but mainly in providing necessary feedback and technical suggestions, proofreading all the writing and submission of all manuscripts.

Co-author contribution (Mr. Rohen Prinsloo)

Mr. Prinsloo has co-author all the publications presented in this thesis. His expertise in organic chemistry has been important in helping me to understand the multiple degradation pathways of the chemical systems studied during my thesis. When possible, Mr. Prinsloo has helped me to isolate organic intermediates and fully characterize them.

Co-author contribution (Ms. Jade Fischer)

Ms. Fischer was a summer undergraduate student working under my supervision during the summer of 2018. She assisted me in preparing solutions, running calibration curves in multiple types of equipment and GC analysis for the study presented in chapter four.

Co-author contribution (Mr. Saud Sunba)

Mr. Saud Sunba was a summer undergraduate student working under my supervision during the summer of 2017. He assisted me in preparing solutions, running calibration curves and GC analysis for the study presented in chapter five.

A.6 Copyright permission

References

(1)   Wang, S. Shale gas exploitation: Status, problems and prospect *Nat. Gas Ind. B* **2018**, *5*, 60–74.

(2)   McIlvaine, R.; James, A. The potential of gas shale *World Pumps* **2010**, *2010*, 16–18.

(3)   Weiland, R. H.; Hatcher, N. A. Overcoming challenges in treating shale gases. Hydrocarb. Process. **2012**, 91,45−48.

(4)   Marriott, R. A.; Pirzadeh, P.; J. J. Marrugo-Hernandez.; Raval, S. Hydrogen Sulfide formation in Oil and Gas *Can. J. Chem.* **2016**, *94*, 406–413.

(5)   Middleton, R. S.; Gupta, R.; Hyman, J. D.; Viswanathan, H. S. The shale gas revolution: Barriers, sustainability, and emerging opportunities. *Appl. Energy* **2017**, *199*, 88–95.

(6)   Kondash, A. J.; Albright, E.; Vengosh, A. Science of the Total Environment Quantity of fl owback and produced waters from unconventional oil and gas exploration. *Sci. Total Environ.* **2017**, *574*, 314–321

(7)   Taylor, R. S.; Fyten, G. C.; Mcneil, F. Acidizing-Lessons from the Past and New Opportunities. **2012**, November, 1–13.

(8)   Extraction, T. E. P. on H. S. and T. to U. the E. I. of S. G. & Science. *Envioronmental Impacts of Shale Gas Extraction in Canada*. (2014).

(9)   Barbot, E.; Vidic, N. S.; Gregory, K. B.; Vidic, R. D. Spatial and temporal correlation of water quality parameters of produced waters from Devonian-age shale following hydraulic fracturing. *Environ. Sci. Technol.* **2013**, *47* (6), 2562–2569.

(10)   Lester, Y.; Ferrer, I.; Thurman, E. M.; Sitterley, K. A.; Korak, J. A.; Aiken, G.; Linden, K. G. Characterization of hydraulic fracturing flowback water in Colorado: Implications for water treatment. *Sci. Total Environ.* **2015**, *512–513*, 637–644.

(11)   Kahrilas, G. A.; Blotevogel, J.; Corrin, E. R.; Borch, T. Downhole Transformation of the Hydraulic Fracturing Fluid Biocide Glutaraldehyde: Implications for Flowback and Produced Water Quality. *Environ. Sci. Technol.* **2016**, *50* (20), 11414–11423.

(12)   FracFocus. What Chemicals Are Used. https://fracfocus.org/chemical-use/what-chemicals-are-used.

(13)   Wang, Q.; Chen, X.; Jha, A. N.; Rogers, H. Natural gas from shale formation - The evolution, evidences and challenges of shale gas revolution in United States. *Renew. Sustain. Energy Rev.* **2014**, *30*, 1–28.

(14)   Dariva, C. G.; Galio, A. F. Corrosion Inhibitors – Principles, Mechanisms and Applications. *Dev. Corros. Prot.* **2014**.

(15)   Boyle, B. A Look at Developments in Vapor Phase Corrosion Inhibitors. *Met. Finish.* **2004**, *102* (5), 37–41.

(16)   Yadav, M.; Sharma, D. Inhibition of corrosion of copper by 2 , 5-dimercapto-1 , 3 , 4-thiadiazole in 3 . 5 % NaCl solution. *Indian J. Chem. Technol.* **2010**, *17* (March), 95–101.

(17)   Ramachandran, S.; Bartrip, K. A. Molecular Modeling of Binary Corrosion Inhibitors. *Corros.* **2003**, No. 03624, 1–8.

(18)   Pähler, M.; Santana, J. J.; Schuhmann, W.; Souto, R. M. Application of AC-SECM in corrosion science: Local visualisation of inhibitor films on active metals for corrosion protection. *Chem. - A Eur. J.* **2011**, *17* (3), 905–911.

(19)   Malcom A., K. *Production of Chemical for the Oil and Gas Industry*, second.; CRC Press: Boca Raton FL, 2014.

(20)   Odgen, R.; Fichter, J.; Johnson, K.; French, K. Use of Microbiocides in Barnett Shale Gas Well Fracturing Fluids to Control Bacteria Related Problems. *NACE Int. Corros. Conf. Expo* **2008**, No. 08658, 1–14.

(21)   Struchtemeyer, C. G.; Morrison, M. D.; Elshahed, M. S. A critical assessment of the efficacy of biocides used during the hydraulic fracturing process in shale natural gas wells. *Int. Biodeterior. Biodegrad.* **2012**, *71*, 15–21

(22)   Kahrilas, G. A.; Blotevogel, J.; Stewart, P. S.; Borch, T. Biocides in Hydraulic Fracturing Fluids: A Critical Review of Their Usage, Mobility, Degradation, and Toxicity. *Environ. Sci. Technol.* **2015**, *49* (1), 16–32.

(23)   Wiencek, K. M.; Chapman, J. S. Water Treatment Biocides: How Do They Work and Why Should You Care? *Corros. 99* **1999**, No. 308.

(24)   Ullah, S. Biocides in Papermaking Chemistry, 2011.

(25)   Aften, C. W.; Roberts, G. New Compounds For Hydrogen Sulfide Scavenging And Iron Sulfide Control. *SPE Int.* **2011**, No. April, 11–13.

(26)   Williams, T. M. Efficacy of Isothiazolone Biocide versus Sulfate Reducing Bacteria (SRB). *NACE Int. Corros. Conf. Expo* **2009**, No. 09059, 1–12

(27)   Clark, P. D.; Hyne, J. B.; David Tyrer, J. Some chemistry of organosulphur compound types occurring in heavy oil sands. 2. Influence of pH on the high temperature hydrolysis of tetrahydrothiophene and thiophene. *Fuel* **1984**, *63* (1), 125–128.

(28)   Kapadia, P. R.; Kallos, M. S.; Gates, I. D. A review of pyrolysis, aquathermolysis, and oxidation of Athabasca bitumen. *Fuel Process. Technol.* **2015**, *131*, 270–289.

(29)   Kapadia, P. R.; Kallos, M. S.; Gates, I. D. A new kinetic model for pyrolysis of Athabasca bitumen. *Can. J. Chem. Eng.* **2012**, *91* (5), 889–901.

(30)   Clark, D. Chemistry of organosulphur compound occurring in heavy oil sands processes hydrolysis and thermolysis of in relation to steam stimulation. *Fuel* **1983**, *62*, 959–962.

(31)   Khansari, Z.; Kapadia, P.; Mahinpey, N.; Gates, I. D. A new reaction model for low temperature oxidation of heavy oil: Experiments and numerical modeling. *Energy* **2014**, *64*, 419–428.

(32)   Struchtemeyer, C. G.; Elshahed, M. S. Bacterial communities associated with hydraulic fracturing fluids in thermogenic natural gas wells in North Central Texas, USA. *FEMS Microbiol. Ecol.* **2012**, *81* (1), 13–25.

(33)   Machel, H. G. Bacterial and thermochemical sulfate reduction in diagenetic settings-old and new insights. *Sediment. Geol.* **2001**, *140*, 143–175.

(34)   Mougin, P.; Lamoureux-Var, V.; Bariteau, A.; Huc . A.Y. Thermodynamic of thermochemical sulphate reduction. *J. Pet. Sci. Eng.* **2007**, 58, 413–427.

(35)   Machel, H. G.; Krouse, H. R.; Sassen, R.; Watkin, L. Products and distinguishing criteria of bacterial and thermochemical sulfate reduction. *Appl. Geochemistry* **2000**, *10*, 373–389.

(36)   Goldstein, T. P.; Aizenshtat, Z. Thermochemical sulfate reduction a review. *J Therm Anal* **1994**, 42, 241–290.

(37)   Xiao, Q.; Sun, Y.; Chai, P. Experimental study of the effects of thermochemical sulfate reduction on low molecular weight hydrocarbons in confined systems and its geochemical implications. *Org. Geochem.* **2011**, *42* (11), 1375–1393.

(38)   R. A Marriott and P. M Davis. Estimation of sulfur deposition during the production of lean sour gas. In *SOGAT III*; Abu Dhabi, United Arab Emirates, 2007.

(39)   Worden, R. H.; Smalley, P. C.; Cross, M. M. The Influence of Rock Fabric and Mineralogy on Thermochemical Sulfate Reduction : Khuff Formation , Abu Dhabi. **1994**.

(40)   Wilson L. Orr. Changes in Sulfur Content and Isotopic Ratios of Sulfur during Petroleum Maturation--Study of Big Horn Basin Paleozoic Oils. *Am. Assoc. Pet. Geol. Bull.* **1974**, *58* (11), 2295–2318.

(41)   Zhang, T.; Ellis, G. S.; Ma, Q.; Amrani, A.; Tang, Y. Kinetics of uncatalyzed thermochemical sulfate reduction by sulfur-free paraffin. *Geochim. Cosmochim. Acta* **2012**, *96*, 1–17.

(42)   Zhang, T.; Ellis, G. S.; Wang, K.; Walters, C. C.; Kelemen, S. R.; Gillaizeau, B.; Tang, Y. Effect of hydrocarbon type on thermochemical sulfate reduction. *Org. Geochem.* **2007**, *38* (6), 897–910.

(43)   Zhang, T.; Amrani, A.; Ellis, G. S.; Ma, Q.; Tang, Y. Experimental investigation on thermochemical sulfate reduction by H2S initiation. *Geochim. Cosmochim. Acta* **2008**, *72* (14), 3518–3530.

(44)   Pirzadeh, P.; Lesage, K. L.; Marriott, R. A. Hydraulic Fracturing Additives and the Delayed Onset of Hydrogen Sul fi de in Shale Gas. *Energy and Fuels* **2014**, *28*, 4993–5001.

(45)   He, K.; Zhang, S.; Mi, J.; Hu, G. The speciation of aqueous sulfate and its implication on the initiation mechanisms of TSR at different temperatures. *Appl. Geochemistry* **2014**, *43*, 121–131.

(46)   Pirzadeh, P.; Raval, S.; Marriott, R. A. On the Fate of Hydraulic Fracturing Fluid Additives : Thermochemical Sulfate Reduction Reaction of Sodium Dodecyl Sulfate. *Org. Geochem.* **2015**.

(47)   Ma, Q.; Ellis, G. S.; Amrani, A.; Zhang, T.; Tang, Y. Theoretical study on the reactivity of sulfate species with hydrocarbons. *Geochim. Cosmochim. Acta* **2008**, *72* (18), 4565–4576.

(48)   Sumner, A. J.; Plata, D. L. Halogenation Chemistry of Hydraulic Fracturing Additives under Highly Saline Simulated Subsurface Conditions. *Environ. Sci. Technol.* **2018**, *52*, 9097–9107.

(49)   Hoelzer, K.; Sumner, A. J.; Karatum, O.; Nelson, R. K.; Drollette, B. D.; O'Connor, M. P.; D'Ambro, E. L.; Getzinger, G. J.; Ferguson, P. L.; Reddy, C. M.; et al. Indications of Transformation Products from Hydraulic Fracturing Additives in Shale-Gas Wastewater. *Environ. Sci. Technol.* **2016**, *50* (15), 8036–8048.

(50)   Xiong, B.; Miller, Z.; Roman-White, S.; Tasker, T.; Farina, B.; Piechowicz, B.; Burgos, W. D.; Joshi, P.; Zhu, L.; Gorski, C. A.; et al. Chemical Degradation of Polyacrylamide during Hydraulic Fracturing. *Environ. Sci. Technol.* **2018**, *52* (1), 327–336.

(51)   Clark, P. D.; Lesage, K. L. Quantitative determination of elemental sulfur in hydrocarbons, soils, and Other Materials. *J Chromatogr. Sci.* **1989**, 27, 259–61.

(52)   https://www.un.org/development/desa/en/news/population/world-population-prospects 2017.html

(53)   Rogers, H. Shale gas--the unfolding story. *Oxford Rev. Econ. Policy* **2011**, 27, 117–143.

(54) Podesta, J; Wirth T. Natural gas – a bridge fuel for the 21st Century. Centre for American progress and energy future coalition paper, **2009**.

(55) National Energy Board. A primer for understanding Canadian shale gas − Energy briefing note, http://publications.gc.ca/site/eng/9.571462/publication.html, **2009**.

(56) US Environmental Protection Agency. Assessment of the potential impacts of hydraulic fracturing for oil and gas on drinking water resources. Extern. Rev. **2015**, 998.

(57) http://www.energybc.ca/cache/fracking/www.csur.com/index431b.html

(58) Howarth, R. W.; Engelder, T. Should fracking stop? *Nature* **2011**,477, 271−275.

(59) Marrugo-Hernandez, J. J.; Prinsloo, R.; Sunba, S.; Marriott, R. A. Downhole kinetics of reactions involving alcohol-based hydraulic fracturing additives with implications in delayed H2S production. *Energy Fuels* **2018**, 32, 4724-4731.

(60) L. Gandossi, An overview of hydraulic fracturing and other formation stimulation technologies for shale gas production, EUR 26347 EN. **2013**, 1-64

(61) Barati, R.; Liang, J. T. A review of fracturing fluid systems used for hydraulic fracturing of oil and gas wells. *J. Appl. Polym. Sci.* **2014**, *131*, 1–11.

(62) Plata, D. L.; Jackson, R. B.; Vengosh, A.; Mouser, P. J. More than a decade of hydraulic fracturing and horizontal drilling research *Environ. Sci. Process.Impacts* **2019**, *21*, 193–194.

(63) Paukert Vankeuren, A. N.; Hakala, J. A.; Jarvis, K.; Moore, J. E. Mineral reactions in shale gas reservoirs barite scale formation from reusing produced water as hydraulic fracturing fluid. *Environ. Sci. Technol*. **2017**, *51*, 9391–9402.

(64) Struchtemeyer, C. G.; Morrison, M. D.; Elshahed, M. S. A critical assessment of the efficacy of biocides used during the hydraulic fracturing process in shale natural gas wells. *Int. Biodeterior. Biodegrad.* **2012**, *71*, 15–21.

(65) Corrin, E.; Harless, M.; Rodriguez, C.; Degner, D.; Archibeque, R. Evaluation of a more environmentally sensitive approach to microbiological control programs for hydraulic fracturing operations in the marcellus shale using a nitrate-reducing bacteria and nitrate-based treatment system. *SPE Int.* **2014**, 27–29

(66) Daly, R. A.; Borton, M. A.; Wilkins, M. J.; Hoyt, D. W.; Kountz, D. J.; Wolfe, R. A.; Welch, S. A.; Marcus, D. N.; Trexler, R. V.; MacRae, J. D.; Krzycki, J. A.; Cole, D. R.; Mouser, P. J.; Wrighton, K. C. Microbial metabolisms in a 2.5-km-deep ecosystem created by hydraulic fracturing in shales. *Nat. Microbiol.* **2016**, *1*, 1–9.

(67) Alhajji, J.; Valliappan, M. Concerns over the selection of biocides for oil fields and power plants: A laboratory corrosion assessment. *15th World Petroleum Congress*; John Wiley & Sons: New York, 1999.

(68) Maillard, J. Bacterial target sites for biocide action. *J. Appl. Microbiol.* **2002**, 92 (s1), 16S–27S.

(69) Dawson, J.; Wood, M. A New approach to biocide application provides improved efficiency in fracturing fluids. *SPE/EAGE Eur. Unconv. Resour. Conf. Exhib.* **2012**, *4*, 1–12.

(70) Lucien, J.; Barrault, J.; Guisnet, M.; Maurel, R. Thiol synthesis from carbonyl compounds. *Ind. Eng. Chem. Prod. Res. Dev.* **1978**, 17, 354–357.

(71) Ruzo. L. O. Physical, chemical and environmental properties of selected chemical alternatives for the pre-plant use of methyl bromide as soil fumigant, *Pest. Manag. Sci.* **2006**, 62, 99–113.

(72) Australian pesticides and veterinary medicine authority NRA special review series 97.2, **1997**, Volume I.

(73) Roberts, T. R.; Hutson, D.H. (Eds.), 1999. Fungicides, in: Metabolic pathways of agrochemicals. Royal Society of Chemistry, Cambridge, pp. 937–960

(74) Taylor G. N.; Prince P.; Matherly, R.; Ponnapati, R.; Tompkins, R.; Panchalingam, V.; Jovancicevic, V; Ramachandran, S. The formation and chemical nature of amorphous dithiazine produced from use of hexahydrotriazine based hydrogen sulfide scavengers and the use of an alternative scavenger to minimize solid formation in sour gas applications. SPE 164134. **2013** no. I, 1–14.

(74) Consolazio, N. Chemical interactions of hydraulic fracturing biocides with natural pyrite. Carnegie Mellon University, Pittsburgh. 2017.

(76) King GE. Thirty Years of Gas Shale Fracturing: What Have We Learned? SPE Annu Tech Conf Exhib 2010:50. doi:10.2118/133456-MS.

(77) Sumner, A. J.; Plata, D. L. Exploring the hydraulic fracturing parameter space: a novel high-pressure, high-throughput reactor system for investigating subsurface chemical transformations *Environ. Sci. Process. Impacts,* **2018**, 0, 1–14

(78) Al-muntasheri GA, Aramco S. SPE 169552 A critical review of hydraulic fracturing fluids over the last decade **2014,** 16–8.

(79) Stringfellow, W. T.; Domen, J. K.; Kay, M.; Sandelin, W. L.; Borglin, S. Physical , chemical , and biological characteristics of compounds used in hydraulic fracturing. *J. Hazard. Mater.* **2014**, *275*, 37–54.

(80)   Şahin, M.; Bilgiç, S.; Yilmaz, H. The inhibition effects of some cyclic nitrogen compounds on the corrosion of the steel in NaCl mediums. *Appl. Surf. Sci.* **2002**, *195* (1–4), 1–7.

(81)   Bentiss, F.; Lagrenee, M.; Traisnel, M.; Hornez, J. C. The corrosion inhibition of mild steel in acidic media by a new triazole derivative. *Corros. Sci.* **1999**, *41* (4), 789–803.

(82)   Quraishi M, Khan M, Ajmal M, Muralidharan S, Iyer S. Technical note Influence of molecular structure of substituted benzothiazoles on corrosion inhibition and hydrogen permeation through mild steel in sulphuric acid. *Br. Corros. J.* **1997**, *32* (1), 72–76.

(83)   Muslim A. Effective Inhibitor for corrosion 1994;36:79–84.

(84)   Lucien, J.; Barrault, J.; Guisnet, M.; Maurel, R. Thiol Synthesis from Carbonyl Compounds. *Ind. Eng. Chem. Prod. Res. Dev.* **1978**, *17* (4), 354–357.

(85)   Gece, G.; Bilgiç, S. Quantum chemical study of some cyclic nitrogen compounds as corrosion inhibitors of steel in NaCl media. *Corros. Sci.* **2009**, *51* (8), 1876–1878.

(86)   Quraishi, M. A.; Khan, S. Inhibition of mild steel corrosion in sulfuric acid solution by thiadiazoles. *J. Appl. Electrochem.* **2006**, *36* (5), 539–544.

(87)   Chen, W.; Luo, H. Q.; Li, N. B. Inhibition effects of 2,5-dimercapto-1,3,4-thiadiazole on the corrosion of mild steel in sulphuric acid solution. *Corros. Sci.* **2011**, *53* (10), 3356–3365.

(88)   Liu, L.; Pan, X.; Xing, J.; Qian, J. Anti-corrosion behavior of thiadiazole derivatives for silver strip in hydrogen sulfide solutions. *Anti-Corrosion Methods Mater.* **2015**, *62* (6), 353–362.

(89)   Qin, T. T.; Li, J.; Luo, H. Q.; Li, M.; Li, N. B. Corrosion inhibition of copper by 2,5-dimercapto-1,3,4-thiadiazole monolayer in acidic solution. *Corros. Sci.* **2011**, *53* (3), 1072–1078.

(90)   Quraishi, M. A.; Wajid Khan, M. A.; Ajmal, M.; Muralidharan, S.; Venkatakrishna Iyer, S. Influence of substituted benzothiazoles on corrosion in acid solution. *J. Appl. Electrochem.* **1996**, *26* (12), 1253–1258.

(91)   Abd El Rehim, S. S.; Sayyah, S. M.; El-Deeb, M. M.; Kamal, S. M.; Azooz, R. E. Adsorption and corrosion inhibitive properties of P(2-aminobenzothiazole) on mild steel in hydrochloric acid media. *Int. J. Ind. Chem.* **2016**, *7* (1), 39–52.

(92)   Elsner, M.; Hoelzer, K. Quantitative Survey and Structural Classification of Hydraulic Fracturing Chemicals Reported in Unconventional Gas Production. *Environ. Sci. Technol.* **2016**, *50* (7), 3290–3314.

(93)   Saba, T.; Mohsen, F.; Garry M.; Murphy, B.; Hilbert, B. Methanol use in hydraulic fracturing fluids prepared by : White paper methanol use in hydraulic fracturing fluids. Alexandria: **2012**.

(94)   Thompson Sr., J. E.; McBain, C.; Gregory, G.; Gerbrandt, D. New Continuous-Mix Process for Gelling Anhydrous Methanol Minimizes Hazards. *J. Pet. Technol.* **1992**, *44* (7).

(95)   Hossaini, M.; Jabs, W.; Grisdale, J. Fracturing with crosslinked gelled methanol: a new approach to well stimulation. *J. Can. Pet. Technol.* **1989**, *28* (5, Sep.-Oct., 1989, pp.49-54.).

(96)   McLeod, H.; Coulter, W. The use of alcohol in gas well stimulation. *Society of petroleum engineers of aime,* 1966.

(97)   Cross, M.; Manning, D.; C, Bottrell S. Worden, R. Thermochemical sulphate reduction (TSR): experimental determination of reaction kinetics and implications of the observed reaction rates for petroleum reservoirs. *Org. Geochem.* **2004**, 35, 393–404.

(98)   Marriott, R. A; Pirzadeh, P.; Raval, S. LRGCC 2015 Conference proceedings and fundamentals manual. On the fate of hydraulic fracturing fluids additives in dry hot shale Reservoirs, **2015**, 287–300.

(99)   Tavan, Y.; Hasanvandian, R. Two practical equations for methanol dehydration reaction over HZSM-5 catalyst - Part I: Second order rate equation. *Fuel* **2015**, 142, 208–14.

(100) Qilin, X.; Yongge, S.; Pingxia, C. Experimental study of the effects of thermochemical sulfate reduction on low molecular weight hydrocarbons in confined systems and its geochemical implications. *Org. Geochem.* **2011**, *42*, 1375−1393.

(101) Yermakova, A. V.; Mashkina, A. V. Kinetic model of the reaction of methanol with hydrogen sulfide. *Kinet Catal* **2004**, 45, 554–561.

(102) Ma, Q.; Ellis, G. S; Amrani, A.; Zhang, T.; Tang, Y. Theoretical study on the reactivity of sulfate species with hydrocarbons. *Geochim Cosmochim Acta* **2008**, 72, 4565–4576.

(103) Miyasaka, A.; Denpo, K; Ogawa, H. Estimation and Measurements of pH in High Temperature and High Pressure Sour Environments. *ISIJ Int* **1989**, 29, 4–5.

(104) Yuan, S.; Chou, I. M.; Burruss, R. C.; Wang, X.; Li, J. Disproportionation and thermochemical sulfate reduction reactions in S-H2O-CH4 and S-D2O-CH4 systems from 200 to 340°C at elevated pressures. *Geochim. Cosmochim. Acta* **2013**, 118, 263–275.

(105) Sharifi-Asl, S.; Macdonald, D. Volt equivalent diagrams as a means of displaying the electrochemical thermodynamics of the sulfur–water system. *Corros. Sci.* **2014**, 81, 102–109.

(106) Oriakhi, C. O. Studies on the thermal decomposition of organic polysulfanes. MSc. Thesis, University of Calgary 1991.

(107) Lu, H.; Greenwood, P.; Chen, T.; Liu, J.; Peng, P. The role of metal sulfates in thermochemical sulfate reduction (TSR) of hydrocarbons: Insight from the yields and stable carbon isotopes of gas products. *Org. Geochem.* **2011**,42,700–706.

(108) Xia, X.; Ellis, G. S. Coupled Kinetic and Fluid Dynamic Models to Understand H2S Occurrence in Unconventional Petroleum Reservoirs.Unconvetional resources technology conference **2017**, 1–10.